# CHIRAL POLYMER ELECTRODES

By Ian Thomson Kinloch

Submitted in part fulfilment

for the degree of

**Doctor of Philosophy**

at

The Department of Chemistry,

University of Glasgow,

Glasgow G12 8QQ.

September 1991



ProQuest LLC.
789 East Eisenhower Parkway
P.O. Box 1346
Ann Arbor, MI 48106 – 1346

For my Mum and Dad.

**ACKNOWLEDGEMENTS**

I would like to thank my supervisor Dr. Robert D. Peacock for all his help and encouragement throughout the last 4 years.

I would also like to thank my family for all their support and for putting up with me over this period of time.

Finally I would like to thank Pamela for all her help with my diagrams and for giving me the love and encouragement needed to write up.

# Contents


Dedication i

Acknowledgements ii

Contents iii

Summary v

Chapter 1 - INTRODUCTION 1

What is a chemically modified electrode? 2

Cyclic voltammetry - a method of studying modified electrodes 9

Covalent Binding to metal oxide electrode surfaces 16

Attachment to carbon electrodes 27

Polymer films on electrodes 43

Chiral electrodes 72

Applications to analysis 80

Chapter 2 - EXPERIMENTAL 84

Instrumentation 85

Experimental procedure 93

Chapter 3 - RESULTS AND DISCUSSION 105

Preparation and resolution of complexes 106

Electrode studies 112

Chapter 4 - CONCLUSIONS 169

Resolution Experiments 170

Electrode Experiments 171

Chapter 5 - FUTURE WORK 179

Chapter 6 - APPENDICES 182

Appendix 1 - Electrode systems 183

Appendix 2 - Abbreviations 184

Chapter 7 - REFERENCES 185

## SUMMARY

When (±)-$[Ru(bipy)_2(vbpy)]^{2+}$ is electrochemically scanned through the potentials -1.00V to -2.05V vs. $Ag/AgNO_3$ in acetonitrile, electropolymerisation occurs and a polymer layer is formed on the working electrode of the electrochemical cell. This polymer modified electrode can be immersed in a solution of tartaric acid in water and conditioned so that subsequent immersions will produce (a) peaks immediately when the tartaric acid is of the same "hand", (b) no peaks immediately when the tartaric acid is of the opposite hand (although peaks will gradually appear over time and the electrode system will now behave with the opposite handed characteristics), or (c) reduced peaks immediately when the tartaric acid has partially the hand used in the conditioning process (In this system, as with (b), the electrode will behave as if it was conditioned with this solution if it is left to soak too long).

If the polymer grown is poly-(-)-$[Ru(bipy)_2(vbpy)]^{2+}$ then the above results do not hold. This polymer will have a fixed helicity and as such will be unable to have further chiral structuring induced in it. Since this further chiral structuring is the prerequisite for the chiral sensing, these electrodes can not be used for such processes. The peaks at +0.45V and +0.65V vs. SSCE still

show up with this system since loose bonding (although no restructuring) occurs.

The actual chemical process involved is as follows:
(i) The $Ru^{II}$ of the polymer is oxidised to $Ru^{III}$.
(ii) This catalyses the oxidation of the tartrate.
(iii) The tartrate or the tartrate oxidation product exchanges with the $PF_6^-$ or the $BF_4^-$ of the polymer.
(iv) This results in the peaks at +0.65V and +0.45V.

For poly-(±)-$[Ru(bipy)_2(vbpy)]^{2+}$, reaction (iii) induces chiral structuring whereas in poly-(-)-$[Ru(bipy)_2(vbpy)]^{2+}$, reaction (iii) does not induce chiral structuring and in fact occurs less strongly for this reason.

Chapter 1

# INTRODUCTION

## What is a Chemically Modified Electrode ?

For many years electrochemists have shown great interest in the occurrence, and in the consequences, of the adsorption of ions and molecules onto the surface of electrodes. Such adsorption can be of a desirable nature or can have disastrous consequences. Research into the adsorption has been associated with insights into the electrical double layer and the kinetics and mechanisms of electrochemical reactions. An adsorbed layer of molecules or ions can accelerate reaction rates, although in most cases it has a retardant effect. It can lead to the passivation of electrodes to corrosion processes, and it can be the basis of electroanalytical measurements. Much information has been obtained on which species adsorb on particular electrodes, on the electrode material and on which solvent and electrolyte to use. In some cases, the above combination can be explained rationally by simple reactions or solubility but in the majority of cases, the discovery was one of "it works!- but why?". In these cases understanding comes later.

Chemically modified electrodes are different from conventional electrode systems in that a layer of a specific material is bonded onto a base electrode in order to produce a new electrode with the properties of the bonded species. Typical properties for the bonded

species to have are: fast outer-sphere electron transfer, catalytic properties, functional groups which scavenge trace ions or molecules from solution for electroanalysis and, as was the aim of this project, chiral discrimination.

The immobilised substrates that have been studied most are those that can, directly or indirectly, exchange an electron with the electrode i.e. are reduced or oxidised in their interacted state with the electrode. In a plot of current versus potential, this is observed as a "surface wave". The interfacial electrochemical transformation is represented in reaction (1).

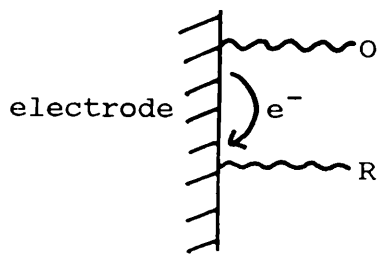


solution,

supporting electrolyte (1)

where ~~O and ~~R are the oxidised and reduced immobilised species respectively. O and R need not necessarily be present in solution for this to be observed. The cyclic voltammetric scan for an example of reaction (1) is shown in Fig 1.[1] This depicts the ferrocene ⇌ ferrocenium electron transfer reaction between a Pt electrode and a ferrocene derivative.

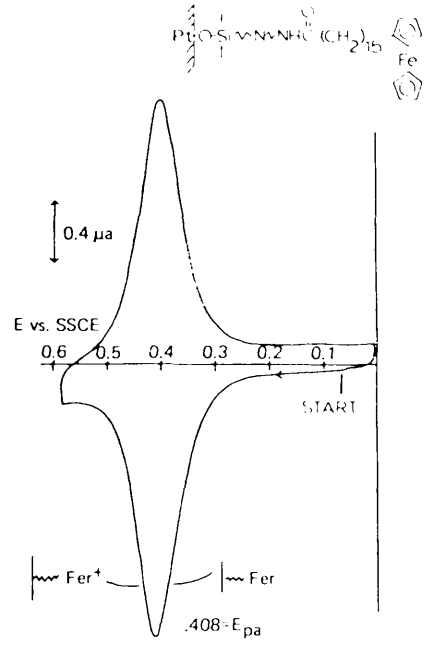


Fig. 1. Covalently immobilised electroactive molecule. The charge under the anodic ferrocene → ferrocenium wave, $Q_a=nFA\Gamma$, gives $\Gamma=0.74 \times 10^{-10}$ mol cm$^{-2}$ for coverage by the indicated structure.

Investigations of these electrochemical reactions make it possible to probe initial/final state thermodynamic differences and the kinetics and mechanisms of electron transfer, to systematically manipulate surface structure and to seek electrode surface reactivity in ways which have no accessible counterpart in the study of electroactive substances dissolved in solution.

There are three types of chemically modified electrodes:-

1. Chemisorbed: Strong or irreversible adsorption of the substance on the electrode surface. The first reported case of this was by Hubbard and Lane[2,3] who chemisorbed quinone-bearing olefins on Pt electrodes.

2. Covalently bonded: Molecules bonded to functional groups of the base electrode. This includes monomolecular layers and (in polymeric form) multinuclear layers.

3. Film deposition: 2 to $10^5$ monolayers can be deposited and held in place by a combination of chemisorption and low solubility in the working solvent. Solubility is usually the more important factor.

An important factor in chemically modified electrodes is that the electrochemical properties of the electrode coating are the same as the nonimmobilised forms. This is evident in the cyclic voltammograms of chemically modified electrodes where the oxidation and reduction potentials are the same as for the solution species. The chemical properties should also, ideally, parallel those of the solution analogues.

Electrocatalysis using a chemically modified electrode is normally a mediation of electron transfer reactions. Using the schematic set up of reaction (1), the electron transfer is by the immobilised O/R couple from the electrode to the substrate (SUBS) which would normally react slowly at the base electrode. This is represented thus in reaction (2).

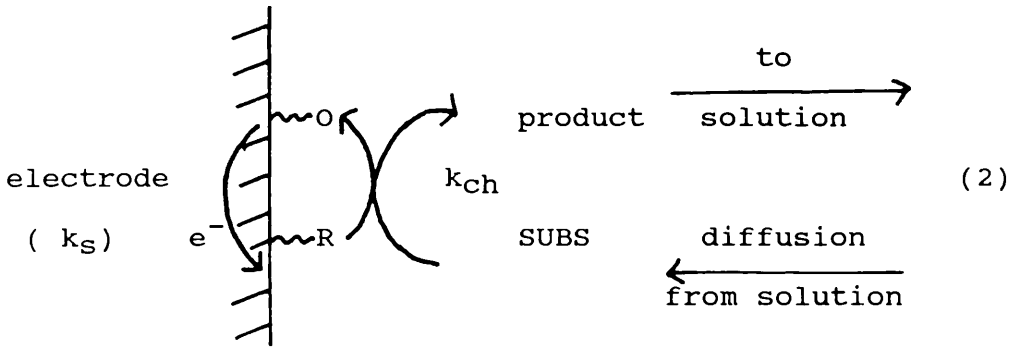


If the rate of mediation ($k_{ch}$) is fast and the rate of reduction of immobilised O ($k_s$) is faster, SUBS is reduced at a potential near to that of the O/R formal potential $E^{o'}_{surf}$.

Reaction (2) can be combined with photoinitiation of the electron transfer step to produce an important phototelectro-catalytic system. For an n-type semiconductor with an immobilised redox couple as before, this would be represented in reaction (3).

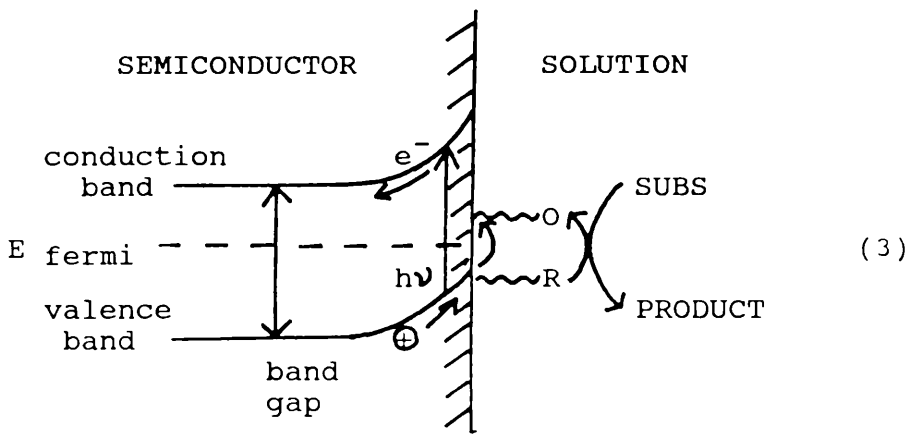

If a photon of energy $h\nu$ is absorbed which is greater than or equal to the band gap of the semiconductor, and in its space charge region, then this causes electron-hole pairs which can separate under the space charge field gradient. The hole migrates to the surface, oxidises R, which in turn is regenerated in the same process as reaction (2). This makes possible the photoelectric oxidation of substrates.

Where there are two distinct polymer layers on an electrode, novel electrochemical properties have been achieved. Rectifying and charge trapping result from bilayers of redox films.[4,5] Using the same system as reaction (2) but where there is an inner film $O_1/R_1$ and an outer film $O_2/R_2$, the electron transfer of $O_2/R_2$ is mediated by that of $O_1/R_1$ as shown in reaction (4).

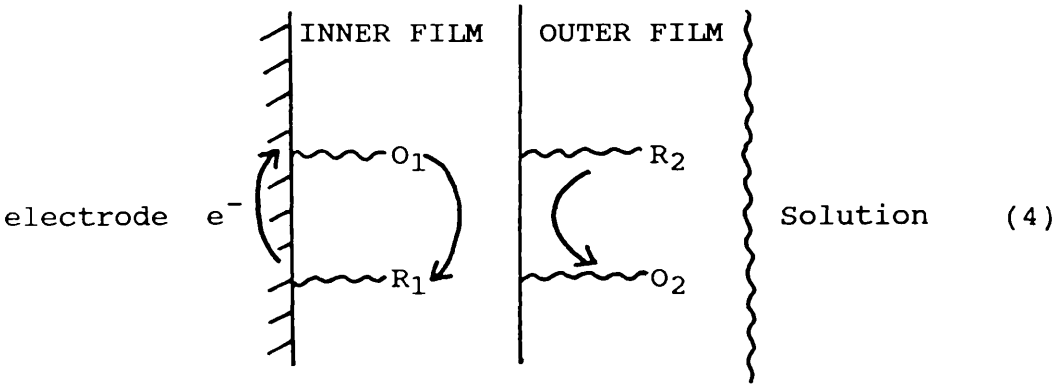


(4)

To tailor-make the electrode it is not necessary to have immobilised electroactive materials. Instead the modification may take the form of a specific functional

group on the electrode surface. An early example of this was the immobilisation of an amino acid ester on carbon so as to create a chiral electrode surface for enantiomerically selective electrosynthesis.[6] Other examples of the "properties" of the molecular layers are hydrophobic, basic, electrically charged etc..

## Cyclic Voltammetry - a method of studying modified electrodes

Cyclic scanning of the potential has been extensively used to characterise the electroactivity of multimolecular and monomolecular layers of redox species. Using the simplified set up of reaction (1), the important quantities measured are shown in Fig. 2.

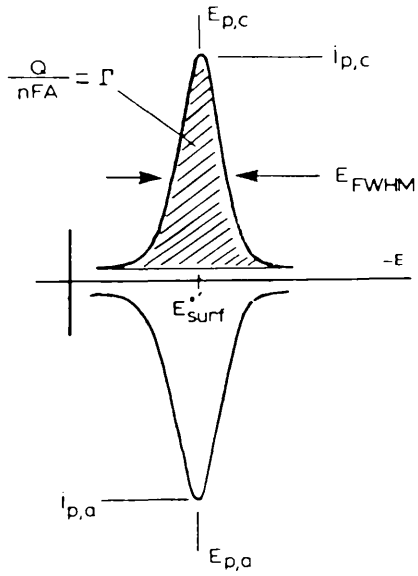


Fig. 2. Schematic representation of a reversible cyclic voltammogram for a monolayer of an immobilised redox species.

Considering reaction (1), if the reaction is reversible i.e. O→R→O→R→O etc. and the activity of O and R are proportional to their surface coverage $\Gamma_O$ and $\Gamma_R$ respectively, then the following equations occur:[7,8]

$$i = \frac{-4ip\exp(\theta)}{[1+\exp(\theta)]^2} \qquad (i)$$

where

$$i_p = \frac{n^2 F^2 A \Gamma_T v}{4RT} \qquad (ii)$$

and

$$\theta = \frac{nF}{RT}(E - E^{\circ\prime}_{surf}) \qquad (iii)$$

$\Gamma_T$ is the total electroactive coverage i.e. the sum of $\Gamma_O$ and $\Gamma_R$. In a reversible reaction, there is proportionality between $i_p$ and potential sweep rate v, the wave shapes and peak potentials for the cathodic and anodic surface waves are identical ($\Delta E_p = 0$) and $E_{FWHM} = 90.6/n$ mV

Electrodes with an immobilised monolayer regularly exhibit a proportionality between $i_p$ and v. It therefore follows that for these electrodes the charge under the current - potential or current - time curve will give the total quantity $\Gamma_T$ (mol $cm^{-2}$) of attached electroactive sites, which is not dependant on v. Charge and $\Gamma_T$ measurements which use a simple current baseline assume that any dispersion in double-layer capacitance current

which may accompany alterations in surface ionic charge caused by oxidation or reduction is insignificant.

For rapid kinetics in the electron transfer reaction (1), $\Delta E_P$ should equal zero at any scan rate v. If, however, the electron transfer is slow, a non-zero $\Delta E_P$ (dependant on potential scan rate) is expected and a change in waveshape will be observed. For monolayers $\Delta E_P$ is normally small (<20mV) but is rarely zero. This could be due to interfacial solvation being asymmetric with respect to the oxidised and reduced species.

Many monolayer electrodes have symmetrical waveshapes about $E_P$ and cathodic and anodic peaks which are almost mirror images but $E_{FWHM}$ and waveshape normally differ from equation (i). Possible reasons for the broadening of the voltammetric peaks are that (a), due to surface structure variations, $E^{\circ\prime}_{surf}$ values are not unique but exist as a narrow range with a mean of $E^{\circ\prime}_{surf}$[7,9,10] and (b) because surface coverage is not perfect. Brown and Anson[11] proposed an equation linking surface activity coefficients with "interaction parameters" $r_O$ and $r_R$ :

$$i = \frac{-4i_P \exp(P)}{[1+\exp(P)]^2-(r_O+r_R)\exp(P)} \qquad \text{(iv)}$$

where

$$P=\theta+(r_O+r_R)\Gamma_O-rR\Gamma_T \qquad \text{(v)}$$

$r_O$ and $r_R$ are normally equal ($r_O=r_R\equiv 2r$). If r is negative then broadening of the waveshape is produced.

Equation (iv) fits experimental waveshapes well for monolayers with discrepancies on the edges possibly due to the $E^{\circ\prime}_{surf}$ value not being unique.[12] $r\Gamma_T$ can be more characteristic of a specific surface species than r since $E_{FWHM}$ does not vary systematically with $\Gamma_T$. $E_{FWHM}$ seems to be independent of $\Gamma_T$.[13]
From fig. 3 it can be seen that $E_{FWHM}$ varies linearly with $r\Gamma_T$.

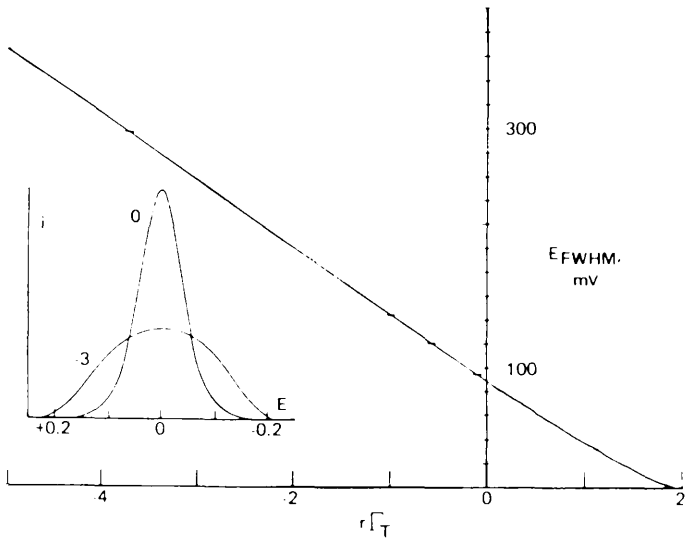


Fig. 3. Graph of $E_{FWHM}$ vs. $r\Gamma_T$ where $r_O=r_R=2r$.

In polymeric or multimolecular films, as would be expected, the variety of mechanisms is greater and more complex. Considerations to be included are (a) electron movement mechanisms where the redox sites are immobile or remote from the electrode, (b) internal movement of the

polymer, and (c) the added complication of solvent and counterions.

In most films, electrochemical charge transport by electrons is thought to be due to electron hopping.[14] This occurs by electron exchange between neighbouring oxidised and reduced sites. To calculate the rate of diffusion a charge transport diffusion coefficient ($D_{ct}$) is introduced.[15] The concentration of fixed oxidised ($c_O$) and reduced ($c_R$) sites depend on the term $D_{ct}\ \tau/d^2$ where $\tau$ is the experimental time-scale and d is the film thickness.

When $D_{ct}\ \tau/d^2 >> 1$, all electroactive sites are in equilibrium with the electrode potential(in a reversible reaction). The voltammetric behaviour is like a monolayer type electrode system. (see fig. 4A)

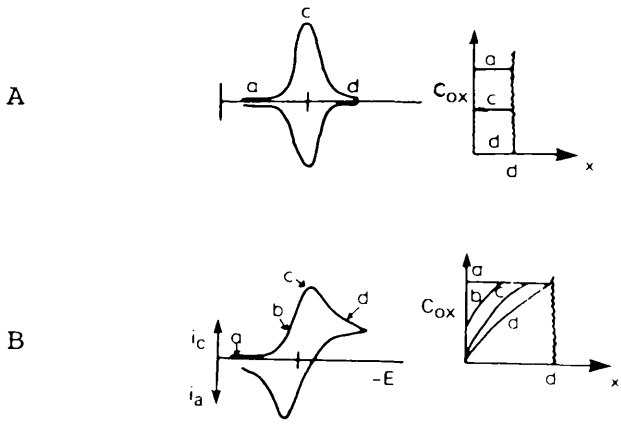


Fig. 4 Schematic reversible cyclic voltammogram and concentration-distance plot for oxidised sites (during negative sweep) for a redox polymer film.

If $D_{ct}\ \tau/d^2 << 1$, a negative potential scan is completed before the sites at the surface are reduced i.e. a semi-infinite electrochemical charge diffusion condition prevails. The current at c is then proportional to $v^{½}$ and given by the equation:

$$i_p = 2.69 \times 10^5 n^{3/2} A D_{ct}^{½} v^{½} c_O \qquad \text{(vi)}$$

The waveform looks like that in fig. 4B. This "diffusion tail" is exaggerated by small $D_{ct}$ (low temperature), polymer film cross linking, fast potential scan rates and thick films.

From fig. 4 it can be seen that the equilibrium condition ($i_p$ proportional to v) has to be achieved so that the charge under the voltammetric peak represents the electroactive coverage $\Gamma_T$.

As in monomolecular layers, the voltammetric waveshapes of multimolecular layers are contributed to by interaction or activity effects and multiple $E^{\circ\prime}_{surf}$ values. This principle has been digitally simulated by Peerce and Bard[16] using a "square reaction scheme" to represent the interconversions.

With relatively thick multimolecular layer films that are poorly swollen by solvent or have sites within them that interact strongly with the electrolyte ions,[17,18,19]

interaction-activity effects can apparently become attractive (e.g. r is positive) meaning that $E_{FWHM}$ is small. Because the solvent and therefore the electrolyte ions can not permeate the polymer to aid in the stability of the oxidised↔reduced site electron transfer, the polymer has an effective ohmic resistance which has to be overcome to allow the oxidation or reduction to occur. This causes the reduction peak and oxidation peak to shift causing an unsymmetrical C.V. "wave". The peaks can separate by 0.2V but the separation depends on the polymer thickness. The peaks also become like current spikes. This "spiking" can be lessened if the scan rate is reduced thus allowing more time for the electrolyte to permeate. The spiking is also related to the solvent used. Acetonitrile will permeate well causing standard C.V. peaks whereas water will cause very sharp peaks. A water/ethanol mixture will cause peaks inbetween.

The physical meaning at the limit of attractive interactions is a kind of phase formation in which the activities $a_O$ and/or $a_R$ become independent of $\Gamma_O$ and $\Gamma_R$ respectively. This has been referred to as a "phaselike" condition.[17]

## Covalent Binding to Metal Oxide Electrode Surfaces

### Immobilisation Chemistry based on Organosilane

One of the first methods of modifying an electrode surface was to use a metal oxide surface. There are several examples of this type of electrode but the most commonly used is $SnO_2$. This also has the added advantage of being transparent so that optical spectroscopy (e.g. UV/vis and circular dichroism) can be performed on the produced layer(s). $SnO_2$ is a wide-bandgap semiconductor which is readily doped to near-degenerate levels. It is obtained commercially as a thin film (~1000-5000 Å thick) coated on glass or quartz.

$SnO_2$, like silica, has many -OH sites on the surface. These are highly reactive towards chlorosilanes and alkoxysilanes[20,21] under anhydrous conditions (see reaction 5).

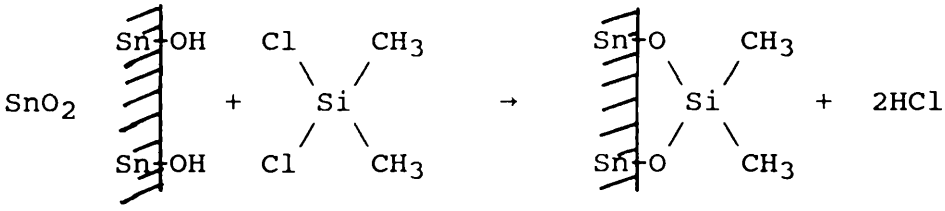


(5)

In this reaction the electrode has a decrease in double-layer capacitance due to the replacement of polar surface hydroxyl groups by methyl groups. This decrease is, however, not as great as would be expected thus indicating that only a small percentage of the hydroxyl sites have been converted.[22]

Other metal oxide electrodes also react with chlorosilanes and alkoxysilanes. These include $RuO_2$,[23] Pt/PtO,[24] Au/AuO,[25] $TiO_2$,[26] GeO,[27] GaAs[28] and Si/SiO.[29] These oxide electrodes can be prepared using a variety of methods. $RuO_2$ is prepared by painting a solution of $RuCl_3$ onto a base titanium electrode.[30] $TiO_2$, being a semiconductor like $SnO_2$, can be coated onto a titanium metal electrode or, if grown as a single crystal,[31] can be used without a support. Pt/PtO, Au/AuO, Si/SiO and Ge/GeO are elemental electrodes, treated in a way in which will induce several layers of oxide on the surface, thus producing a good conducting electrode with the appropriate functionality at the surface. All these electrodes can be reacted with organosilanes as in reaction (5). The M/MO nomenclature in no way assumes the metal oxide exists in that form. The theory is complex and differs from oxide to oxide. It can also vary from the pre-silanized oxide to the post-silanized form.

Reaction (5) is a simplistic example and does not produce an interesting electrode system. Much chemistry has been

done on more complex molecules. They tend to be synthesised so that once the appropriate functionality is present, a chlorosilyl derivative is attached and the functionality can be attached to the oxide electrode. The most useful organosilanes are either already electroactive or contain secondary reaction coupling functionalities i.e. functional groups that can be reacted with other atoms/molecules which are electroactive. Attempts to use the functional groups as ligands for metal ions has proved difficult with concurrent adsorption of the ions onto the unreacted surface oxide c.f. the limited reaction of $SnO_2$ with $SiCl_2Me_2$. Further reactions with the functional groups can be done to produce complex pendant chains of varying length (several atoms up to polymer chains).

Organosilanes can also be electrochemically reacted with a Pt surface[32] since chlorosilanes can be reduced in acetonitrile to produce $R_3Si^{\bullet}$ as a radical intermediate. From XPS data the surface would seem to contain $Pt\text{-}O\text{-}SiR_3$ species.

Electrochemical Reactions of Reagents Immobilized on Silanized Metal Oxides.

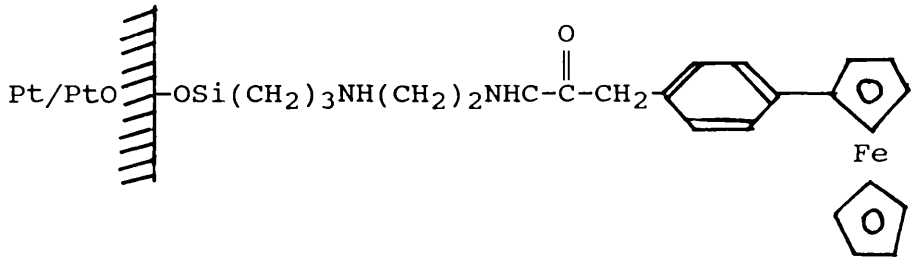


(I)

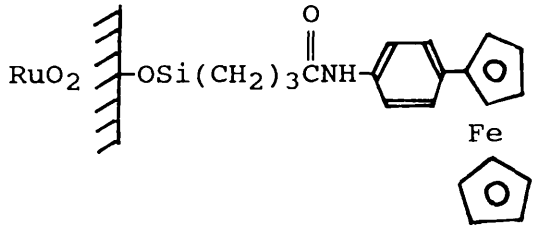


(II)

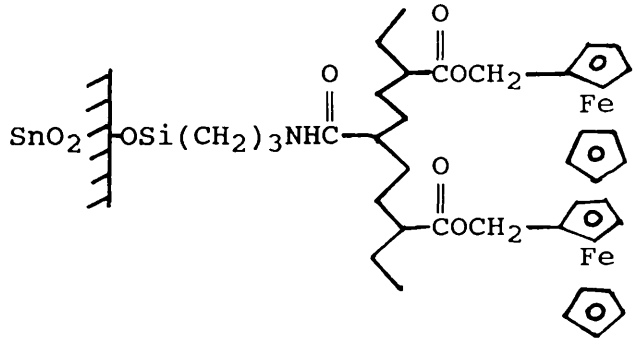


(III)

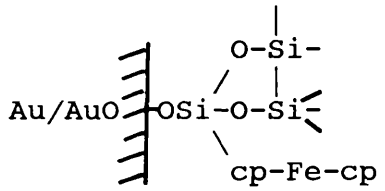


(IV)

The C.V. of (I)[33] has only one significant current peak at +0.44 V vs. SSCE. This is almost identical to that of ethyl-4-(ferrocenyl)phenyl acetate (+0.43V) so the current peak can be assumed to be the reaction: ferrocene ↔ ferrocenium. The current peak is not observed

if $(CH_3O)_3Si(CH_2)_3NH(CH_2)_2NH_2$ is omitted or if the ferrocene used lacks a carboxylic acid group. This verifies the theorised structure of (I). The peak remains after washing with solvent thus indicating the fixed nature of the functionalities.

The C.V. of (II)[10] is almost identical to that of (I) except the background current is higher. The reason for this is not known and is contrary to the coverage of ferrocene on $RuO_2$ being higher than on Pt/PtO.

(III),[34] having more than one ferrocene per silanized surface site, produces a strong current peak in the C.V. relative to background current. It is stable to multiple electrochemical cycling between ferrocene and ferrocenium.

As in the above three cases, (IV)[25] also has a one electron oxidation/reduction about the same potential as the ferrocene↔ferrocenium couple of the isolated ferrocene derivative. All four electrode systems have quite different structures but in effect are electrochemically similar.

This not only holds for ferrocene. Murray et. al.[13] fixed Ruthenium complexes to a Pt/PtO electrode using two different methods. Firstly using a condensation reaction as above and secondly by attaching a silyl molecule to the surface which has a functional group that can be used

as a transition metal ligand. This ligand once fixed to the electrode surface can be reacted with an appropriate Ruthenium complex so that after the ligand has bound to the Ruthenium, the Ruthenium is bound to the electrode. In both these cases, although the chemistry is quite different, the electrochemical properties are very similar.

The first reported case of this surface ligand displacement was by Burt et. al.[35] who displaced a t-$BuS^-$ thiolate ligand from the cluster $[Fe_4S_4(tBuS)_4]^{2-}$ using a $SnO_2$ electrode silanized with $(CH_3O)_3Si(CH_2)_3SH$.

In most (if not all) cases, the formal potential of reversibly reactive non-complex surface immobilized molecules is similar to their solution-dissolved analogues.[23] From this it can be assumed that the bonding of a molecule to a substrate electrode does not alter its oxidised or reduced electronic structure. In electrocatalysis and photoelectrocatalysis, knowing the surface reaction potential is critical. Here we have a method of coating an electrode with a substance of known thermodynamic electron free-energy levels.

The ability of a modified electrode to be used for electrocatalysis, photoelectrocatalysis or other electrochemical systems is dependant on the stability of the electrode towards continuous cycling. If the linkage(s) between the electrode and redox site are

broken causing the electroactive constituent to be dissolved into solution then the electrode loses its required properties. This can be caused by the solvent used or by the electrochemical reaction conditions and can occur at different rates.

Although covalent attachment gives greater stability than chemisorbed or polymer deposited electrodes towards solvent stability, the oxidised states are less stable compared with the corresponding un-immobilised species. In particular, the radical anions of nitro-aromatics immobilised on $RuO_2$ and Pt/PtO[23,24] seem less stable than expected from solution chemistry. This is more severe when bonded to $SnO_2$, even in aprotic solvents.[36] Reasons for this are not certain, but water and proximity to a metal oxide site seems to be involved in the degradation.

There is also the possibility of decomposition via secondary reactions. Since the concentration of molecules on the electrode surface is relatively high, the possibility exists of other processes occurring such as dimerisation and disproportionation. The high concentration can however have the opposite effect with reaction between constrained molecules being slower than expected from the free molecule reaction data.

An example of this is shown in reaction (6).[37]

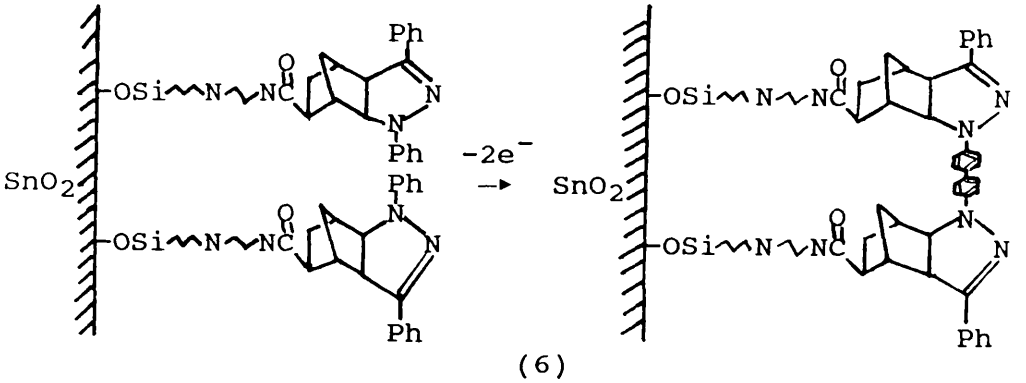

(6)

In this case the reaction rate is less than that for the analogous solution reaction.

In the case of (I),[33] it was found that as with ferrocene, the electrode coating was almost indefinitely stable while in contact with solvents. The slow decay of the surface wave was due to the time spent as the ferrocenium ion and not due to the conversions from ferrocene to ferrocenium. Therefore its use as an electrocatalyst is possible if the scan rate is made large and so the time spent as the ferrocenium ion is kept as short as possible.

How the silanized surface can be pictured is quite complex as there are many possibilities. i.e.

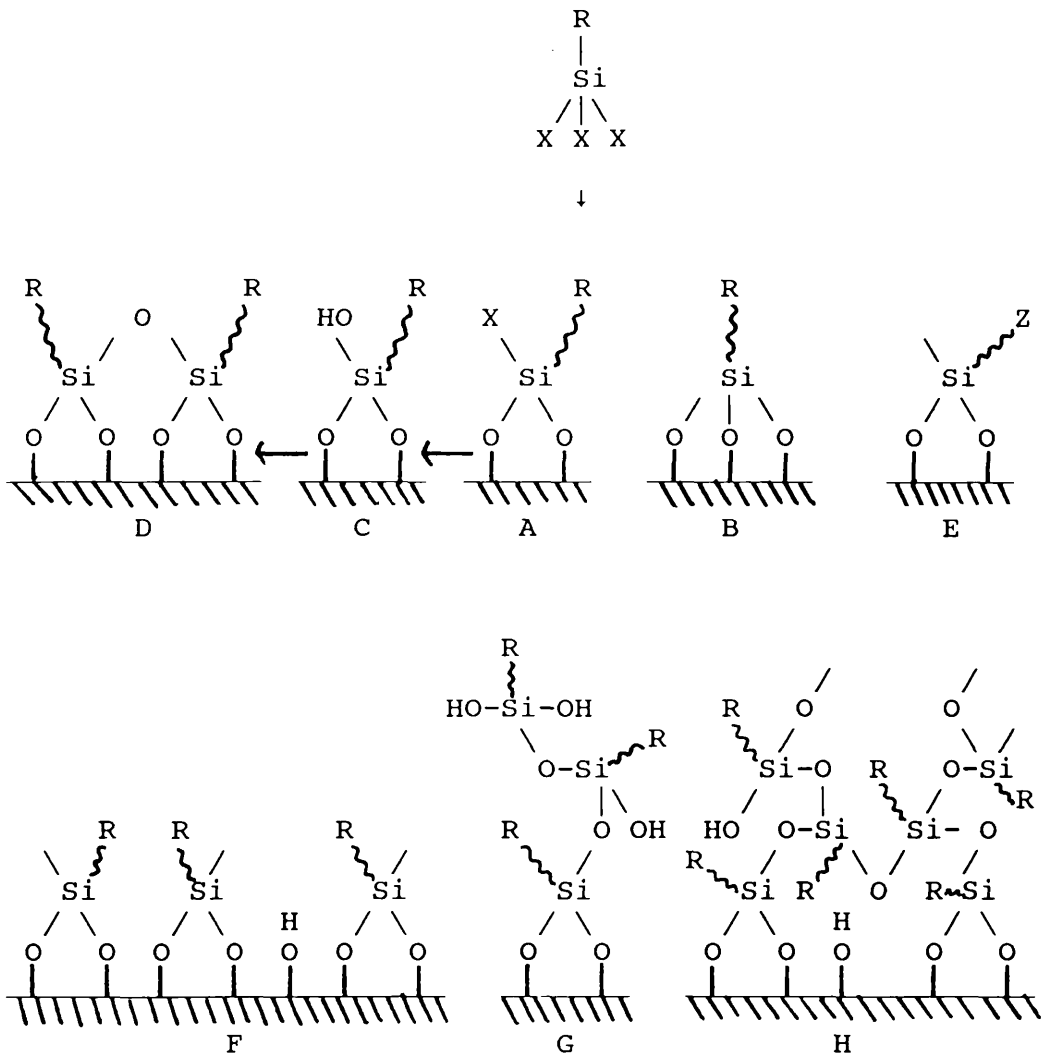


Fig. 5. Schematic structures at a silanized surface.

Aspects to be considered are:-

1. How many surface M-O-Si bonds are formed? (A vs. B)

2. Is the functional part of the organosilane reagent intact and fully reactive? (A vs. E)

3. What is the surface density, or coverage, of the bonded organosilanes? (how many -R groups in F?)

4. Is the surface structurally heterogeneous? (more than one surface structure present)

5. What is the average conformation and dynamic mobility of the organosilane chains?

6. Are siloxane polymer groups present, uniformly or in patches, and are they long or short or cross linked chains? (G and H)

Understanding the complexities of surface coverage is quite difficult with nonuniformity across the silanized surface possibly causing nonuniform electrochemical behaviour of immobilised sites. In the case of electrocatalysis this, however, would not be of significant importance.

Work has also been done on other methods of bonding to metal oxide electrodes. This can be done using ester bond linkages,[38] cyanuric chloride[39] and basic chromium complexes.[40] An appropriate example of the ester linkage was done by Anderson et al.[38] reacting $TiO_2$ with $Ru(bipy)_2(4,4'\text{-di(carbonylchloride)-}2,2'\text{-bipyridine})^{2+}$.

The proposed attachment is via two

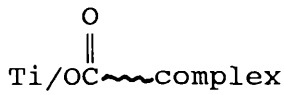

bonds. This led to apparent photosensitisation of the $TiO_2$ semiconductor. These linkages have proved to work but are not as successful as the silanized electrode surfaces. Surface coverage and stability are less and the complexity of the system is greater.

## Attachment to Carbon Electrodes

### Chemical Nature of Carbon Surfaces

Carbon electrodes are well suited for modification by covalently attached groups. To understand this it is necessary to explain the basal plane-edge structure of carbon. The structure of graphite is as shown in fig. 6. An infinite basal plane is nonionic, of low polarity, hydrophobic and rich in pi-electron density. It lacks functionality but due to high pi-electron density is a good conductor. Functionality does, however, occur at the edge of a basal plane and if these functionalities are unsaturated then this gives rise to strong electroactive sites.

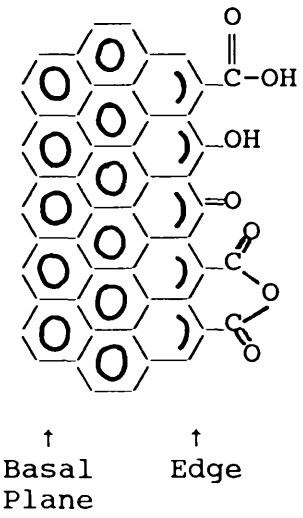


Fig. 6. Schematic representation of chemical functionalities at edge plane of pyrolytic graphite.

Chemical functionalities abound on the edges of the graphite planes and any cleavage process, whether chemical or mechanical, creates reactive edge plane dangling valencies which usually react with oxygen and water to become stable. Although the ratio of basal to edge plane surfaces is unknown, it is thought that the edge planes account for the reactivity.[41] For sites that have been generated by oxidative treatment (thermal or chemical), the sites produced are thought to include phenolic, quinone, carboxylic, lactone and other ketonic functions (see fig. 6). As such graphite electrodes are ideal for modification processes via these reactive sites. Edge planes are also polar and therefore hydrophilic and so contain ionic sites which cause the double-layer capacitance of the edge plane to be larger than that of the basal surface.[42]

Carbon can be obtained in many different forms:-

1. Graphite single crystals.
2. Pyrolytic graphite.
3. Highly orientated pyrolytic graphite (HOPG).
4. Glassy (vitreous) carbon.
5. Compacted polycrystalline structures of varying porosity (such as high density spectroscopic rods).
6. Powders.
7. Whiskers.
8. Fibres.
9. Yarns.

10. Cloth.

etc.

With each of these groups, there are a variety of different shapes, grades and degrees of irreproducibility from sample to sample associated with different manufacturers and the method by which they make them. The most commonly used (so far) for electrode modification processes are pyrolytic graphite (a highly imperfect graphite equivalent to single crystal graphite with a basal edge plane surface) and glassy carbon (a random tangle of graphite strips consequently exhibiting a mixture of basal and edge plane characteristics). As stated before, the reproducibility from one sample to another can differ greatly due to production methods and also pre-treatment steps e.g. mechanical polishing of the basal plane of pyrolytic graphite will expose edge plane sites as will polishing of edge plane surfaces expose some basal plane areas if structural folding occurs. Consequently, the density of attached sites to a carbon electrode will vary over the whole surface.

In order to enhance the carboxylic acid and hydroxylic groups on a carbon electrode, several pretreatment processes have been used: heating in air at 400-500°C, treatment in a radio frequency (RF) $O_2$ plasma,[43] and simply polishing in air.

Reaction of Carboxylic and other Ketonic Groups on Carbon

Analogies can be drawn between carbon surface carboxylic acid groups and their solution analogues. Therefore in order to couple a dissolved amine or alcohol to the surface requires a reactive intermediate to be formed. Three such reactions are:[6]

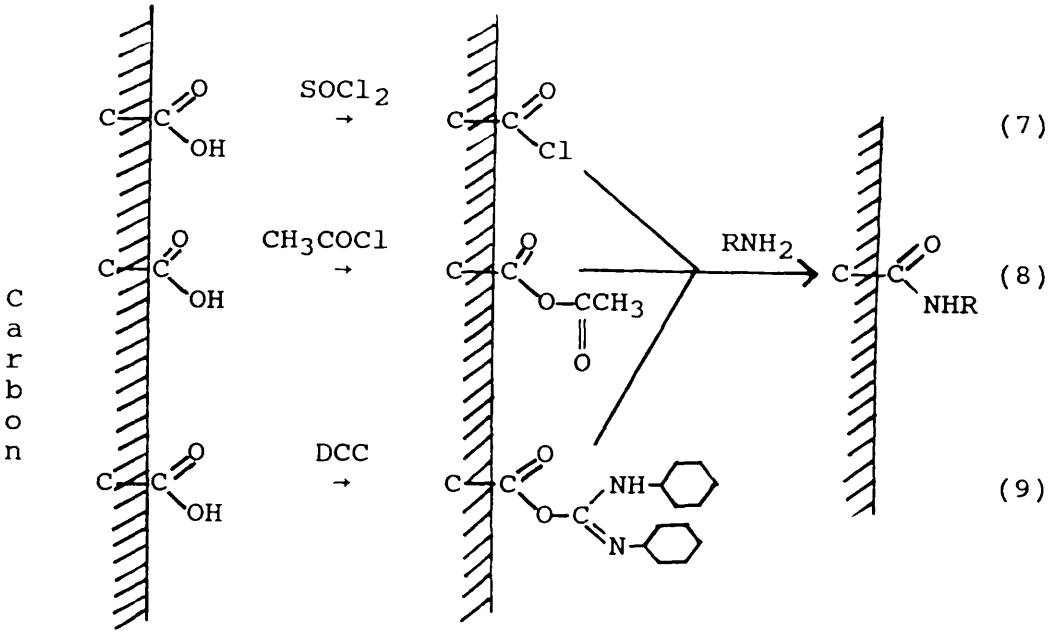


Problems with this methodology have occurred. Thionyl chloride adsorbs on carbon but since it is an oxidant it is necessary to wash the surface. This, however, causes loss of acid chloride sites so the next step of amide coupling occurs in very small yields. Washing should be kept to a minimum.

Reactions (8) and (9), using substances other than thionyl chloride, by-pass this problem but have other

drawbacks. Reaction (8) has the problem of dissolved acetamides being produced rather than surface amides and reaction (9), although occurring with mild conditions, introduces steric effects and therefore causes low conversion to the surface amide.

Another problem is that although the reactions above are analogous to their solution counterparts, they occur at a much slower rate and as such require heating and longer reaction times.

An early example of a chiral electrode[6] (1975) was based on a carbon electrode. A spectroscopic carbon rod was thermally oxidised, thionyl chloride activated and reacted with S(-)phenylalanine methyl ester.

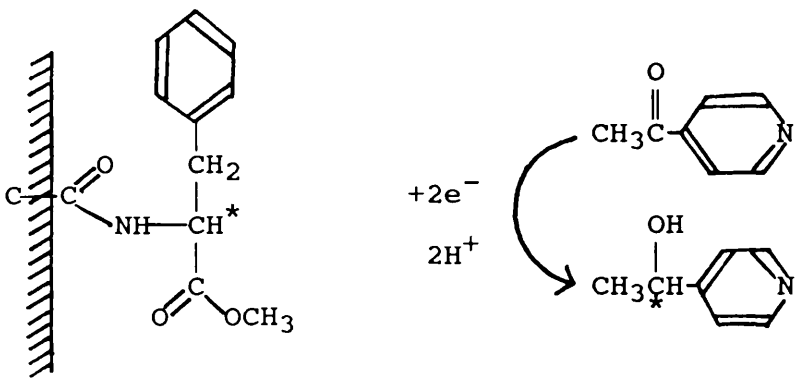


(10)

This electrode was used to reductively electrolyse a solution of 4-acetylpyridine (see reaction (10)), an enantiomeric excess of 10% being recorded. The sign of

this excess changed when R(+)phenylalanine methyl ester was bound to a carbon electrode.

Proof that the above reaction was not just due to adsorption but to actual bonding was provided by the following experiments using highly oriented pyrolytic graphite (HOPG). When the reaction was carried out using the "modified" basal plane surface, no enantiomeric excess was recorded whereas when the modified edge plane electrode was used, an enantiomeric excess was observed.

The first covalent attachment to a carbon electrode of a reversibly electroactive redox substance was of the tetra(aminophenyl)porphyrins,[9] $(m\text{-}NH_2)_4TPP$ and $(p\text{-}NH_2)_4TPP$. These were attached to a glassy carbon electrode pretreated by thermal oxidation and then thionyl chloride.

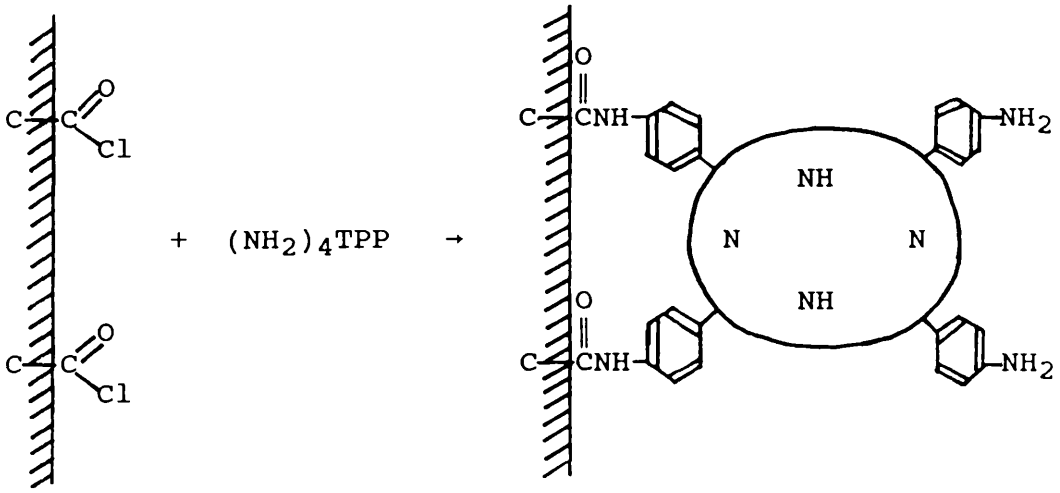

where

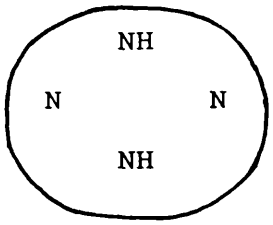


≡

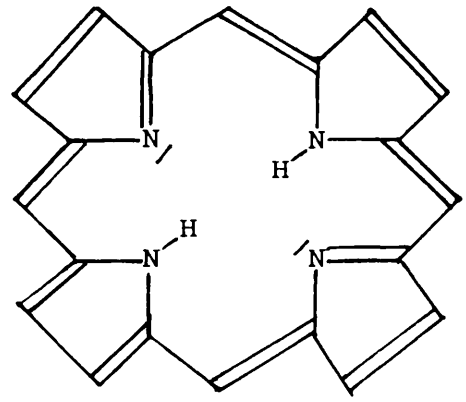


(11)

If there is residual thionyl chloride then this can react with the free amine of the porphyrin to produce multilayer coverage (2-10 layers).[44] In well rinsed electrodes, multilayering does not occur.[45] Reactions have been done to prove that the majority of the porphyrin is bonded via two acid sites.[9]

When reaction (11) is carried out on glassy carbon electrodes, the C.V.'s produced have two reversible reductions corresponding to the radical anion and dianion formation. These waves occur at potentials close to those observed for the solution analogues.

Transition metals can be inserted into the porphyrin system either before[44] or after[9] attachment to the carbon surface. The reduction potentials are again similar to the solution analogues and with a series of reduced porphyrin donor sites, electron transfer mediation is possible. Electrocatalysis has been done with metallated

porphyrin coated carbon electrodes but the electrode stability was not impressive.

By manipulating the axial chemistry of the porphyrin, a greater degree of control might be introduced to electrocatalytic reactivity towards dissolved substrates. For the cobalt-metallated $(NH_2)_4TPP(py)_2$ complex on carbon, as an electron is added, a pyridine is lost.[46] In most other similar complexes, however, retardation is introduced with the loss of a ligand, X, where X has been theorised to be carboxylic acid groups present on the carbon surface.

Ruthenium complexes (discussed more fully later) have been immobilised on carbon using the following reactions:[47,48]

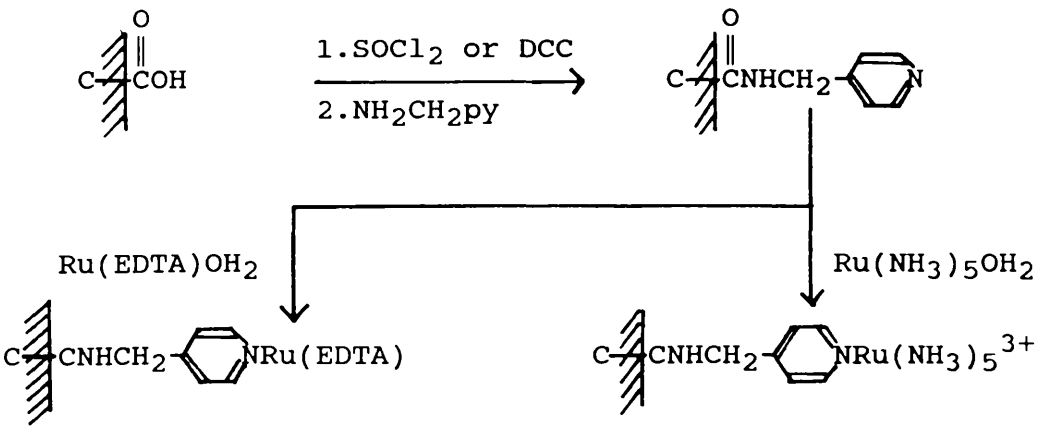


(12)

While cycling the above electrode systems electrochemically between Ru(II) and Ru(III), a decay

occurred which followed a first-order rate law. The half life was 1080 min for the $Ru(NH_3)_5OH_2$ case. The electrode could, however, be rejuvenated almost entirely by re-exposure to a fresh solution of the appropriate Ruthenium complex. This seems to indicate that the cycling causes a cleavage of the Ru-py bond. From work done on the solution analogues, the complexes are less stable with respect to ligand dissociation in the Ru(III) state.[49]

One of the first attempts to use a modified electrode for electrocatalysis was done using a benzidine modified carbon electrode:[50]

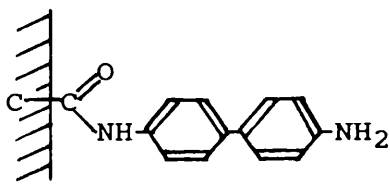


(V)

Two electron oxidation to the diimine was observed, but the oxidised form soon decayed to show a more stable daughter wave at $E_{p,a}$=+0.28V vs. Ag/AgCl. It was suggested that the structure was as follows:

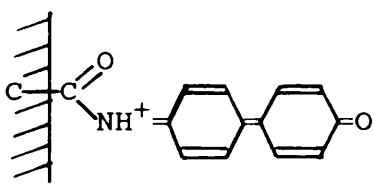


(VI)

and occurred by hydrolysis. This system was effective in the electrocatalytical oxidation of ascorbic acid.

Due to insufficient stereoselectivity in electrode reactions, electro-organic synthesis has not been very successful. Using cyclodextrins (cyclic 1,4-linked D-glucopyranose oligomers),however, greater control over stereoselectivity has been achieved since the electroactive site is totally enclosed. In aqueous solution, many organic compounds are associated or partitioned into the cavity of the cyclodextrin. These are called inclusion complexes and exhibit dissociation constants corresponding to the "guest" molecule and the accommodating cyclodextrin. An example of a good "host" and "guest" pair are α-cyclodextrin (which contains six glucose units) and benzene respectively.

An example of this selectivity was shown by Osa et al..[51,52,53] Anodic chlorination of anisole can produce either para or ortho monochlorinated product but if the benzene of the anisole is within the cyclodextrin then chlorination at the ortho position is hindered by the walls of the "host" molecule. (see reaction (13))

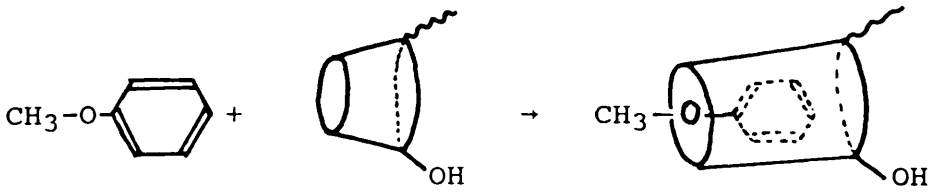


(13)

The chlorination is carried out by oxidising $Cl^-$ to chlorine (at the anode) which hydrolyses to produce HOCl and HCl. The HOCl chlorinates the benzene. Although it is not a perfect reaction, the para/ortho ration = ~20:1 , the selectivity being greater than for chiral electrode systems!

Another use of cyclodextrins is to selectively oxidise or reduce a specific isomer due to one isomers greater ability to complex with the cyclodextrin although reported cases show greater selectivity for free cyclodextrins compared with cyclodextrins directly bonded to carbon.[53]

Reactions of Hydroxylic Groups on Carbon Surfaces.

It is possible to modify a carbon surface using the hydroxylic groups reacted with organosilanes and cyanuric chloride. The reaction of a carbon surface with cyanuric chloride is as follows:[54]

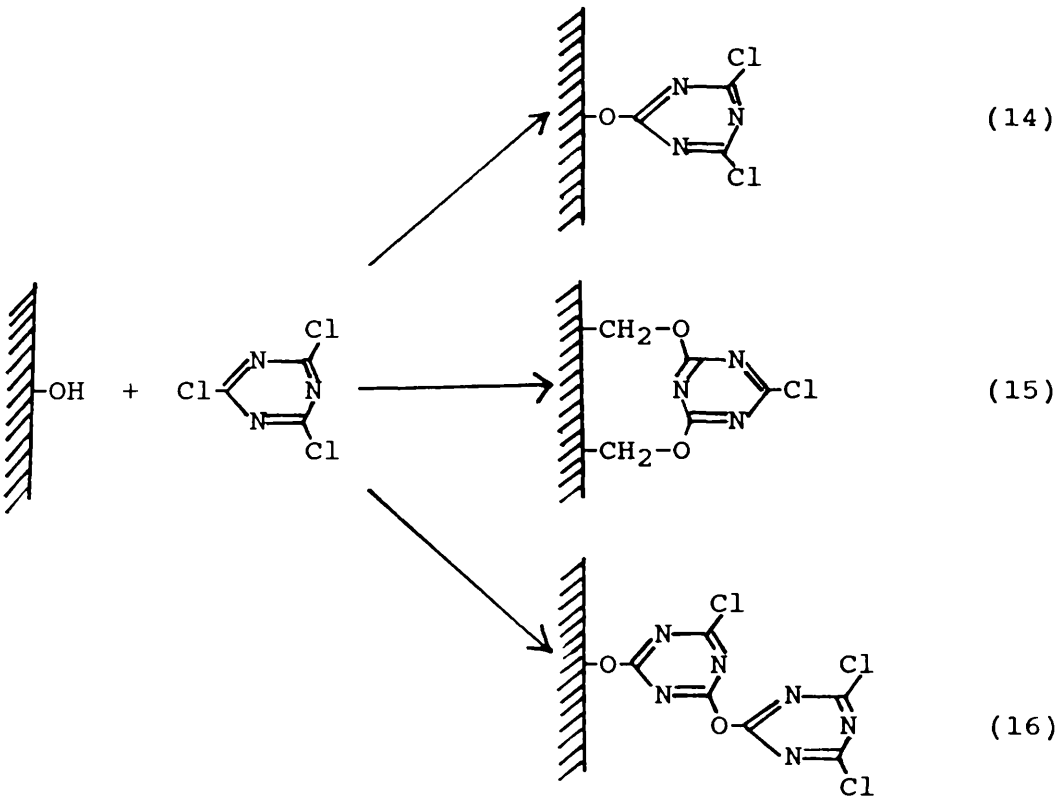


Unless the reacted electrode is deliberately exposed to water vapour, reaction (16) does not occur. Normal results are consistent with monolayer or submonolayer

coverage. Distinguishing between the products of reactions (14) and (15), however, is difficult.

Cyanuric chloride, immobilised on carbon, is reactive towards amines, alcohols, Grignard reagents and hydrazines.[55] Attached species again have reduction/oxidation potentials close to the solution analogues.

Cyanuric chloride can also be used to activate metal oxide electrodes but to a much lesser extent.[54]

Organosilanes, although used on metal oxide electrodes, do not give any appreciable electronic functionality on carbon even though initial XPS data seemed to give encouraging results.[56]

"Oxide-Free" Carbon

Freshly exposed basal plane edge reacts with dioxygen resulting in oxygen containing surface functionalities.[57] From this it was predicted that carbon could be bonded directly to olefins via a cycloaddition reaction.

Carbon fibre (high specific surface area of 240 $m^2g^{-1}$) was heated in vacuo, cooled and exposed to several olefinic compounds.[57] These compounds (methyl acrylate, acrylyl chloride and allene) were adsorbed to the extent

of 0.83, 0.72 and 0.63 mmol $g^{-1}$ respectively. This compares with 0.62 mmol $g^{-1}$ coverage for $O_2$ which seems to indicate that all sites that could react with oxygen are reacting with the olefins. Some olefins, however, (e.g. cyclopentadiene) adsorb less (0.35 mmol $g^{-1}$) and the remaining sites are still capable of bonding to oxygen.

Omaya et al.[58] came up with another method of making oxide free carbon. Analogous to oxidation in an oxygen plasma, oxide free carbon is produced by exposure to an argon plasma and the resulting electrode surface reacted with amine reagent gases. This was then coupled with nicotinic acid and then reacted with a solution of $[Ru(NH_3)_5OH_2]^{3+}$ using cyclic voltammetry. A peak at +0.13V vs. SSCE resulted due to substitution of the $H_2O$ by pyridine. The following structure resulted:

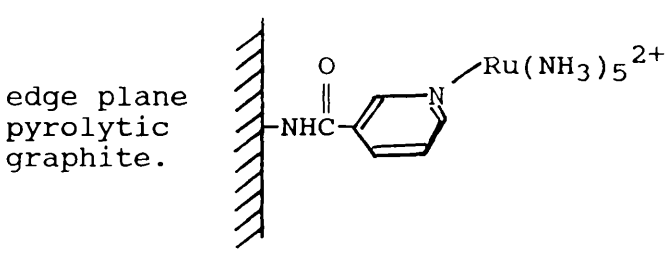


(VII)

Cyclic voltammetry gave the expected potential compared with the analogous complex $[Ru(NH_3)_5(nic)]^{2+}$.

A similar system was reacted with $[Ru(EDTA)(OH_2)]^{3+}$ to produce the following structure:[59]

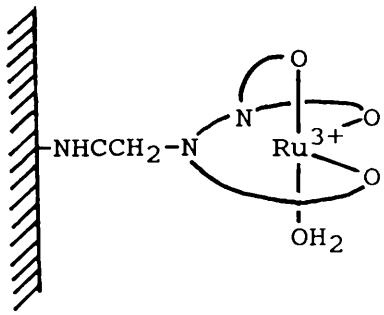


(VIII)

This system was analogous to the solution analogue in that ligand displacement of the water was possible in the presence of base such as pyridine and nicotinamide. This means that when the electrode is reduced in the presence of base, the C.V. changes to that of the base-ligand substituted complex.

Another method of binding directly to carbon is to mechanically abrase or fracture a carbon electrode in an inert atmosphere thus exposing oxide-free carbon.[60] If this is also carried out in a "puddle" of e.g. vinyl pyridine then the "pyridine carbon surface" is produced. This can be reacted with complexes such as $[Ru(bipy)_2Cl(iso\text{-}nic)]^{2+}$ to produce ruthenium bound species similar to those above.

Carbon Paste Electrodes

Carbon paste electrodes do not fit in with the theory as described above for carbon electrodes or metal oxide electrodes. Carbon paste electrodes are produced by mixing a solid sample of the electroactive species with carbon powder and nujol.[61] These electrodes are then used in the usual way. The electroactive species becomes, "in some unexplainable way", transported/transferred to the carbon powder-solvent interface. There it exhibits stable characteristic electroactivity which can be regenerated by removing the top layer of the electrode.

## Polymer Films on Electrodes

### Introduction

In the past, polymer films on electrodes have been used for analytical purposes.[62,63] Present day work, however, differs in that the polymers now contain electrochemically and/or chemically reactive centres. This is similar to the processes undergone in the monolayer electrode system but since the polymer contains the equivalent of many monolayers worth of electroactive sites, the electrochemical response is much greater and therefore more easily observed. A polymer can contain the equivalent of from <1 to >20,000 monolayers which means the concentration of electroactive sites in the polymer can range from 0.1 to 5 mol $l^{-1}$.

Electroactive polymers can be produced in many ways. Some are bonded via functional groups to the electrode surface in a method similar to those used in the graphite and non-metal oxide monolayer systems. Others are bonded via a poorly understood combination of adsorptive attraction to the electrode and a poor solubility in the working solvent.

The polymers can be divided into two types, redox polymers and ion exchange polymers. Redox polymers contain the electroactive site as part of the polymer

chain backbone or have it bonded after the polymer is applied to the electrode. Ion exchange polymers rely on drawing ionic redox substances from their solutions into the films as counterions having favourable ion exchange partition coefficients. This process is called "electrostatic binding".[64]

The polymers can be further sub-divided into polymers that are polymerised directly onto the electrode or ones that are applied to the electrode after polymerisation.

The different methods of making polymer modified electrodes are as follows:-

(i) Dip Coating.

This is done by exposing the electrode to a solution of the polymer, during which time a film is adsorbed on the surface.[65] The polymer may contain the redox moiety[66] or it may be bonded later via amide links[67] or metal complex formation.[68]

(ii) Droplet Evaporation.

This is done by spreading and evaporating a few microlitres of a dilute solution of a polymer.[17,64] Films produced by this method can be rough unless the evaporation is slow.[69] Even films can be produced by rotating the electrode.[70,71]

(iii) Oxidative or Reductive Deposition.

Polymer solubility can depend on its redox state. By reducing or oxidising a specific polymer, it can be converted to a less soluble and more adsorbable state thus coating the electrode.[34,72]

(iv) Spin Coating.

A solution of a polymer is dropped on a spinning electrode and allowed to air dry.[14] This is then swabbed dry. For pinhole-free films, many layers are required.

(v) Binding a monolayer of polymer.

e.g. A sylanised metal oxide surface reacted with poly(acryloyl chloride) then with hydroxymethyl-ferrocene.[34]

(vi) Electrochemical Polymerisation.

A solution of monomer is oxidised[73] or reduced[4,74] to produce intermediates (e.g. radicals) which polymerise rapidly to form a film on the electrode. This method does not produce pinholes as these sites react more rapidly than the polymer coated sites thus "filling in the gaps".[75] For coating to continue further, the polymer itself must be redox active and capable of oxidising or reducing fresh monomer. Otherwise, electrode passivation occurs and film growth is halted.

(vii) Organosilanes.

Organosilane monomers can be polymerised under dip coating or droplet evaporation to produce polymers bound to the electrode as well as cross-linked (-Si-O-Si-).

(viii) RF Plasma Polymerisation.

Polymer is produced by exposing monomer to a radio-frequency plasma discharge.[76] On exposing to air, however, plasma films typically take up oxygen and behave differently to conventionally polymerised systems.

Properties of Redox Polymer Electrodes

For a polymer to be electroactive, it must have ionic conductivity. This can occur by electrolyte ions penetrating the film through pores or the film must contain many fixed charged sites plus mobile counterions. This ionic conductivity is needed so that a potential applied to the electrode can produce a potential gradient at the electrode-polymer interface. This will drive electron transfer between the electrode and adjacent redox centres in the polymer. In many polymers, solvent penetration into the polymer causes "swelling". This will aid ionic mobility and therefore conductivity.

Related to ionic conductivity is the permeability of the polymer film to electroactive constituents of the

solution. These may react in several different ways. Oxidised or reduced constituents of the polymer can act as electron transfer mediators and as such can act as catalytic sites (electrocatalysis). With a larger number of sites compared to a monolayer functionalised electrode, polymer electrodes have the potential to be better catalysts. This, however, depends on the ability of the substrate in solution to penetrate the polymer and encounter the properly oxidised or reduced catalyst site.[17,77]

If the polymer redox sites do not act as electron transfer mediator catalysts, then the solution constituents must permeate the polymer to the electrode surface via pinholes or channels in the film. This can occur freely[17,78] or be totally inhibited[17,79] due to the steric bulk of the substrate and the thickness and solvent swelling of the polymer.

If the polymer is highly conducting, then electron transfer can occur at the film-solution interface.[80,81]

Charge transport within an electroactive polymer occurs (as described before) by a succession of electron transfer self-exchange reactions between neighbouring oxidised and reduced sites (see fig. 7).[5]

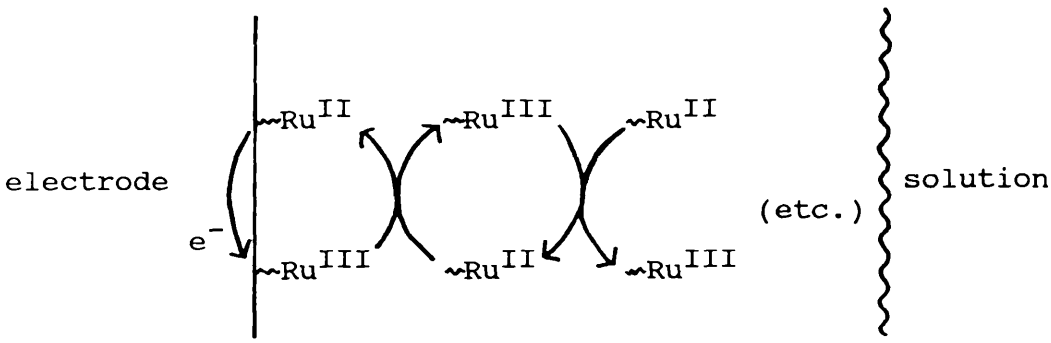


fig. 7. Schematic electron self-exchange mechanism in poly $[Ru(vbpy)_3]^{2+}$ .

Although this is the mechanism for electron transport, the overall mechanism is much more complex since the above system requires the movement of counterions and associated solvent in the opposite direction to electron flow. Therefore, the rate limiting factor is often unknown.

Fortunately, however, charge transport in a polymer seems to follow the laws of diffusion.[15,17,82] This means that by studying the rate at which a polymer becomes oxidised or reduced in response to a potential applied, a diffusion coefficient for charge transport can be calculated. This is expressed as the product $\sqrt{D_{ct}}.C$ where $D_{ct}$ is the effective diffusion coefficient for charge transport and C is the concentration of redox centres in the polymer film. Where charge transport is important, the cyclic voltammogram of a polymer loses the peak symmetry associated with monolayer and solution systems.

Other cyclic voltammetric peak shape anomalies have been observed for polymer-coated electrodes. They involve complex issues and are not fully understood. Wave sharpening (current spikes)[18,72,83] have been attributed to attractive site interaction effects in which the limits constitute phase-like behaviour or site dimerisation. Cathodic-anodic dissimilarities[14,17,78] and multiple waves,[14,66] have been attributed to the presence of electrochemically nonequivalent (different E°) redox sites in a polymer (although only one type seems to be present) which are interconvertable on the voltammetric time scale. These phenomena seem very sensitive to the solvent and supporting electrolyte ions employed. The above phenomena will be described fully later.

If the wave for a surface-confined redox species rises gradually and falls abruptly, then slow electron transfer rate occurs between the electrode and immediately adjacent redox sites,[16,84,85] although this phenomenon could also be due to uncompensated iR drops in the polymer film.[16,17]

Ruthenium, Iridium, Osmium and Rhenium Complexes.

Many ruthenium complexes are electrochemically and substitutionally robust in solution and as such make good polymer modified electrodes. They have also been used successfully as monolayers in electrode systems. Much attention has been given to ruthenium polymers due to the interesting properties of ruthenium i.e. the electron transfer rate is normally very fast, the possibility of multielectron transfer reactions exist, the interesting exited states and the high possibility of catalytic chemistry.[13,86]

The ruthenium polymers can be made in two different ways. Firstly, the polymer can be produced on the electrode and the ruthenium ion then complexed[87,88] (this results in not all the possible sites having a ruthenium atom complexed). Alternatively, the ruthenium complex can be synthesized as the monomer and this can be directly polymerised onto the electrode.[4,89]

The earliest reported ruthenium-containing polymers were produced by Oyama and Anson.[88,90] Using poly(vinylpyridine) and polyacrylonitrile as the base polymer, ruthenium was attached by dipping the electrodes into solutions of $[Ru^{III}(EDTA)]$, $[Ru^{II}(EDTA)]$ and $[Ru(NH_3)_5OH_2]^{3+}$. The electrodes gave electrochemical responses similar to the solution analogues. Anson and

Omaya also showed that by dipping a poly(vinylpyridine) electrode into two solutions, a mixed polymer film electrode was produced that gave rise to both electrochemical responses in the C.V. . Unless one site impedes the other electrochemically, this result can be generally expected.

The original films of poly(vinylpyridine) reacted with [Ru(EDTA)] were interesting in several respects. Poly(vinylpyridine) reacted quicker with dilute $[Ru^{II}(EDTA)]$ than with dilute $[Ru^{III}(EDTA)]$. When concentrated solutions were used, however, both reacted at the same rate. This shows that the intrinsic reactivity of coordination sites in thin polymer films towards substrates is best expressed when the coordination reaction does not saturate the film. Another interesting result was achieved where the [Ru(EDTA)] reacts with two pyridine molecules from two polymer chains thus producing the structure in fig. 8(b).[88] This produces a different electrochemical response (see fig. 8(a)), but the bis-pyridine complex is not stable and dissociates when the complex is maintained in the $Ru^{III}$ state.

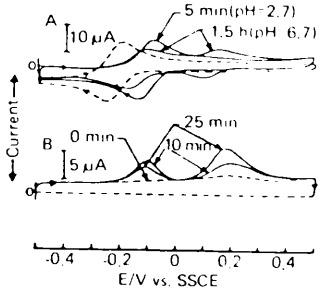


Fig. 8.(a) Curve A: cyclic voltammetry in 0.2mol $l^{-1}$ dissolved [$Ru^{II}$(EDTA)] (dashed line) plus 5mmol $l^{-1}$ pyridine (solid line) at various pH and t min and 1.5 hr after pyridine added; curve B: cyclic voltammetry of a poly(vinylpyridine)-coated electrode at various times after immersion in $2x10^{-6}$ mol $l^{-1}$ [$Ru^{II}$(EDTA)] solution, pH 3.3.

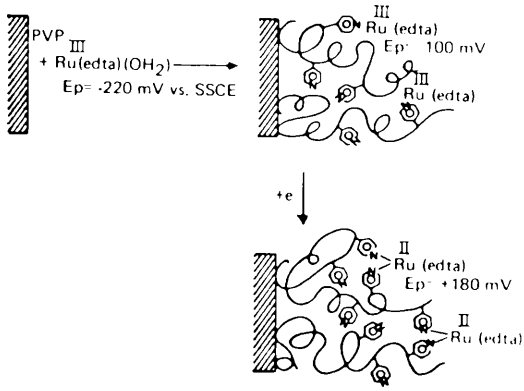


Fig. 8(b). Schematic structures of chemistry occurring in curve B.

As the thickness of the polymer film is increased, the symmetry of the cyclic voltammetry waves were lost and a display similar to that in fig. 4(b) resulted. This shows the diffusional character of charge transport in redox polymer films with one theory suggested being that the segmental motion of polymer chains out of the way of

counterions entering the film was the rate determining step.[15]

The above experiments were carried out on optically transparent carbon-film electrodes so that the number of pyridine sites could be spectrophotometrically calculated and compared with the electrochemically determined Ru sites.[91] As the number of pyridine sites was increased, the Ru incorporation decreased from 40% down to 7%. This suggests that the $[Ru^{III}(EDTA)OH_2]$ reacts less freely with pyridine sites deep within the polymer film and therefore the Ru will not be distributed homogeneously within the film.

Carbon/poly(vinylpyridine)-$[Ru^{II}(bipy)_2OH_2]^{2+}$ films are interesting because the $Ru^{IV}$ state can be electrochemically produced.[71] $Ru^{IV}$ can oxidise primary and secondary alcohols and aromatic hydrocarbons in solution and can be produced in the above film by the following electrochemical reactions:

$$[\text{poly(vinylpyridine)}\text{-}Ru^{II}(bipy)_2OH_2]^{2+}$$

$$\downarrow -e^- \qquad (16)$$

$$[\text{poly(vinylpyridine)}\text{-}Ru^{III}(bipy)_2OH]^{2+} + H^+$$

$$\downarrow -e^- \qquad (17)$$

$$[\text{poly(vinylpyridine)}\text{-}Ru^{IV}(bipy)_2O]^{2+} + H^+$$

In this state, the polymer catalytically oxidises toluic acid, xylenes and aqueous solutions of isopropanol (to acetone). The polymer was, however, not stable to continuous usage due to self-attack of the polymer by $Ru^{IV}$. It was, however, although not producing good yields, better at oxidising than the solution analogues.

An interesting dynamic cyclic voltammogram is shown in fig. 9.[92] This resulted when the film [poly(vinylpyridine)$_{10}$Ru(bipy)$_2$Cl]$^+$ (+0.64 V vs. SCE=E°') was immersed in aqueous acid and whilst in the Ru(II) state was irradiated with visible white light. The resulting substance (E°'=+0.84V vs. SCE) was thought to be [poly(vinylpyridine)$_{10}$Ru(bipy)$_2$($H_2O$)]$^{2+}$. Substitution by [$ClO_4$]$^-$ and $CH_3CN$ is also possible depending on the medium.

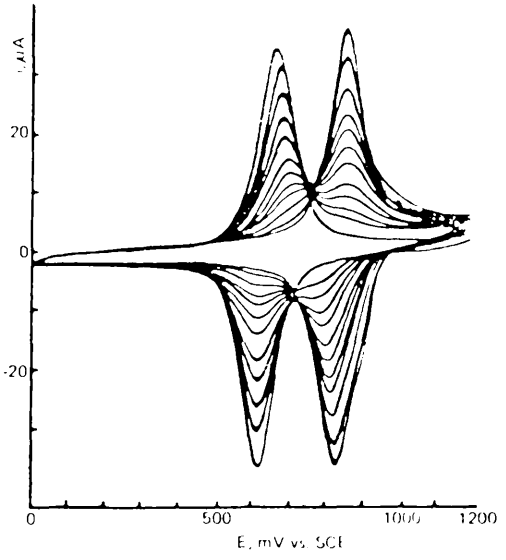


Fig. 9. Cyclic voltammetry during photolysis of a [poly(vinylpyridine)$_{10}$-Ru(bipy)$_2$Cl]$^+$ film on glassy carbon in 1mol $l^{-1}$ $HClO_4$. The wave at +0.64V decreases while that at +0.84V increases. Time between scans is 0.5-2 minutes.

Metal complexes can be bonded to preformed ligating polymers on electrodes via reduction of the chlorinated metal complex.[93] With loss of chlorine, the unsaturated metal complex rapidly bonds to the ligating polymer. The first examples of osmium and rhodium containing polymers were produced by this method using mer-$Os^{III}(Me_2PhP)_3Cl_3$ and mer-$Rh^{III}(Me_2PhP)_3Cl_3$ electrochemically reacted with poly(vinylpyridine).

Because there is uncoordinated pyridine in the polymer, protonation of the free pyridine occurs. This results in fixed cationic sites within the film which will expand the polymer framework and increase its ionic conductivity.[94] This therefore, at certain pH's, results in abnormal electrochemistry which is not present in the fully metallated analogues.

Electropolymerisation of redox active monomers is perhaps the most versatile way of producing a modified surface. The process can be carried out on a broad range of electrode materials including metals, semiconductors, carbon, conducting metal oxides and others. The coverage produced can be exquisitely and reproducibly controlled through the polymerisation conditions.

H. Abruña hypothesized that the combined ligand-centeredness of $Ru^{II}$ bipyridine reactions and anionic polymerisability of vinylpyridines and vinylbipyridines

could upon reaction lead to polymerisation of appropriately vinyl-substituted ruthenium complex monomers. This proved to be the case. When a Pt (or C or $SnO_2$) electrode was repeatedly scanned through a negative potential in a solution of the monomer $[Ru^{II}$(4-vinyl-4'-methyl-"2,2'-bipyridine)$_3]^{2+}$, a polymer film accumulates.[74] The film is electroactive and causes an electrochemical signal which grows as further polymer is deposited (fig. 10).

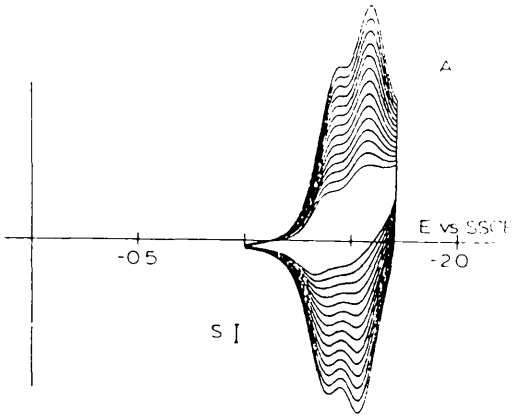


Fig. 10(A). Cyclic voltammograms for $[Ru(vbpy)_3]^{2+}$ depicting electropolymerisation.

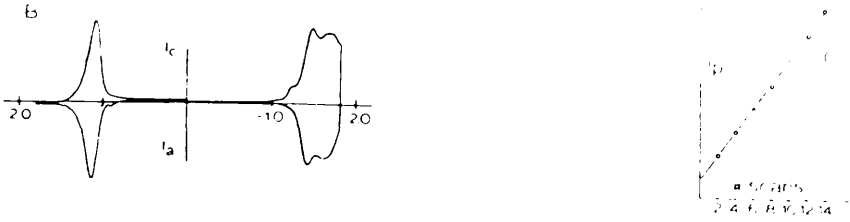


Fig. 10(B and C). A cyclic voltammogram of the modified electrode in a solution of supporting electrolyte only (B) and the linear correlation between growth and number of scans (C).

The polymerisation process was thought to be due, in part, to the fact that the reduction processes are ligand localised and in addition there is a significant degree of $\pi$-backbonding, thus localising a significant amount of charge on the ligands. This charge distribution was then believed to be responsible for the polymerisation, especially in light of the fact that vinylpyridine undergoes anionic polymerisation. Extensive work by Murray et al.[89] has proven, however, that the dominant mechanism involves radical coupling through the ligands. Monomers with more than one vinyl group are more easily polymerised than monomers which are singly vinylated. The former produce crosslinked structures of the type shown in fig. 11(a).[74] These are substantially composed of hydrodimer links and as such are equivalent to ligand-bridged macrocluster complexes. Singly vinylated monomers polymerise to produce structures of the type shown in fig. 11(b) and as such are totally metallated vinylpyridine (vinylbipyridine) polymers.[74] Work done on ruthenium monomers containing 1,10-phenanthroline as a ligand showed that radical growth could produce coupling to the 4- and 7- positions of the phenanthroline ligand and also that an ESR-active species could be isolated.[95]

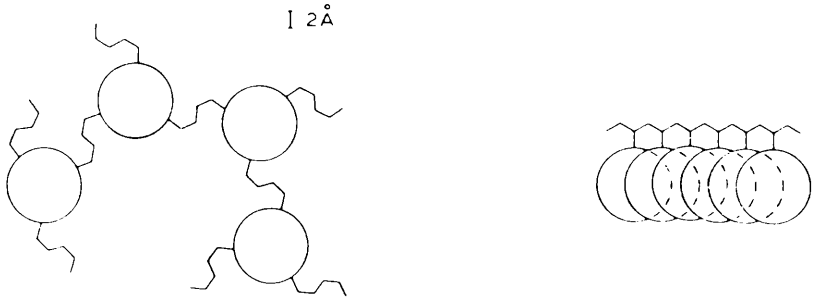


(a) (b)

Fig. 11. Structure of a "tri-vinyl" metal complex polymer (a) compared with a "singly-vinylated" metal complex polymer (b).

The polymers produced are stable and can be cleaned and used in new solvents. Poly-$[Ru(bipy)_3]^{2+}$ produces C.V. peaks similar to those of $[Ru(bipy)_3]^{2+}$ and the films exhibit many of the properties of $[Ru(bipy)_3]^{2+}$ i.e. exceptional $Ru^{III/II}$ couple stability in many solvents and aqueous acid, a similar optical spectrum (when grown on $SnO_2$ coated glass electrodes) and rapid (diffusion-limited) electron transfer mediation reactions with substrates dissolved in the surrounding solution.

An electropolymerised film of poly-$[Ru(vbpy)_3]^{2+}$ has been used in solutions of other redox species having formal potentials placed so that the dissolved redox species must penetrate the film to the electrode in order to react[74,75] and where the electron transfer reactions of the dissolved redox species can be mediated by the

ruthenium redox states in the polymer.[96] The polymer is polycationic and highly cross-linked and therefore has a low permeability, especially to dissolved cationic redox couples. The diffusion coefficient for such species does not depend on the polymer thickness but is highly dependant on the redox size and charge of the redox species and to film cross-linking. This indicates that such films are relatively pinhole-free even at thicknesses as low as ~60Å. They should be considered as viscous, concentrated polyelectrolyte solutions into which the redox species "dissolve" and diffuse.

Ferrocene Polymers

As was the case in monolayer systems, ferrocenes are a popular area of research for redox polymer-coated electrodes. Poly(vinylferrocene) has been dip coated,[72] droplet evaporated,[97] spin coated,[98] oxidatively electrochemically deposited[72] and oxidatively photochemically deposited[97] on Pt. Ferrocene polymers have been attached using organosilane reactions to $SnO_2$ electrodes. Following derivatisation with alkylaminesilane, the following reaction was carried out:[34]

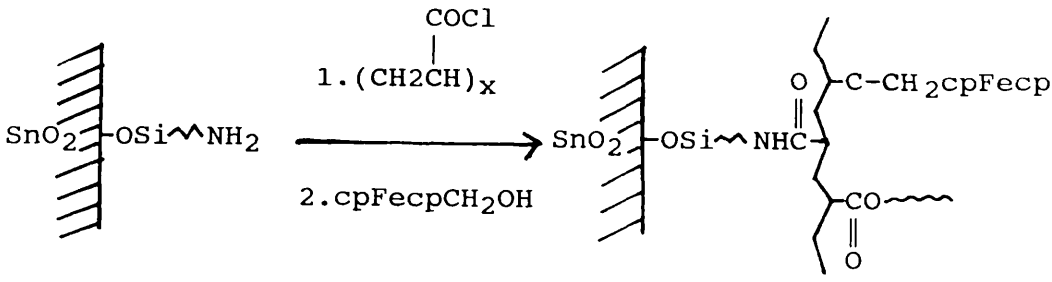


(18)

Since the silanised surface only bears a monolayer of amine sites, the above system is in effect a "monolayer of polymer".

The ferrocene polymers produced all have electrochemical surface waves understandable in terms of the ferrocene/ ferrocenium couple. The waveshapes, however, are quite varied depending on polymer structure, solvent, supporting electrolyte, and temperature. In acetonitrile, ferrocene polymer films which are not too thick (<30 layers), slightly polar (i.e. based on organosilane linkages),[25,27] have dilute ferrocene coverage of ferrocene sites[16] or are examined by cyclic voltammetry at slow potential scan rates have broad symmetrical waveshapes (see fig. 4A). If the films are thicker, are scanned quicker or are observed at low temperatures, charge transport rates become important and the waveshape becomes unsymmetrical (see fig. 4B) due to diffusion.

When the above simple ferrocene polymers are used in aqueous media, however, the waveshape changes (see fig. 12). [18]

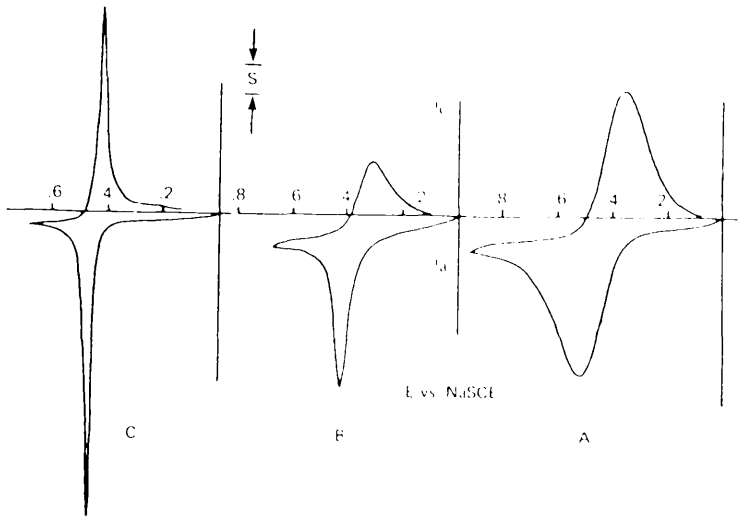


Fig. 12 cyclic voltammetry of aminophenylferrocene coupled to spin coated $(CH_3O)_3Si(CH_2)_3NH(CH_2)_2NH_2$ on Pt, in (A) 0.1 mol $l^{-1}$ $Et_4NClO_4/CH_3CN$,2mV $sec^{-1}$, $1.5x10^{-7}$ mol $cm^{-2}$; (B)0.2 mol $l^{-1}$ $LiClO_4/H_2O$, 2mV $sec^{-1}$, $1.5x10^{-8}$ mol $cm^{-2}$; (C) 0.1 mol $l^{-1}$ $H_2SO_4/H_2O$, 1mv $sec^{-1}$, $3.0x10^{-8}$ mol $cm^{-2}$.

The oxidation wave becomes much narrower and the ferrocenium reduction remains broad.

Sharp peaks for oxidation of ferrocene are also seen for films of poly(vinylferrocene) in acetonitrile at slow potential sweep rates, especially when a polymer with high coverage is used. From fig. 13, it can be seen that multiple peaks occur at slow scan rates but disappear at faster rates becoming charge transport dependant.[16]

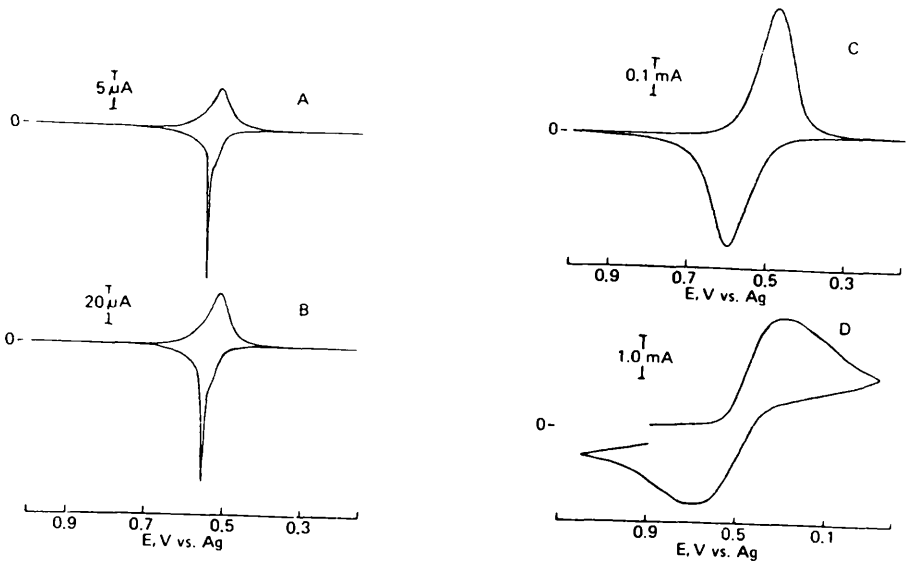


fig. 13. Cyclic voltammetry of $8x10^{-8}$ mol $cm^{-2}$ poly(vinylferrocene) (molecular weight 50,000) on Pt in $Et_4N$(p-toluenesulphonate). (A)-(D) potential scan rate 0.002, 0.01, 0.2, 10 V $sec^{-1}$.

The sharp peaks are a result of attractive interaction effects between the ferrocene sites (or between a site and the polymer lattice). These effects are enhanced by poor solvating media (e.g. water) or by low polarity (or high molecular weight) of the polymer so that acetonitrile is also a poor solvent. This agrees with ruthenium redox polymers where poor solvent swelling led to insufficient electrolyte intrusion for the electrochemical processes to occur.[94] For ferrocene, however, electrochemistry does occur under these conditions and the sharp anodic / broad cathodic voltammogram are considered as an indication of the presence of domains or islands of ferrocene polymer, in

which there is a phaselike behaviour in terms of ferrocene activity (i.e. activity independent of quantity of ferrocene).[17]

The multiple peaks in fig. 13 require the ferrocene to exist in different states in the polymer. Using the following reaction scheme,:[16]

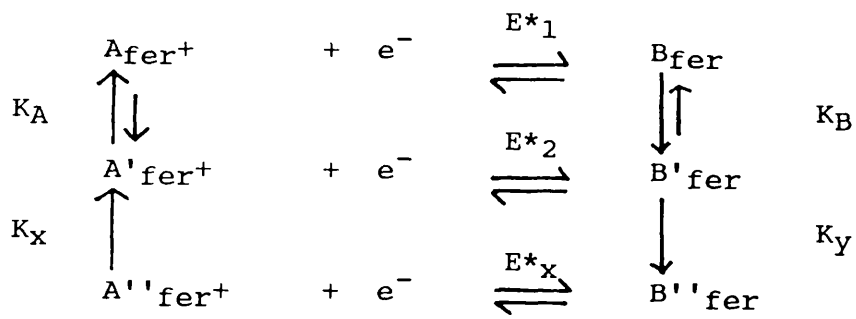


(19)

where $A_{fer}^+$, $A'_{fer}^+$ and $A''_{fer}^+$ are different kinds of ferrocenium sites in the polymer and $B_{fer}$, $B'_{fer}$ and $B''_{fer}$ are different kinds of ferrocene sites, digitally simulated C.V. spectra were produced which were almost identical to those in fig. 13.

Ion Exchange or Electrostatic Trapping in Polyelectrolyte Films

Ionic redox species can be incorporated into polyelectrolyte polymer films on electrodes as the counter ion of the film.[99] This process is called electrostatic trapping and is actually an ion exchange mechanism. It does not require chemical derivatisation of the redox couple.

The principle has been demonstrated by the binding of anionic species $[Fe(CN)_6]^{3-}$ and $[IrCl_6]^{3-}$ by poly(vinylpyridine) on carbon (the C.V.'s observed during this process showing gradually increasing peaks for $[Fe(CN)_6]^{3-/4-}$ and $[IrCl_6]^{2-/3-}$ respectively) and for binding of cationic species $[Ru(NH_3)_6]^{3+}$ by poly(acrylic acid) on carbon.

Work was done on poly(vinylpyridine) films with $[Fe(CN)_6]^{3-}$ and $[IrCl_6]^{3-}$ ions bound, to see how this affected electron transfer-mediated reactions between electrostatically trapped catalyst and redox species in solution.[64,79] The films exhibited low permeability towards dissolved reactants e.g. the above electrodes in aqueous solutions of Fe(II) and Fe(III) did not display electrochemical peaks at the expected potential. Three reactions were investigated:

$$[PVP\text{-}IrCl_6]^{2-} + Fe^{2+} \rightarrow [PVP\text{-}IrCl_6]^{3-} + Fe^{3+} \quad (20)$$

$$[PVP\text{-}IrCl_6]^{2-} + [IrCl_6]^{3-} \rightarrow [PVP\text{-}IrCl_6]^{3-} + [IrCl_6]^{2-} \quad (21)$$

$$[PVP\text{-}Fe(CN)_6]^{4-} + [Fe(CN)_6]^{3-} \rightarrow [PVP\text{-}Fe(CN)_6]^{3-} + [Fe(CN)_6]^{4-} \quad (22)$$

Where PVP is poly(vinylpyridine)

Rotated disc electrodes coated with the above films gave, in each case, a linear Koutecky-Levich plot ( (limiting current)$^{-1}$ vs (rotation rate)$^{-½}$ ), whose intercepts were inversely proportional to the bulk concentration of reactant. This result means that the rate is not controlled by charge transport through the film. The rate constants for reactions (21) and (22) derived by dividing the product $(k_{ex})_{app}$ obtained from fig. 14 by the total quantity of electrostatically bound $[Fe(CN)_6]^{3-}$ or $[IrCl_6]^{3-}$, varied with the quantity of the polymer film on the electrode, ( $(k_{ex})_{app}$ decreased when polymer films were "thick").[64] This shows that only a fraction of the $[Fe(CN)_6]^{4-}$, for reaction (22), in the film is accessible for reaction with the solution $[Fe(CN)_6]^{3-}$.

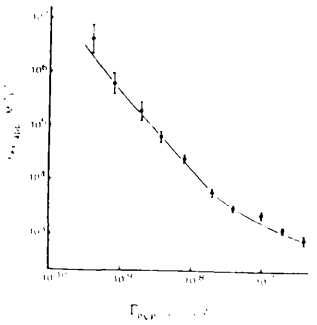

Fig. 14. Apparent rate constants for electron exchange between $[Fe(CN)_6]^{4-}$ confined within a poly(vinylpyridine) film and $[Fe(CN)_6]^{3-}$ in the 0.2 mol $l^{-1}$ $CF_3CO_2Na$ - 0.1 mol $l^{-1}$ $CF_3CO_2H$ solution as a function of the amount of poly(vinylpyridine) used to form the film.

This is what would be expected if the rate of charge transfer in the film and the rate of self-exchange between the film and solution species are both greater than the rate of permeation of solution reactant into the film.

Another feature of fig. 14 is that the value of $(k_{ex})_{app}$ for the thinnest films, which from above is the closest to the actual mediated rate, is larger than the known self exchange rates in homogeneous solution. This was thought to be due to rate-slowing coulombic repulsion effects between $[Fe(CN)_6]^{4-}$ and $[Fe(CN)_6]^{3-}$ by the polycationic film environment.

Electrostatic bound redox ions have been put to a variety of uses. Poly(vinylpyridine) with bound $[Mo(CN)_8]^{4-}$ ions has a similar E°' to that for aqueous Fe(III/II). This film can therefore be used to electron transfer mediate both the oxidation of Fe(II) and the reduction of

Fe(III).[100] $[Fe(CN)_6]^{4-}$ ions exchanged into polymerised $(CH_3O)_3Si(CH_2)_3NH(CH_2)_2NH_2$ films mediates the oxidation of ascorbic acid.[70] At low concentrations of $[Fe(CN)_6]^{4-}$ in the film, all the redox ions oxidise the ascorbic acid, but if the concentration is increased, only the outermost $[Fe(CN)_6]^{4-}$ sites are effective. Electrochemical oxidation of $[Ru(bipy)_3]^{2+}$ in Nafion films in the presence of oxalate, leads to a chemiluminescent emission (by $[Ru(bipy)_3]^{2+}$).[101]

Bilayers

Royce Murray et al. have done much work recently into bilayer modified electrode systems where the inner and outer films are of a different redox species.[4,5] If the E°' values of these two layers are appropriately chosen, the interface between the two polymer films acts as a charge rectifying junction. This is illustrated in fig. 15 where the inner layer is poly[$Ru(vbpy)_3$]$^{2+}$ and the outer layer is poly(vinylferrocene).

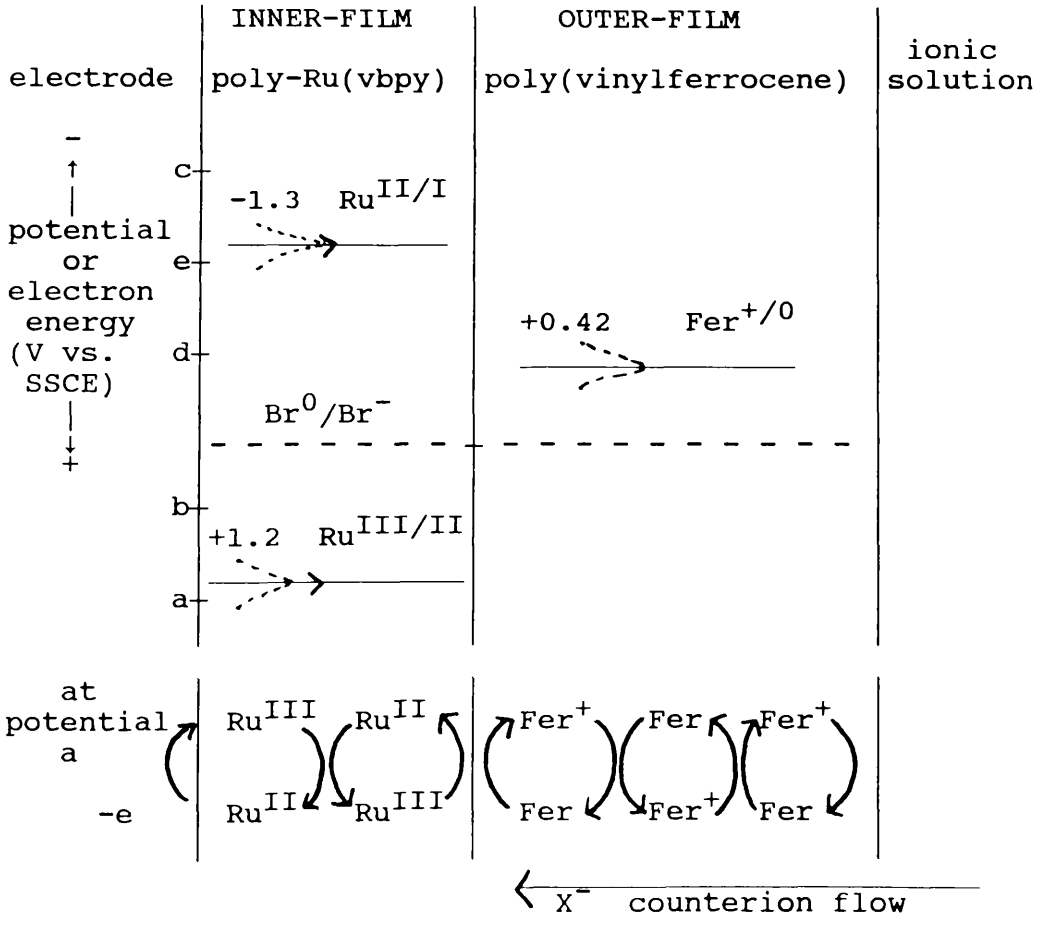


Fig. 15. Energy level diagram for a bilayer electrode where the outer film is poly(vinylferrocene) and the inner film is poly[$(vbpy)_3$]$^{2+}$.

By setting the potential to a, the outer film can be oxidised by the charge trapping reaction:

$$\text{poly-}[Ru(vbpy)_3]^{2+} + PVF^{+} \rightarrow \text{poly-}[Ru(vbpy)_3]^{3+} + PVF \quad (23)$$

Where PVF is poly(vinyferrocene).

When the potential is returned to d, the outer film should be re-reduced, but this does not occur as there is no level by which electrons can flow from the electrode to the outer film. The trapped poly(vinylferrocene)$^{+}$ therefore remains for long periods and can be removed from solution and the Fe $2p_{3/2}$ XPS band observed to confirm the still oxidised state of the outer film. The outer film can be reduced (discharged) by changing the voltage to c where the following reaction occurs:

$$\text{poly-}[Ru(vbpy)_3]^{+} + PVF^{+} \rightarrow \text{poly-}[Ru(vbpy)_3]^{2+} + PVF \quad (24)$$

This is observed in the C.V. (see fig. 16) where it can be seen how the oxidation and reduction of the poly(vinylferrocene) does not occur until the inner layer [poly$(vbpy)_3^{2+}$] undergoes some sort of redox process. The poly(vinylferrocene) waves therefore occur as spikes

with a large voltage separating the oxidation wave from the reduction wave.

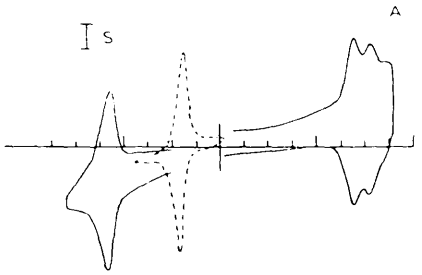


Fig. 16A. Cyclic voltammetry of Pt/poly-$[Ru(vbpy)_3]^{2+}$ (solid line) one layer electrode at 0.1V $s^{-1}$, and Pt/poly(vinylferrocene) (dashed line) one layer at 0.1V $s^{-1}$.

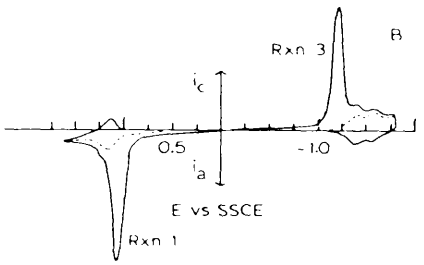


Fig. 16B. Cyclic voltammetry of Pt/poly-$[Ru(vbpy)_3]^{2+}$ /poly-$[Ru(vbpy)_3]^{2+}$ bilayer where $\Gamma_{Ru}=2.4\times10^{-9}$ mol $cm^{-2}$ and $\Gamma_{Fe}=1.2\times10^{-8}$ mol $cm^{-2}$. The solid line represents 0V→+1.6V→-1.6V→0V potential excursion and the dashed line represents result of reversing the scan at 0.6V or (for the negative potential region) if the virgin scan was 0V→-1.6V→0V. (all work done in 0.1mol $l^{-1}$ $Et_4NClO_4/CH_3CN$).

The above systems have similar properties to semiconductors although neither material is a semiconductor. In a semiconductor, rectification of current is possible because of space charge layers or

gradients of potential which drive electrons in their conduction band away from or towards the interface. In a bilayer electrode, the redox levels for the charge trapping reaction form the gradient for irreversible electron flow.

## Chiral Electrodes

The first reported case of a chiral modified electrode was by Larry Miller and co-workers in 1975.[6] This was also the first reported example of a covalently modified carbon surface (see page 31). The system comprised of a spectroscopic carbon rod made active by heating in air. The electrode was functionalised by soaking in dry thionyl chloride in benzene solution. They were reacted with (S)-(-)-phenylalanine methyl ester.

4-acetylpyridine (1) can be electrolytically reduced at relatively positive potentials to the alcohol (2). If the above electrode system is dipped in a solution of 4-acetyl pyridine and left at a constant voltage, a 48:52 mixture of (1) to (2) is produced.

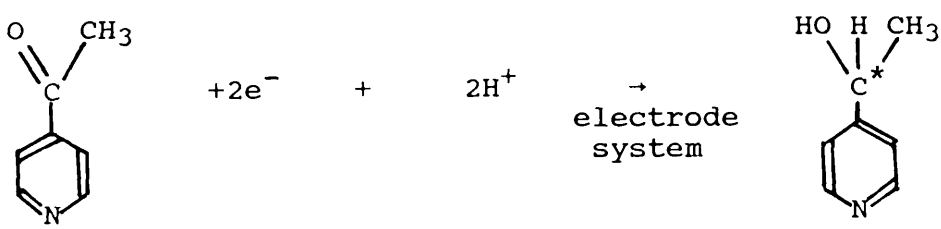


(1) (2)

The optical rotation of (2) was found to be $[\alpha]^{20}_{D}$-7.22°. The process is repeatable with the same electrode producing (2) with an optical rotation of $[\alpha]^{20}_{D}$-4.2°. If the electrode is made up with (R)-(+)-phenylalanine methyl ester then the optical rotation of (2) obtained is $[\alpha]^{20}_{D}$+6.1°.

It is known that optically active alkaloids in solution can lead to asymmetric induction[102] (the reduction of 4-acetyl pyridine on a mercury electrode in the presence of alkaloids gives optically active (2) ). Therefore the reduction was done using a plain carbon electrode in the presence of (S)-(-)-phenylalanine. Alcohol (2) was produced but the optical rotation was $\alpha_{OBS}$=-0.015 and on a second run $\alpha_{OBS}$=+0.025.

It could also be argued that the activity of the electrodes was due to adsorbed phenylalanine methyl ester and not covalently attached phenylalanine methyl ester. This was disproved by carrying out the reactions with basal and edge planes of highly orientated pyrolytic graphite. The modified edge plane graphite electrode produced product with an enantiomeric excess but the "modified" basal plane graphite electrode produced optically inactive product.

A year later, Miller and Firth reported similar results using $SnO_2$ electrodes and DSA electrodes (commercial electrodes which contain tantalum and iridium oxides).[103]

The above work seemed to be quite conclusive but attempts by Horner and Brick[104] to repeat the experiments proved unsuccessful. Enantiomeric excess was only achieved when using an optically active electrolyte.

The work done by Miller et al. was only reported as a communication to the Editor of the Journal of the American Chemical Society. It has never been written up as a full paper. This suggests that perhaps the results were not consistently reproducible.

In 1982, Fujihira, Osa et al.[105] published work on a chiral electrode based on Raney nickel modified with tartaric acid. Ketones were selectively reduced to their alcohols depending on whether the electrode had been modified with (+)- or (-)- tartaric acid. Enantiomeric excesses were , however, low with average values of 4% obtained.

In 1983, Nonaka et al.[106] showed durability as well as specificity was possible with graphite electrodes modified with poly(L-valine) and poly(N-acryloyl-L-valine methyl ester). Although better enantiomeric excesses were possible with dip coated electrodes, covalently attached

systems had better durability; dropping only slightly over 4 runs. Dip coated electrodes dropped to ~0 after 4 runs.

Further work by Nonaka based on poly(amino acid) coated electrodes produced enantiomeric excesses of up to 93% when specifically oxidising sulphides to chiral sulphoxides.[107] This optical purity was for tertiary-butyl phenyl sulphide oxidised to tertiary-butyl phenyl sulphoxide using a platinum electrode coated doubly with polypyrrole and poly(L-valine).

An untouched idea was then developed by Nonaka.[108] This was the specific reaction of one hand of a racemic mixture. Nonaka used a lead dioxide anode coated doubly with polypyrrole and poly(L-valine). This electrode was capable of the enantiomer-differentiating oxidation of racemic 2,2'-dimethyl-1-phenyl-1-propanol (I) to the corresponding ketone (II).

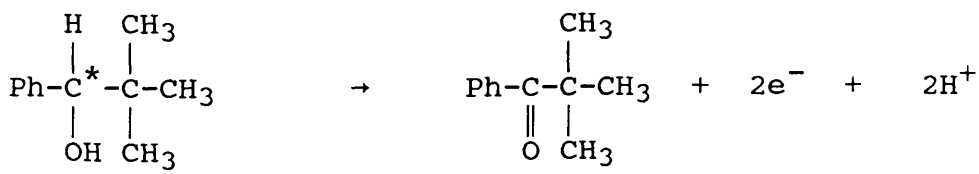

(I) (II)

After the above reaction, 43% optically pure (S)-(-)-2,2'-dimethyl-1-phenyl-1-propanol was recovered as an unreacted part.

In 1985[109] (and again in 1989),[110] Salmón and Bidan published methods of producing chiral polymers (based on pyrrole) that are comparably stable although no actual work on their stereoselectivity was done in either report.

In recent years, attempts at more practical chiral electrode systems have been made. Much work has been done on clay modified electrodes and their unusual intercalating properties. Work done by several research groups on complexes like $[Ru(phen)_3]^{2+}$, $[Fe(phen)_3]^{2+}$ and $[Cr(bipy)_3]^{2+}$ has shown that half the amount of complex is intercalated into a clay electrode when one enantiomer is used compared to the racemic mixture[111] (see fig. 17).

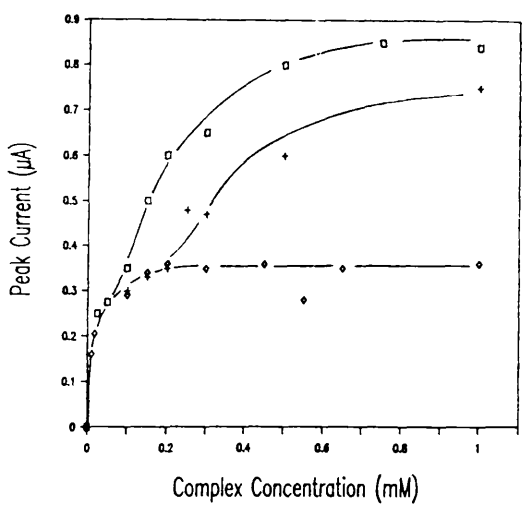


Fig. 17. Cathodic peak height of positive shifted peak as a function of complex bulk solution concentration: (□) racemic $[Cr(bipy)_3]^{3+}$ in 0.01 mol $l^{-1}$ $Na_2SO_4$; (+) (-)d-$[Cr(bipy)_3](PF_6)_3$ in 0.01 mol $l^{-1}$ $Na_2SO_4$; (◊) racemic $[Cr(bipy)_3]^{3+}$ in 0.02 mol $l^{-1}$ NaCl.

The theory assumes that racemic adsorption occurs in pairs as in fig. 18 i.e. sites within the clay bond to pairs of oppositely configured enantiomers.[112] If, however, a solution of only one enantiomer is used, then adsorption occurs as in fig. 19. The quantity of electroactive complex adsorbed on the electrode can be calculated in two ways. If the adsorbed species has a UV/vis absorption the quantity can be calculated spectroscopically or since it is electroactive, the quantity can be calculated using cyclic voltammetry (the quantity present being relative to the peak height).

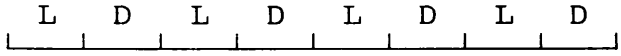


fig. 18

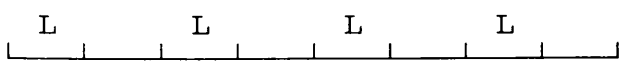


fig. 19

This theory can be confirmed by adding the electrode to a new racemic solution. If the structure in fig. 19 is correct then the D enantiomer will be adsorbed on the electrode leaving an enantiomeric excess of L in solution. This is in fact the case.

The above theory is not as simple as was first thought. In 1990, Villemure and Bard[113] produced a paper not only

disagreeing with the above results but producing a system that gave the opposite results. Villemure and Bard showed that one enantiomer of $[Ru(bipy)_3]^{2+}$ will be adsorbed twice as readily as racemic $[Ru(bipy)_3]^{2+}$ into clay electrodes. They also claim that these results can not be obtained electrochemically as the electronic properties of clay are far too complex.

This disagrees with all the above theories and to date no satisfactory conclusions have been produced to explain the differences. $[Ru(bipy)_3]^{2+}$ and $[Ru(phen)_3]^{2+}$ both have similar sizes and structures, yet both produce opposite effects with clay.

As a consequence of this work, $[Ru(bipy)_3]^{2+}$ was incorporated into cholesteric liquid crystals as a support analogous to clay.[114] Discrimination between the two enantiomers was obtained to a degree (0.78). Further work on this topic has not been continued.

Also in the last few years, the first case of chiral recognition by a chemically modified electrode was reported.[115,116] A chiral thiophene was electropolymerised onto a platinum disk electrode and the electrode used to distinguish between (+)- and (-)-10-camphorsulphonic acid (fig. 20) using cyclic voltammetry. The results are not very conclusive with the differentiation possibly due to a varying background current.

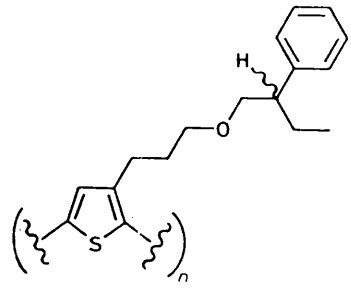


(IX)

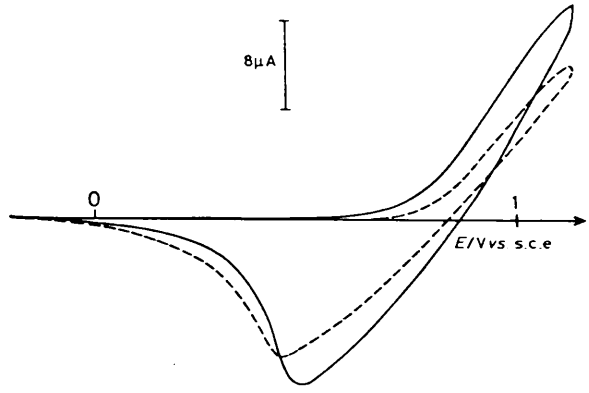


Fig. 20. Cyclic voltammogram of chiral poly(thiophene) (IX) using chiral anions as doping agents; deposition charge 400mC $m^{-2}$, electrolyte (+)- (————————) and (-)- (------------) 10-camphorsulphonic acid in acetonitrile (0.1 mol $l^{-1}$), scan 50mV $s^{-1}$.

Other work on chiral poly(thiophenes) has also been reported in the literature but none has been continued to the stage where chiral recognition (or other practical processes) have been attempted.

Very recently (April 1991), a paper was published where electrodes had been modified using carbohydrates.[117] These systems could have strong potential for chiral recognition, but as above only the synthesis has been carried out with no attempt at chiral sensing reported.

## Applications to Analysis

Monomer coated electrodes, which were the first to be developed, have not proved to have any significant uses within analytical chemistry largely because these systems are relatively fragile and difficult to make. Polymer coated electrodes, however, have been shown to have a number of uses. These are summarised as follows:

### (i) Preconcentration

Modified electrode surfaces can act as preconcentrating surfaces, in which the analyte species (or some product thereof) is concentrated on the electrode by chemical reactions with the groups attached to the surface. The species can then be detected by the electrochemical response. If the electrode selectively detects the analyte then the response will be due totally to it. If the electrode concentrates more than one species, then the electrochemical response for these different species must be suitably different so that they may be distinguished. For the method to succeed, the electrochemical response should ideally have a good signal to noise ratio so that good sensitivity is possible.

Comprehensive work by Price and Baldwin[118] on alkylamine modified platinum electrodes in a solution of ferrocenecarboxaldehyde showed the following species to be produced:

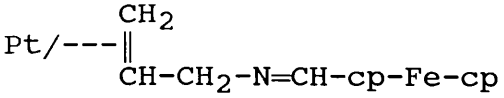

(X)

The ferrocene/ferrocenium couple was detected by pulse voltammetry at concentrations as low as $10^{-7}$ mol $l^{-1}$.

(ii) Analysis with Biological Redox Systems

Redox active biological systems often give sluggish electrochemical responses due to the inaccessibility of the redox site and/or unfavourable adsorption. For successful detection, an intermediate redox reaction is required to aid the redox species react. With such sites attached to the electrode in modified systems, a simple solution has been found.

Wrighton et al.[119] have coated platinum electrodes with polymers of the following species:

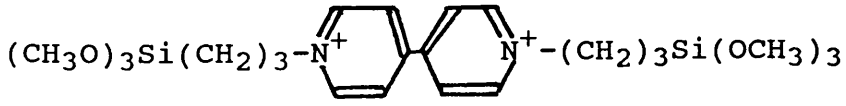

(XI)

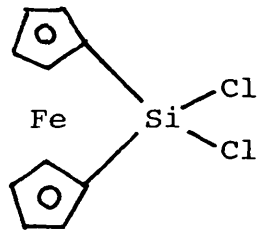


(XII)

and

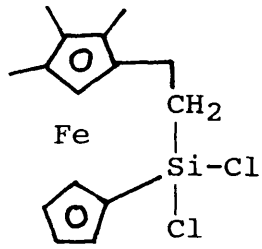


(XIII)

The three electrode systems work as follows:

Reduced Pt-poly(XI) mediates the reduction of cytochrome c (ox) but not the oxidation of cytochrome c (red).

Pt-poly(XII) mediates the oxidation of cytochrome c (red) but not the reduction of cytochrome c (ox).

Pt-poly(XIII) mediates both the oxidation and reduction of cytochrome c.

In the latter case, the cytochrome c reacts nearly reversibly at the electrode. The mediator reaction therefore is not required to occur at exactly the same potential as the biological reaction, only close to it.

In other work done it is not the biological species that is directly detected but the $H_2O_2$ (or other substrate) released when the modified surface oxidises the species.[120]

(iii) Chiral Detection

To date chiral detection has not been performed satisfactorily with modified electrodes. Attempts have been made but no conclusive results have so far been produced. It is, however, an area of increasing research and in the future (I suspect) it will produce satisfactory results.

# Chapter 2

## EXPERIMENTAL

## Instrumentation

### Cyclic voltammetry

All voltammetric experiments were carried out using Princeton Applied Research equipment. A conventional cell using a three electrode configuration was used; the electrodes being a working electrode, an auxiliary electrode and a reference electrode. The auxiliary electrode was platinum wire, the working electrode was platinum wire (with tin oxide coated glass used for spectroscopic studies) and the reference electrode was Ag/AgCl for aqueous work and $Ag/Ag^{+}$ for work in acetonitrile.

For aqueous work, the reference electrode (fig. 21) consisted of a silver wire coated with silver chloride. This was immersed in a 3 mol $l^{-1}$ aqueous solution of sodium chloride in an air-tight compartment with a porous Vycor glass frit. This was placed in a salt bridge compartment (0.1 mol $l^{-1}$ KCl in $H_2O$) which was separated from the electrolytic cell solution by a porous Vycor frit.

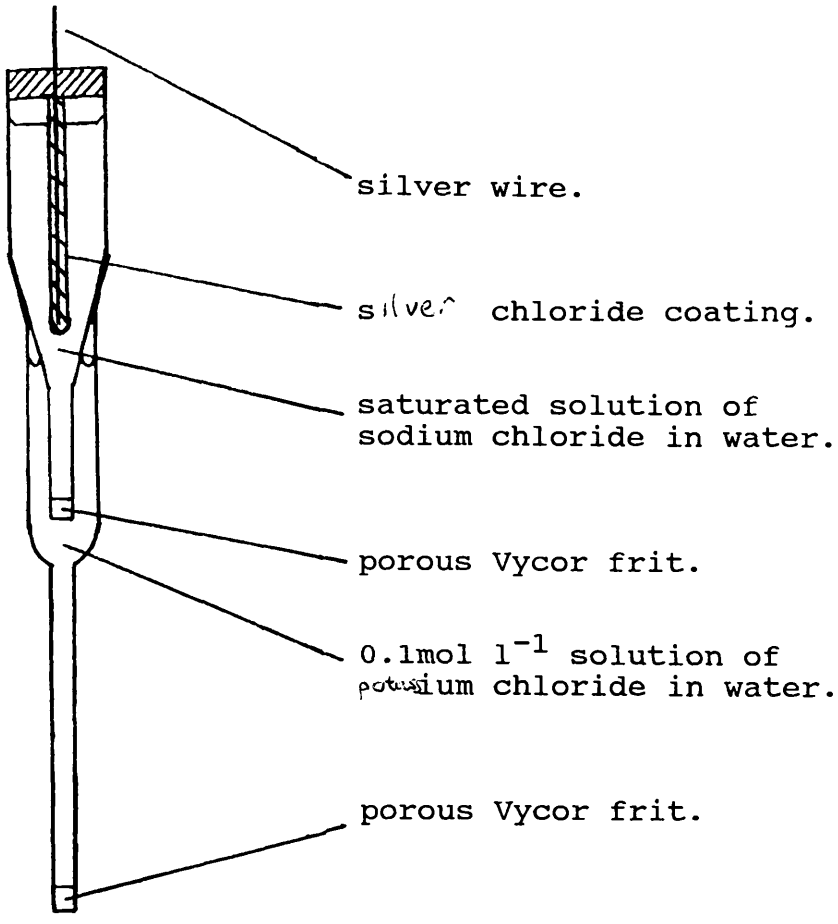


Fig. 21. Schematic diagram of aqueous work reference electrode - Saturated Sodium Chloride Electrode (SSCE).

For acetonitrile work the reference electrode (fig. 22) consisted of a silver wire dipped in a solution of 0.1 mol $l^{-1}$ $AgNO_3$ in acetonitrile. This was in an air- and light- tight compartment with a porous Vycor frit. This electrode compartment was placed in a salt bridge compartment (0.1 mol $l^{-1}$ TBA $BF_4$ in acetonitrile) which was separated from the electrolytic solution by a porous Vycor frit.

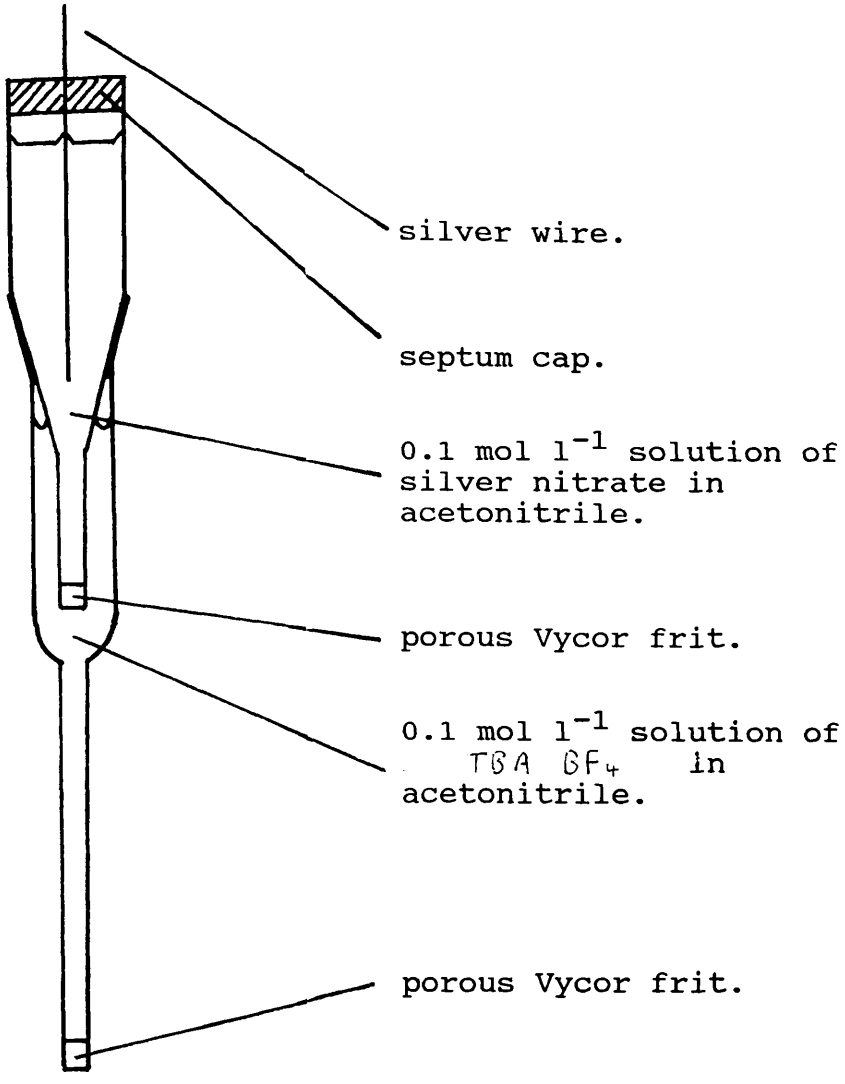


Fig. 22. Schematic diagram of silver / silver nitrate electrode.

The electrochemical cell (fig. 23) was air-tight . It had inlet and outlet taps to allow deoxygenation of the solutions by purging with dried Argon .

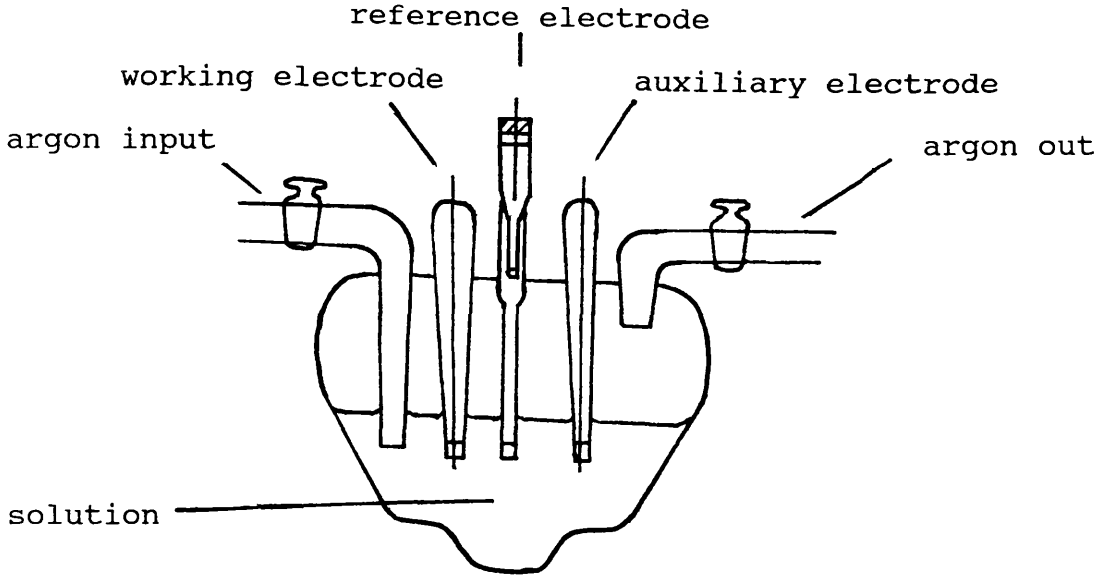


Fig. 23. Schematic diagram of electrochemical cell.

Cyclic voltammograms were recorded using an EG+G Princeton Applied Research Model 175 Universal Programmer coupled to an EG+G Princeton Applied Research Model 173 Potentiostat / Galvanostat with a Lloyd XY plotter model PL3. All of the C.V.'s recorded had peak heights of approximately 30μA.

Circular Dichroism

THE C.D. spectrometer (fig. 24) was constructed around a Jobin-Yvon 0.6m monochromator. The source was a Xenon arc lamp powered by a Rofin power supply focussed by means of a parabolic reflector. The light energy from the single grating monochromator was passed through a filtering system and was then plane-polarised in the vertical plane by a quartz Rochon prism. The plane polarised light was

then circularly-polarised by passing it through a silica photo-elastic modulator (powered by a PEM-80 Photoelastic Modulator System Controller) held at 45° to its optic axes. The circularly-polarised light passed through the sample and was collected by an EMI model 9558 QB photomultiplier. The modulated signal was measured using a synchronous lock-in amplifier (Bentham) referenced to the photo-elastic modulator vibration frequency of 50kHz. The lock-in amplifier detected the periodic difference in light intensity due to the presence of an optically active sample. The lock-in output was plotted on a Servoscribe chart recorder as the monochromator was scanned in wavelength, producing a spectrum of $\Delta A$ varying with wavelength, where $\Delta A$ is the fractional circular dichroism absorbance.

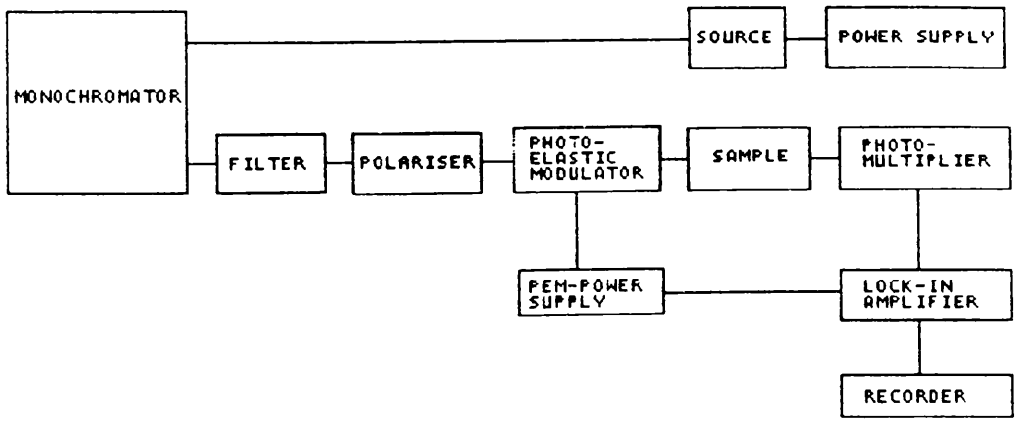


Fig. 24. Schematic diagram of C.D. spectrometer.

Operation of the photo-elastic modulator

The photoelastic modulator consists of a bar-shaped crystal of calcium fluoride or fused silica which is driven into oscillation by mechanical coupling to a bonded-on piezoelectric transducer made of crystal quartz. The stretching and compression of the optical element results in an oscillating birefringence ($n_x$-$n_y$). This is due to a time varying difference between the two refractive indices, $n_x$ and $n_y$, applying to light polarised parallel or perpendicular to the x and y axes of figure 25.

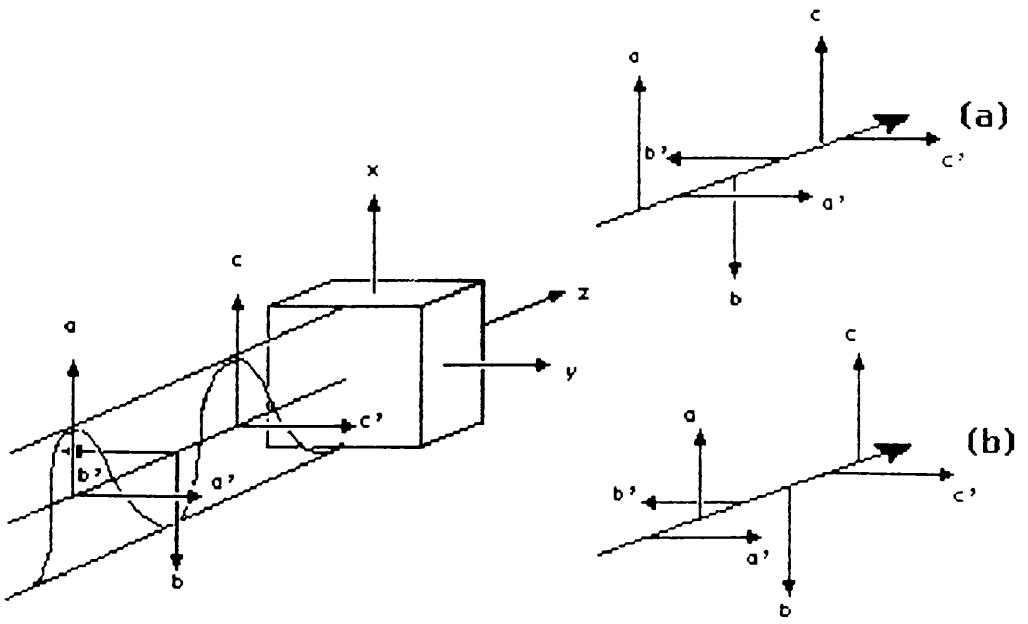


Fig. 25. Polarisation modulation:
(a) $n_x > n_y$, $\delta = \lambda/4$, right-circular polarisation.
(b) $n_x < n_y$, $\delta = \lambda/4$, left-circular polarisation.

The extensional displacements along the x-axis of the bar are given by,

$$\delta=\delta_o \sin(\pi x/\lambda)\sin\omega t \qquad \text{(vii)}$$

where $\delta_o$ is the maximum extension, $\lambda$ is the wavelength, $\omega$ is the oscillating frequency and t is the time. The corresponding strain is proportional to $(\partial\delta/\partial x)$, that is, to $\cos(2\pi x/\lambda)$ and is a maximum at the centre of the bar. The birefringence $(n_x-n_y)$ is proportional to the strain and varies with time as $\sin(\omega t)$.

Consider a linearly polarised light beam which is the resultant of two linear components abc and a'b'c' (fig. 25). This light beam, with its resultant linear axis orientated at 45° to the pressure axes, now passes through a block of isotopic fused silica rendered linearly birefringent by pressure exerted along the x or y axis. The induced differential refractive index $(n_x \neq n_y)$ causes one of the linear components of the light beam (abc or a'b'c') to travel through the silica faster than the other. If $n_x > n_y$ then the x component (abc) will travel more slowly than the y component (a'b'c'). As drawn in fig. 25(a), an x component retardation is exactly ¼ wave ($\lambda/4$) leads to right-circular polarisation ($-\lambda/4, 3\lambda/4, 7\lambda/4, \ldots$ etc. retardation will give left-circular polarisation)-fig. 25(b). A half wave retardation, plus or minus, will cause a 90° rotation of

the original plane of linear polarisation. Zero ($n_x=n_y$) of full-wave retardation leaves the polarisation of the incident beam unchanged. The general phase retardation, $\delta$, leads to elliptically polarised light. A programmed variable pressure on the optical block is the basis of a device to generate a controllable polarisation. This is polarisation modulation.

UV/vis spectroscopy

Electronic absorption spectra were recorded on a Perkin-Elmer λ9 UV/vis/NIR spectrophotometer. In addition, a Perkin-Elmer data-base (PECSS) was used to manipulate and save spectra.

NMR spectroscopy

NMR spectra were recorded on a Perkin Elmer R32 90MHz machine and a Varian XL100 100MHz machine.

## Experimental Procedure

### Chemical purification

#### (a) Acetonitrile (for electrochemistry)

Bulk acetonitrile was purified using the 6 stage distillation of Winfield and then stored over activated 3Å molecular sieves

#### (b) Tetrabutylammonium Tetrafluoroborate

TBA $BF_4$ was bought from Fluka ( >99% pure). It was further purified by the following procedure: 50g was added to 400ml of water and heated to 50°C for 2 hours, stirring continuously. This was allowed to cool and was then filtered and washed with 100ml of water. The solid was dried in a vacuum desiccator and then recrystalised from ethylacetate/pentane.

#### (c) Ethyl acetate

The water, ethanol and acid impurities were removed by washing with 5% aqueous sodium carbonate, then with saturated calcium chloride, followed by drying over anhydrous potassium carbonate and finally distilling from $P_2O_5$.

(d) Pentane

Pentane was stirred with successive portions of concentrated sulphuric acid until there was no further colouration after leaving for 12 hours. It was then stirred with 0.5N $KMnO_4$ in 3 mol $l^{-1}$ $H_2SO_4$ for 12 hours, washed with water and aqueous $NaHCO_3$, dried with $MgSO_4$ and fractionally distilled from $P_2O_5$.

(e) Tetrahydrofuran

THF was purified by drying over sodium wire and distilling from sodium.

(f) Dichloromethane

Dichloromethane was distilled from calcium hydride.

(g) Diethyl ether

Ether was stored over sodium wire, distilled from sodium / potassium amalgam and used immediately.

(h) Dimethylformamide

DMF was stirred over calcium oxide for 24 hours then distilled under vacuum.

(i) Water (for electrochemistry)

The water was doubly distilled from alkaline potassium permanganate.

## Synthetic Preparations

### Preparation of 4-hydroxyethyl-4'-methyl-2,2'-bipyridine

4-hydroxyethyl-4'-methyl-2,2'-bipyridine was prepared using the method of Ghosh and Spiro.[121] n-BuLi (35ml of 1.6 mol $l^{-1}$ in hexane) was added to a solution of 8ml of diisopropylamine in 30ml of THF. The resulting mixture was stirred for 15 minutes. 10g of 4,4'-dimethyl-2,2'-bipyridine in 250ml of THF was slowly added from a dropping funnel; the colour changing to orange brown. After 2 hours, 1.7g of gaseous formaldehyde was bubbled through the solution whose colour slowly turned green. After an additional 1 hour of stirring, the reaction was quenched with ice water and extracted with ether.

This proved to be only fairly successful so the method by Guarr and Anson was used.[95] 40ml of 1.6 mol $l^{-1}$ n-BuLi in hexane was carefully added to a solution containing 4ml of diisopropylamine in 15ml of THF. The resulting mixture was stirred for 15 minutes. A solution of 5g of 4,4'-dimethyl-2,2'-bipyridine in 125ml of THF was then slowly

added via a dropping funnel to produce an orange-brown solution. A stream of formaldehyde was then bubbled through the solution for 2 hours. The reaction was then quenched with ice water and extracted with ether.

In purifying the oily product, it was discovered that crystals of 4,4'-dimethyl-2,2'-bipyridine precipitated out after leaving for several weeks. The oil could then be filtered producing pure 4-hydroxyethyl-4'-methyl-2,2'-bipyridine.

Preparation of Formaldehyde

Dry formaldehyde was produced by passing dry argon over heated paraformaldehyde.

Preparation of 4-methyl-4'-vinyl-2,2'-bipyridine

4-methyl-4'-vinyl-2,2'-bipyridine was prepared using the method of Guarr and Anson.[95] 2.0g of 4-hydroxyethyl-4'-methyl-2,2'-bipyridine was heated to 130°C in a vacuum sublimator with 0.5g of powered NaOH. The vacuum was approximately 0.001mm of Hg (mercury diffusion pump used as well as a rotary pump) and pure white crystals were deposited on the cold finger (dry ice and acetone).

The method by Ghosh and Spiro[121] was initially used i.e. refluxing 4-hydroxyethyl-4'-methyl-2,2'-bipyridine with

$P_2O_5$ in Xylene but this method produced black tar from which no product could be isolated.

Preparation of cis Bis(2,2'-bipyridine) Bis(chloride) Ruthenium(II) Dihydrate

cis-$Ru(bipy)_2Cl_2.2H_2O$ was produced using the method of Weaver.[122] 7.8g of $RuCl_3.3H_2O$, 9.36g of bipyridine and 8.4g of LiCl were refluxed in 50ml of DMF for 8 hours; the reaction being stirred throughout. After cooling to room temperature, 250ml of Analar acetone was added and the resultant solution cooled to 0°C overnight. Filtering produced a red to red-violet solution and a dark green-black micro-crystalline product. The solid was washed 3 times with 25ml portions of water followed by three 25ml portions of diethyl ether and dried in a vacuum desiccator.

Preparation of cis Bis(1,10-phenanthroline) Bis (chloride) Ruthenium(II) Dihydrate

cis-$Ru(phen)_2Cl_2.2H_2O$ was produced using a similar method as cis-$Ru(bipy)_2Cl_2.2H_2O$. 3.9g of $RuCl_3.3H_2O$, 5.4g of 1,10-phenanthroline and 4.2g of LiCl were refluxed in 250ml of DMF. This produced dark green-black crystals.

Preparation of cis Bis(1,10-phenanthroline) Bis(4-vinylpyridine) Ruthenium(II) Bis(hexafluorophosphate)

cis-$[Ru(phen)_2(vpy)_2](PF_6)_2$ was prepared using the method of Murray et. al.[89] 127mg of cis-$Ru(phen)_2Cl_2.2H_2O$ was added to a deoxygenated solution containing 15ml of ethanol, 15ml of water and 0.8ml of 4-vinylpyridine. This was refluxed under nitrogen for 3.5 hours and then reduced in volume by approximately half by rotary evaporation. Addition of 1ml of a saturated aqueous solution of $NH_4PF_6$ causes immediate precipitation of orange crystals. These were filtered, dried, reprecipitated by ether from a minimum volume of acetone and collected by filtration.

Preparation of cis Bis(2,2'-bipyridine) Bis(4-vinylpyridine) Ruthenium(II) Bis(hexafluorophosphate)

cis-$[Ru(bipy)_2(vpy)_2](PF_6)_2$ was produced using a similar method as for the production of cis-$[Ru(phen)_2(vpy)_2](PF_6)_2$. 116mg of cis-$Ru(bipy)_2Cl_2.2H_2O$ was added to a solution of 15ml ethanol, 15ml water and 0.8ml of 4-vinylpyridine. This produced a similarly coloured orange solid.

## Preparation of cis Bis(1,10-phenanthroline) Bis(pyridine) Ruthenium(II) Bis(hexafluorophosphate)

cis-$[Ru(phen)_2\ py_2](PF_6)_2$ was produced using the slightly modified method of Bosnich and Dwyer.[123] 0.5g of cis-$Ru(phen)_2Cl_2.2H_2O$ was refluxed for 3 hours in a solution containing 10ml of water and 5ml of pyridine. During this time, the solution changed colour from red-brown to light orange. The solution was filtered and then evaporated to dryness. The brown residue was then taken up in 10ml of methanol and the complex precipitated as fine yellow needles on addition of diethyl ether. After standing for 1 hour, the crystals were filtered and washed with ether. The hex afluorophosphate was prepared by dissolving a small amount of the yellow crystals in water containing a little methanol then adding a saturated solution of $NH_4PF_6$.

## Preparation of Sodium Arsenyl-(+)-Tartrate

Sodium Arsenyl-(+)-Tartrate was produced using the method of Schlessinger.[124] Twenty grams of arsenic (III) oxide was added to a mixture of 30g of (+)-tartaric acid and 25ml of water. After heating just to the boiling point, a solution of 8g of sodium hydroxide in 20ml of water was added dropwise with stirring. The suspension was digested by heating until only a small amount of undissolved oxide remained. After cooling, 25ml of water was added and the

residue was filtered off. The filtrate was evaporated to a syrup and then heated for an additional 1-2 hours at 105-110°C in a vented oven. On cooling, with occasional stirring, a semi-solid crystalline mass was obtained consisting of the 2½ hydrate of the product. This was triturated to a smooth slurry with 100ml of absolute ethanol, cooled in ice, and filtered. The hydrated material was heated to constant weight at 105-110°C; at this temperature the anhydrous compound results.

Preparation of Sodium Antimonyl-(+)-Tartrate

Sodium Antimonyl-(+)-Tartrate was prepared using an analogous method to that for Sodium Arsenyl-(+)-Tartrate. Antimonyl (III) Oxide was used in the corresponding quantity.

Preparation of Silver Antimonyl-(+)-Tartrate

Silver Antimonyl-(+)-Tartrate was prepared by mixing an aqueous solution of Sodium Antimonyl-(+)-Tartrate and an aqueous solution of Silver Nitrate. Silver Antimonyl-(+)-Tartrate was precipitated out and collected by filtering. The crystals were washed with water and dried in a vacuum desiccator.

Preparation of Tris(2,2'-bipyridine) Ruthenium(II) Bis(bromide)

$Ru(bipy)_3.Br_2$ was produced using the method of Braddock and Meyer.[125] 1.0g of $RuCl_3.3H_2O$ and 1.8g of bipyridine were refluxed for approx. 3 hours in 50ml of N,N'-DMF. After 3 hours, the DMF was slowly distilled off until the solution volume was approx. 10ml. The solution was added dropwise to a saturated solution of Tetra-n-butylammonium Bromide in reagent grade acetone, which precipitated $Ru(bipy)_3.Br_2$. The crystals were filtered and dried *in vacuo*.

Preparation of Tris(4-methyl-4'-vinyl-2,2'-bipyridine) Ruthenium(II) Bis(hexafluorophosphate)

$Ru(vbpy)_3.PF_6$ was produced using a similar method as for the production of $Ru(bipy)_3.Br_2$. 1.0g of $RuCl_3.3H_2O$ was refluxed with 2.25g of 4-methyl-4'-vinyl-2,2'-bipyridine in 50ml of DMF. $Ru(vbpy)_3.Br_2$ was isolated as above, then dissolved in a minimum quantity of water. A few drops of a concentrated solution of $NH_4PF_6$ in water was added and the $Ru(vbpy)_3.PF_6$ salt was precipitated out. This was filtered, washed with water and dried *in vacuo*.

Preparation of Bis(2,2'-bipyridine) (4-methyl-4'-vinyl-2,2'-bipyridine) Ruthenium(II) Bis(hexafluorophosphate)

$Ru(vbpy)(bipy)_2.(PF_6)_2$ was produced using the method of Ghosh and Spiro.[121] 1.3g of cis-$Ru(bipy)_2Cl_2.2H_2O$, 0.5g of vinyl-bipyridine and 0.7g of sodium bicarbonate were refluxed together in 60ml of 2:3 methanol:water solution, until the $Ru(bipy)_2Cl_2$ was used up (as indicated by the absorption spectrum). 4ml of aqueous 3 mol $l^{-1}$ ammonium hexafluorophosphate was added and a red solid precipitated out. The final product was recrystallised from acetone/dichloromethane.

Attempted Resolution of cis-Bis(2,2'-bipyridine) Bis(4'-vinyl-pyridine) Ruthenium(II) Bis(chloride), cis-Bis(1,10-phenanthroline) Bis(4'-vinyl-pyridine) Ruthenium(II) Bis(chloride) and cis-Bis(1,10-phenanthroline) Bis(pyridine) Ruthenium(II) Bis(chloride)

The attempted resolution of cis-$[Ru(bipy)_2(vpy)_2]^{2+}$, cis-$[Ru(phen)_2(vpy)_2]^{2+}$ and cis-$[Ru(phen)_2\ py_2]^{2+}$ was done using the literature method of Bosnich and Dwyer,[123] for the resolution of cis-$[Ru(phen)_2\ py_2]^{2+}$. A solution of sodium arsenyl-(+)-tartrate (0.61g) in warm water (10ml) was added to a solution of cis-$[Ru(phen)_2\ py_2]Cl_2$ (0.63g) in water (10ml). On scratching the sides of the beaker, a canary yellow diastereoisomer precipitated, and after

cooling the solution slowly to 5°C, the crystals were collected, washed with water (5ml), followed by acetone.

To the filtrate, which contained the 5ml of water used for washing, excess ammonium nitrate was added and the mixture was allowed to stand at 0°C for 15 minutes. The yellow crystals of the "laevo" nitrate thus precipitated were filtered, washed with ice cold water, and sucked dry at the pump.

The diastereoisomer was suspended in a solution of water (5ml) containing 0.75ml of 15N nitric acid. The mixture was stirred and warmed to 40°C, whereupon the solid dissolved to give a yellow solution which deposited the "dextro" nitrate when excess ammonium nitrate was added. After collecting the solid, it was recrystallised from acetone by the addition of ether.

This method was used on both of the vpy complexes with no success. It was then repeated using sodium antimonyl-(+)-tartrate as the resolving agent again with no success. It was repeated using the exact compounds stated in the literature i.e. cis-$[Ru(phen)_2\ py_2]^{2+}$ and sodium antimonyl-(+)-tartrate. This also produced no resolution.

Resolution of Tris(2,2'-bipyridine) Ruthenium(II) Iodide

$Ru(bipy)_3I_2$ was resolved using the method of Dwyer and Gyarfas.[126] The racemic iodide (2.0g) was converted into

the antimonyl-(+)-tartrate, by shaking with silver antimonyl-(+)-tartrate (0.9g), silver iodide precipitating out and removed by filtration. The solution was concentrated on a rotary evaporator and then cooled in ice, whereupon the antimonyl-(+)-tartrate salt crystallised out. The red crystals were washed with a small quantity of ice cold ethanol to remove traces of more soluble salts. The red crystals were then dissolved in hot water and fractionally precipitated by addition of potassium iodide solution.

This only produced partial resolution so additional fractional crystallisation was required so as to produce the (+) and (-) enantiomers in 100% optical purity.

Resolution of Tris(4-methyl-4'-vinyl-2,2'-bipyridine) Ruthenium(II) Bis(Iodide) and Bis(2,2'-bipyridine)4-methyl-4'-vinyl-2,2'-bipyridine Ruthenium(II) Bis(Iodide)

$Ru(vbpy)^{2+}$ and $Ru(bipy)_2(vbpy)^{2+}$ were resolved using the same method as for the resolution of $Ru(bipy)_3^{2+}$. Again the literature method had to be extended to produce optically pure enantiomers by further fractional crystallisation.

# Chapter 3

# RESULTS AND DISCUSSION

## Preparation and Resolution of Complexes

### Synthesis of 4-methyl-4'-vinyl-2,2'-bipyridine (vbpy)

The first reported synthesis of 4-methyl-4'-vinyl-2,2'-bipyridine was by Ghosh and Spiro. The first stage of the synthesis (the production of 4-hydroxyethyl-4'-methyl-2,2'-bipyridine) worked well but the second stage (dehydration to give the vinyl group) produced no detectable yields at all. Refluxing in xylene with $P_2O_5$ seems to have been much too harsh a procedure with the 4-hydroxyethyl-4'-methyl-2,2'-bipyridine decomposing to produce a black tar. The inability of the second stage to produce the vinyl compound is confirmed in the literature. Several other groups have failed to isolate any vbpy.

The alternative method by Guarr and Anson (heating the 4-hydroxyethyl-4'-methyl-2,2'-bipyridine in a vacuum sublimator with sodium hydroxide) worked very well and also purified the vbpy considerably. Pure white crystals were produced, the only problem being "splashing" of the "oily" 4-hydroxyethyl-4'-methyl-2,2'-bipyridine directly onto the cold finger.

4-vinylpyridine complexes

Since 4-vinylpyridine (vpy) is commercially available from Aldrich, work was done on the ruthenium complexes containing at least one "vinylpyridine" ligand. The complexes produced were cis-$[Ru(bipy)_2(vpy)_2]^{2+}$ and cis-$Ru(phen)_2(vpy)_2^{2+}$. The resolution of both complexes was attempted using a method analogous to the one of Bosnich and Dwyer for the resolution of $Ru(phen)_2(py)_2^{2+}$ (where py is pyridine). This involved making the diastereoisomers by reacting the ruthenium complex with sodium arsenyl-(+)-tartrate. Neither cis-$Ru(bipy)_2(vpy)_2^{2+}$ nor cis-$Ru(phen)_2(vpy)_2^{2+}$ were resolved using this method. In fact no degree of enantiomeric excess was recorded after several attempts (including a comprehensive series of fractional crystallisations).

The above procedures were repeated using sodium antimonyl-(+)-tartrate in order to produce the diastereoisomers. Again no resolution at all was detected.

It was therefore assumed that the vinyl-pyridine was causing the problems with resolution so another reaction scheme was devised:-

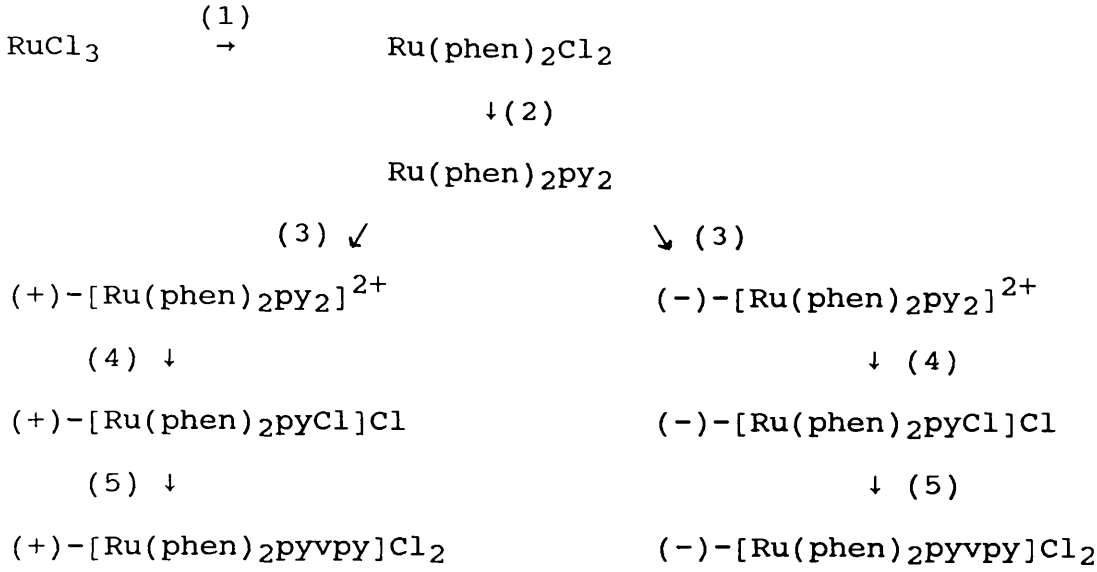


The resolution (step 3) of $Ru(phen)_2py_2$ is reported in the literature. Step (4) is also a literature method. The only non-literature preparation is the last step (reaction (5) ) although it is based on the analogous reaction with pyridine to produce $[Ru(phen)_2py_2]Cl_2$.

Therefore it was assumed that the above process would work easily. It failed, however, at stage (3). No notable resolution was recorded. It was therefore assumed that the resolution process was at fault. Sodium antimonyl-(+)-tartrate was being used although the literature specified sodium arsenyl-(+)-tartrate. The use of sodium arsenyl-(+)-tartrate, however, did not produce resolution either.

A subsequent method for the resolution of these complexes was found which used silver antimonyl-(+)-tartrate. The

advantage with this method is that on production of the diastereoisomers, the other ions in solution are precipitated out (i.e. silver chloride) leaving only the ruthenium complex with the antimonyl-(+)-tartrate counter ion in solution. This resulted in low resolution of the ruthenium complexes. In the first literature method above, the sodium and chloride ions in solution must have hampered the resolution. Perhaps on crystallisation the sodium and chlorine ions impede the formation of the diastereoisomers.

With the successful production of vinyl-bipyridine, no more work was carried out on the vinyl-pyridine complexes. For future work, resolution would be carried out using silver antimonyl-(+)-tartrate. During the search for a method of resolution, a synthetic process for the production of a singly vinylated monomer ( (-)-$[Ru(phen)_2$ py vpy$]Cl_2$) was theorised. This should produce the desired polymer type although its stability would probably be less than that of (-)-$[Ru(bipy)_2(vbpy)]Cl_2$.

"Vinyl-bipyridine" complexes

The first "vinyl-bipyridine" complex to be synthesised was $[Ru(vbpy)_3]^{2+}$. this was a one step process from the starting materials of $RuCl_3$ and vbpy. Polymerisation of this was carried out successfully but work on this system was not continued as it used up three moles of vinyl-bipyridine to make one mole of the ruthenium monomer. Also with three vinyl groups per monomer, cross-linking would occur. This would produce a much more stable polymer but might not have the ordered structure required of a chiral sensor.

It was therefore decided to concentrate work on a single vinyl-bipyridine containing ruthenium complex. These are harder to polymerise but the polymer chains will have no cross-linking and as such will produce second order spiralling. It was postulated that with the resolved monomers, the spiralling would be of a single helicity.

Resolution of $[Ru(bipy)_2(vbpy)]^{2+}$

$[Ru(bipy)_2(vbpy)]^{2+}$ was synthesised as described before. Attempted resolution was then carried out using silver antimonyl-(+)-tartrate. Immediately, partial resolution was effected but, unlike the literature method, precipitating half of the sample did not produce 100% (R) or (S). The testing was made more difficult by the fact that a batch of crystals precipitated in one attempt were not all of the same resolution. Crystals taken from the top could be of different resolution compared with crystals taken from the bottom. As such, each sample had to be dissolved, tested for resolution, and recrystallised before continuing. In an extreme case, almost pure (+) was discovered in the same crystallisation as almost pure (-) (different crystal sizes allowed the possibility of testing both separately).

Eventually both (+)- and (-)-$[Ru(bipy)_2(vbpy)]^{2+}$ were resolved.

## Electrode Studies

### Polymerisation of $[Ru(bipy)_2(vbpy)]^{2+}$

$[Ru(bipy)_2(vbpy)]^{2+}$ was polymerised as a 0.1mol $l^{-1}$ solution of TBA $BF_4$ in acetonitrile. The counter-ion was hexafluorophosphate. The potential was scanned from -1.00V to -2.05V (vs. $Ag/Ag^+$) and the build up of polymer (although not visible to the eye initially) could be seen from the increasing peak height on the cyclic voltammogram (see fig. 26). Polymerisation was slow and had to be left for several hours before a noticeable build up of polymer was achieved.

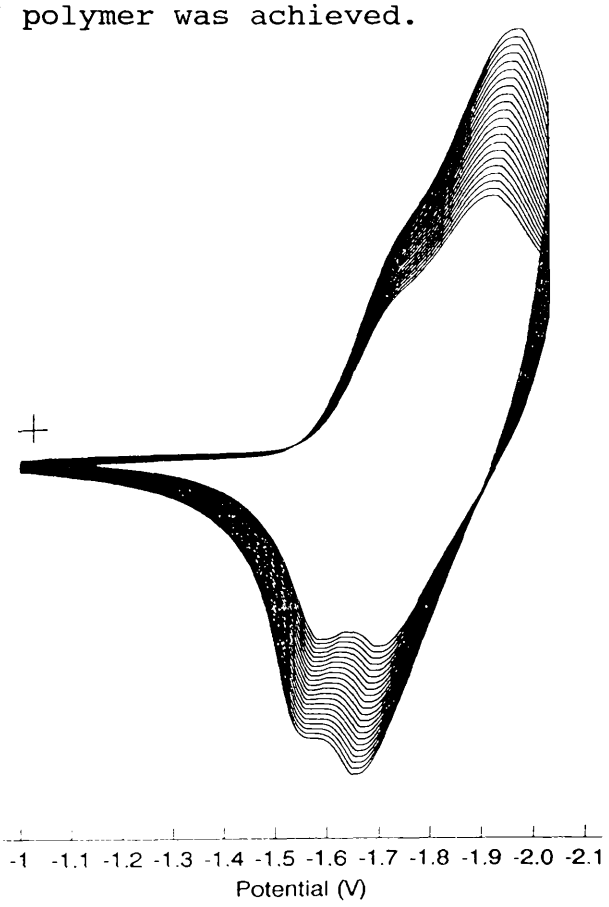


Fig. 26. Cyclic voltammogram of $[Ru(bipy)_2(vbpy)]^{2+}$ in a 0.1 mol $l^{-1}$ solution of TBA $BF_4$ in acetonitrile. The first 22 scans recorded.

In the literature there are varying reports on $[Ru(bipy)_2(vbpy)]^{2+}$ polymerisation - from slow to non-existent. From fig. 27 it can be seen that the polymerisation follows the linear build-up of previous cycling electropolymerised polymers.

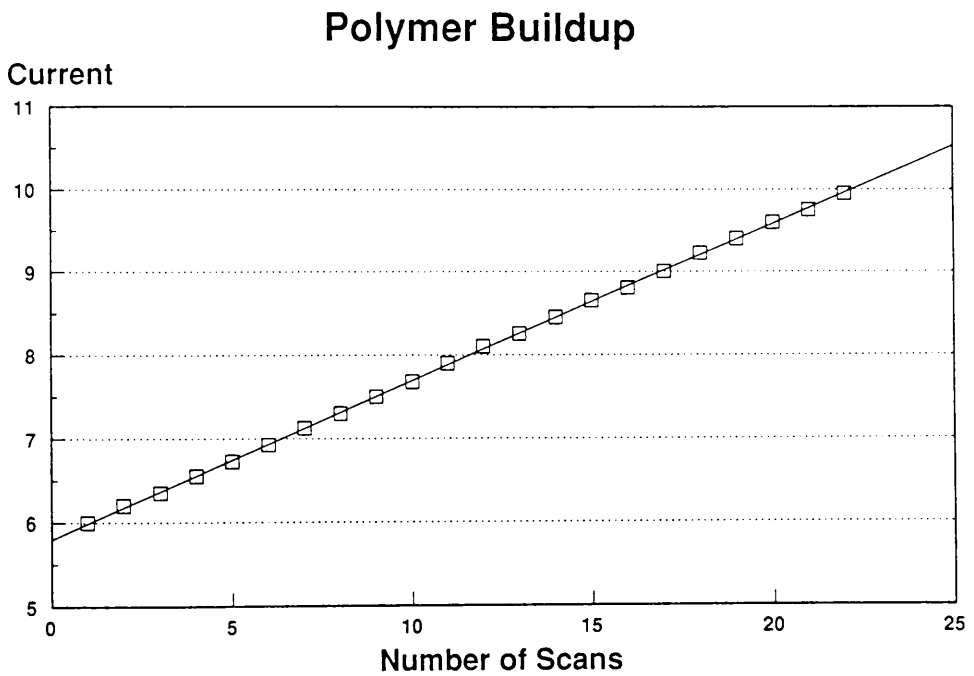


Fig. 27. Graph of Current vs. Number of scans for the build up of $[Ru(bipy)_2(vbpy)]^{2+}$ in a 0.1 mol $l^{-1}$ solution of TBA $BF_4$ in acetonitrile.

It was noticeable, however, that a lot of polymer seemed to drop from around the electrode (on reduction) and formed a layer at the bottom of the electrochemical cell. This layer re-dissolves back into solution but the ruthenium is not in the same state as the starting monomer since no polymerisation occurs after the solution

has been used for a certain time. The extinction coefficient of the solution is not significantly lower than the original solution indicating that most of the ruthenium is still present. The peaks of the U.V. of the exhausted solution seem not to differ from the peaks of the original monomer solution. It was therefore assumed that some kind of soluble "polymer" material (of almost identical structure to the monomer) is produced which cannot undergo further polymerisation due to lack of vinyl groups.

The original polymer grown was relatively uneven and therefore magnetic stirring in the electrochemical cell of the monomer solution was introduced. This, however, produced electrodes with a hole in the polymer consistently at the point where the auxiliary and working electrode were closest together. It was thought that this was due to the warping of the flux lines between the electrodes by the magnetic field of the magnetic stirrer.

As such, polymerisation was continued with no stirring and subsequent electrodes had no holes in the polymer covering.

## $[Ru(bipy)_3]^{2+}$ interactions with poly-$[Ru(bipy)_2(vbpy)]^{2+}$

Initially it was thought that polymers of $[Ru(bipy)_2(vbpy)]^{2+}$ would interact best with $[Ru(bipy)_3]^{2+}$ as they both have in effect the same structure. Therefore, $[Ru(bipy)_3]^{2+}$ was resolved into its (+)- and (-)- enantiomers using the same method as for $[Ru(bipy)_2(vbpy)]^{2+}$.

Three solutions of (+)-$[Ru(bipy)_3]^{2+}$, (-)-$[Ru(bipy)_3]^{2+}$, and (±)-$[Ru(bipy)_3]^{2+}$ were made up to exactly the same concentrations (~$5x10^{-3}$ mol $l^{-1}$) and checked using UV/vis spectroscopy. The $[Ru(bipy)_3][PF_6]_2$ was dissolved in a solution of 0.1 mol $l^{-1}$ TBA $BF_4$ in acetonitrile.

The chiral electrode, Pt/poly-(-)-$[Ru(bipy)_2(vbpy)]^{2+}$, was then immersed in these solutions and the first cycle of the C.V. recorded (see fig. 28).

(a)

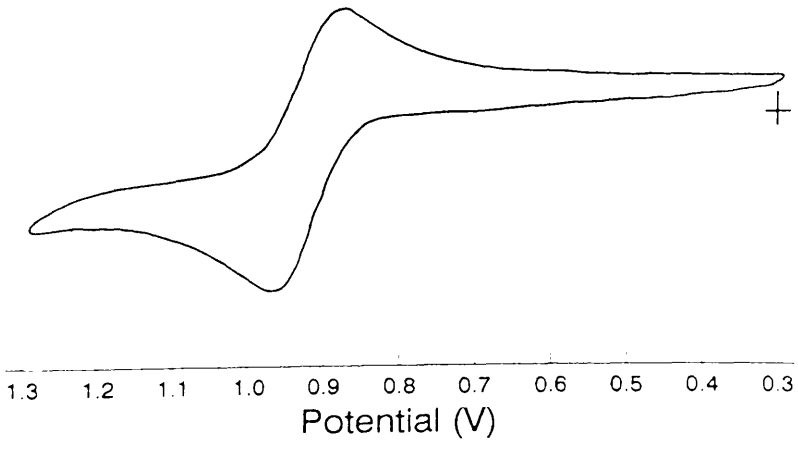

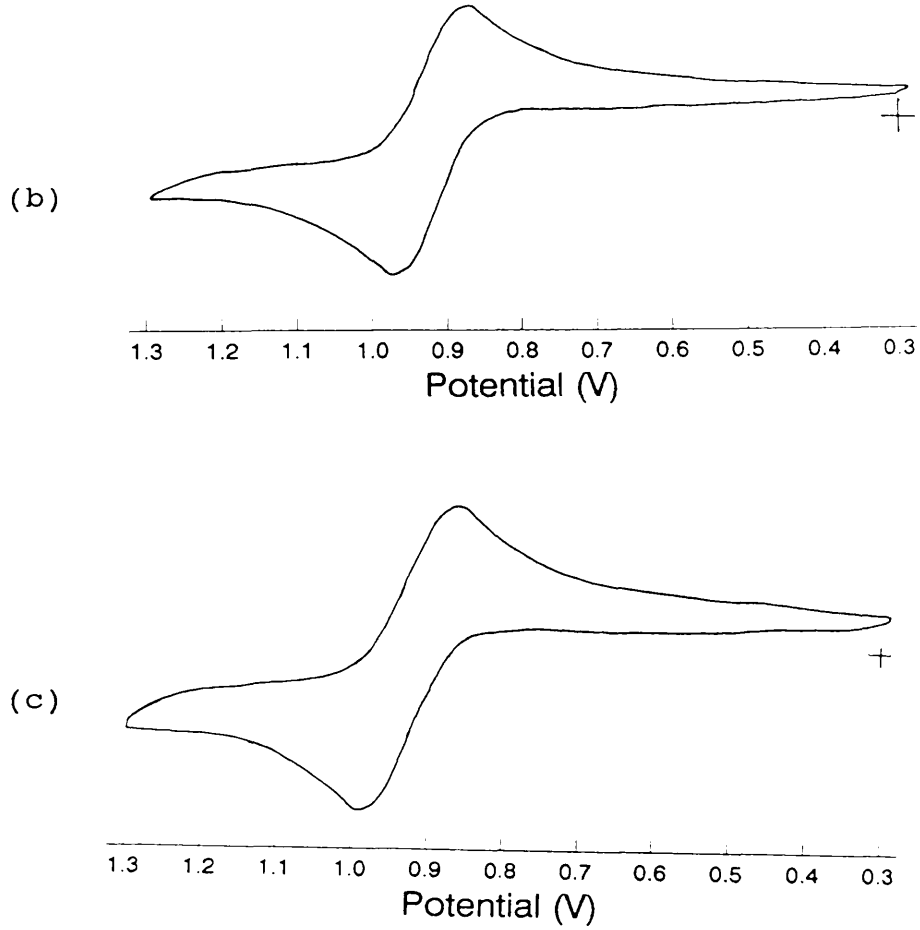


Fig. 28. Cyclic voltammogram of a Pt/poly-(-)-$[Ru(bipy)_2(vbpy)]^{2+}$ electrode immersed in (a) (+)-$[Ru(bipy)_3]^{2+}$, (b) (-)-$[Ru(bipy)_3]^{2+}$ and (c) (±)-$[Ru(bipy)_3]^{2+}$.

The first cycle was used consistently since the peak height of subsequent cycles changes. The polymer was also run in a 0.1mol $l^{-1}$ solution of TBA $BF_4$ to obtain the peak due to the polymer on its own (see fig. 29).

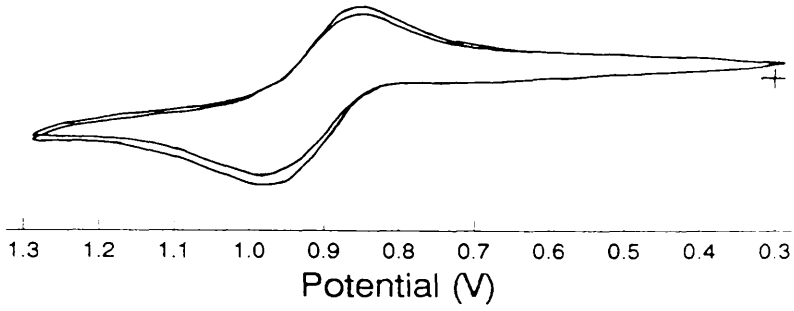


Fig. 29 Cyclic voltammogram of a Pt/poly-(-)-$[Ru(bipy)_2(vbpy)]^{2+}$ electrode immersed in a 0.1 mol $l^{-1}$ solution of TBA $BF_4$ in acetonitrile (peak height decreasing).

On over-lapping the C.V.'s of the electrode in (+)-$[Ru(bipy)_3]^{2+}$ and (-)-$[Ru(bipy)_3]^{2+}$ (see fig. 30) it can be seen that there is a slight difference in peak height between the two (the (+)-$[Ru(bipy)_3]^{2+}$ was run first followed <u>immediately</u> by the (-)-$[Ru(bipy)_3]^{2+}$).

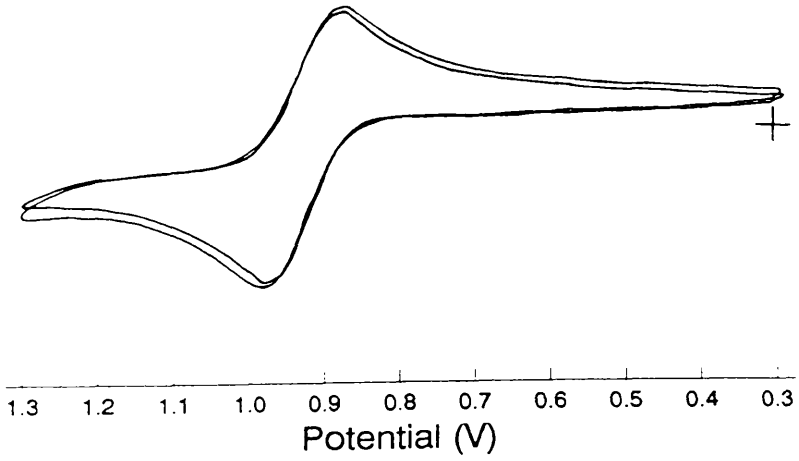


Fig. 30 Cyclic voltammogram of a Pt/poly-(-)-$[Ru(bipy)_2(vbpy)]^{2+}$ electrode immersed in (+)-$[Ru(bipy)_3]^{2+}$ and (-)-$[Ru(bipy)_3]^{2+}$ overlapped.

If the (±)-$[Ru(bipy)_3]^{2+}$ C.V. is now over-lapped onto fig. 30, it can be seen that it has slightly lower peak height again (see fig. 31).

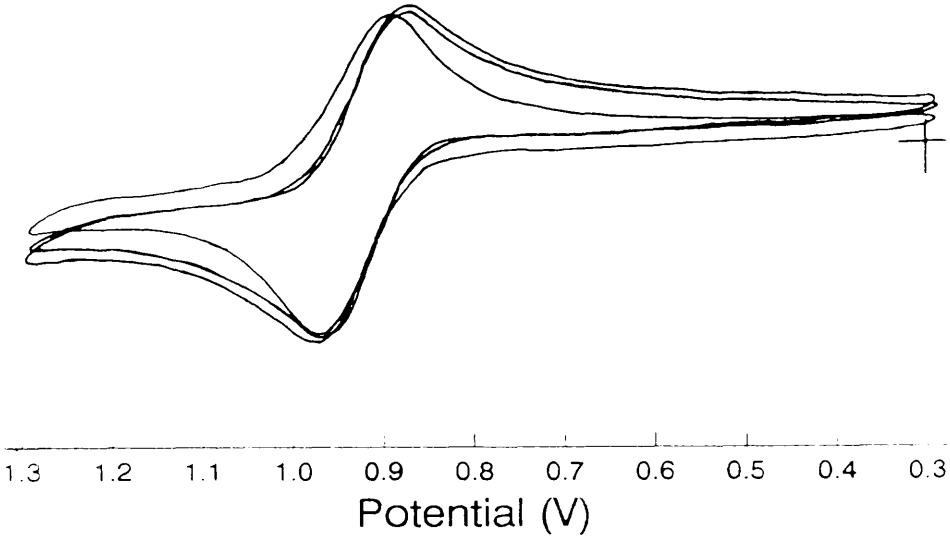


Fig. 31 Cyclic voltammogram of a Pt/poly-(-)-$[Ru(bipy)_2(ybpy)]^{2+}$ electrode immersed in (+)-$[Ru(bipy)_3]^{2+}$, (-)-$[Ru(bipy)_3]^{2+}$ and (±)-$[Ru(bipy)_3]^{2+}$ overlapped.

To confirm that no changes are present, the experimental was repeated, except that the (-)-$[Ru(bipy)_3]^{2+}$ was run first followed <u>immediately</u> by the (+)-$[Ru(bipy)_3]^{2+}$. Fig. 32 shows how the results from fig. 30 are reversed with the (-)-$[Ru(bipy)_3]^{2+}$ peak now being bigger than the (+)-$[Ru(bipy)_3]^{2+}$ peak. Obviously, the order that the solutions are run determines the peak height.

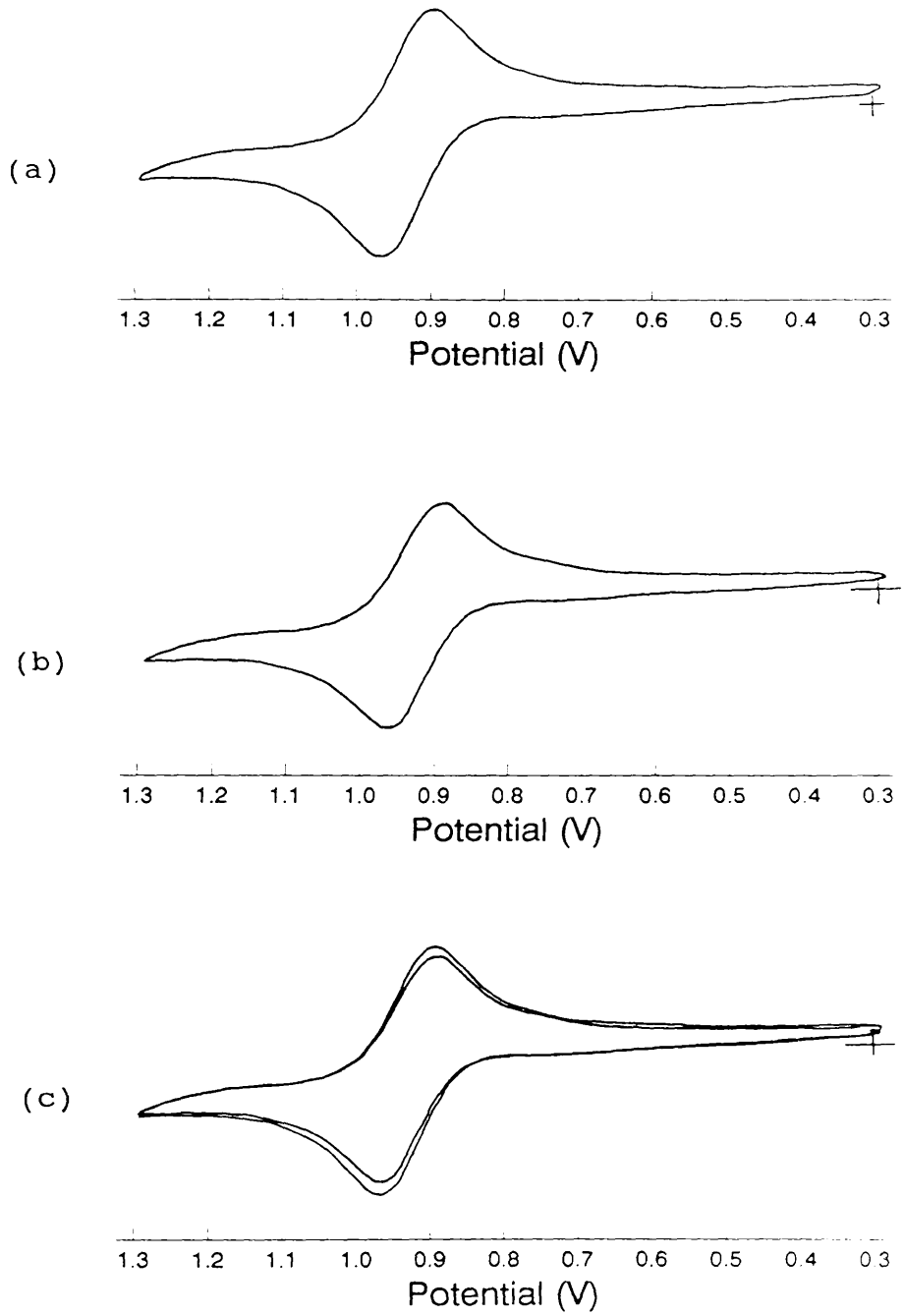


Fig. 32. Cyclic voltammogram of a Pt/poly-(-)-$[Ru(bipy)_2(vbpy)]^{2+}$ electrode immersed in (a) (-)-$[Ru(bipy)_3]^{2+}$, (b) (+)-$[Ru(bipy)_3]^{2+}$ and the two overlapped in (c).

This reduction in peak height must be due to polymer degradation since it was observed that the polymer run consecutively in 0.1 mol $l^{-1}$ TBA $BF_4$ in acetonitrile solution had a reduction in peak height (see fig. 33).

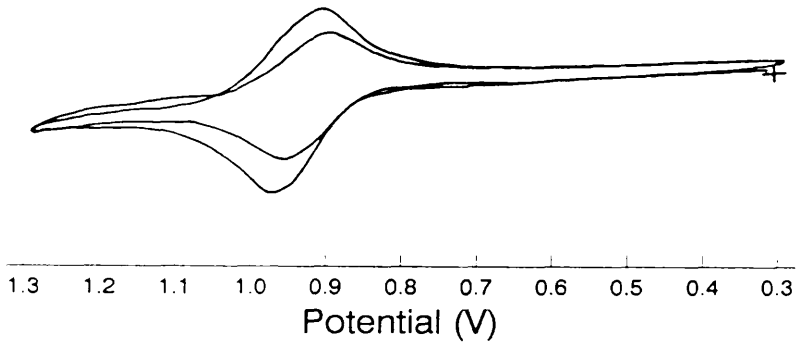


Fig. 33. Cyclic voltammogram of a Pt/poly-(-)-$[Ru(bipy)_2(vbpy)]^{2+}$ electrode immersed in a 0.1 mol $l^{-1}$ solution of TBA $BF_4$ in acetonitrile overlapped with the C.V. of the same system run 1 hour later (larger peak is first scan).

This degradation was quantified by immersing a new electrode into a solution of 0.1 mol $l^{-1}$ TBA $BF_4$ in acetonitrile. The polymer was scanned over a period of time and the C.V.'s recorded (see fig. 34).

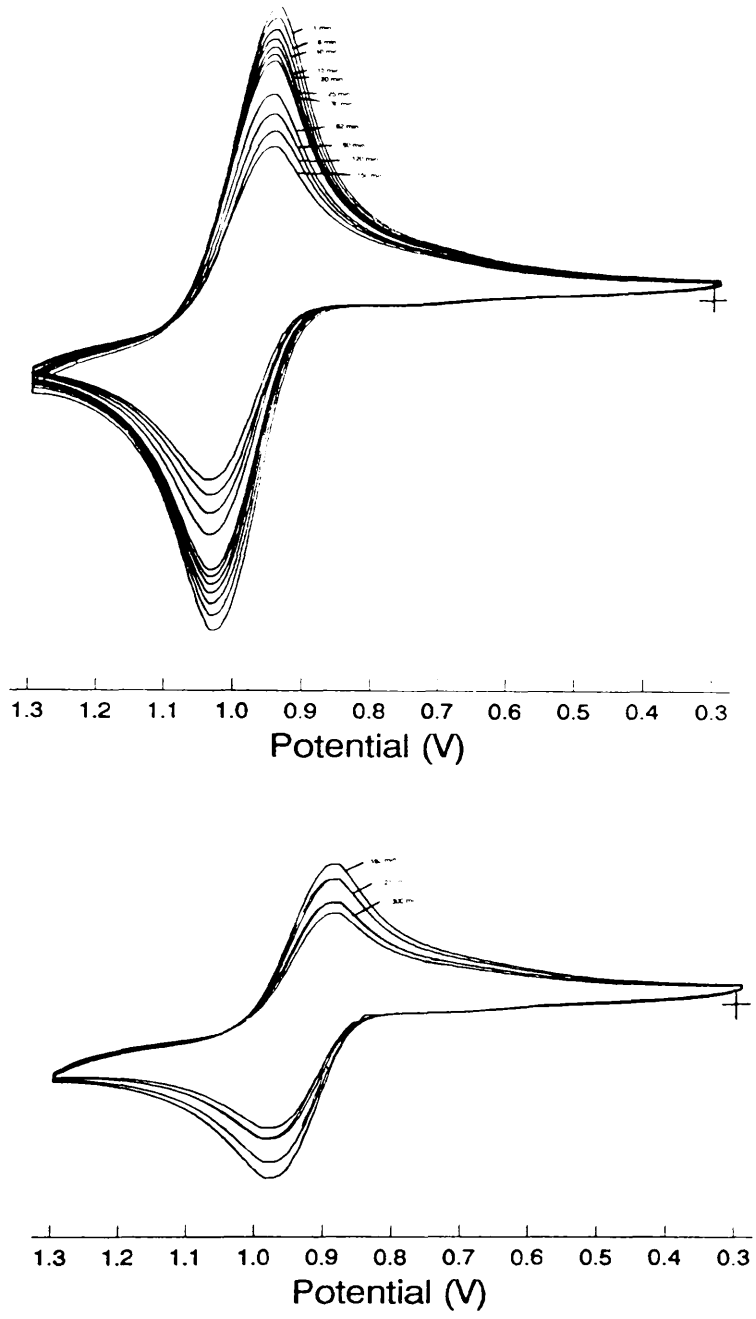


Fig. 34. Cyclic voltammogram of Pt/poly-(-)-$[Ru(bipy)_2(vbpy)]^{2+}$ electrode immersed in a 0.1 mol $l^{-1}$ solution of TBA $BF_4$ in acetonitrile over 5 hours.

It can be seen that, with time, the polymer is decomposing and the $Ru^{II/III}$ peak is decreasing in height (see fig. 35).

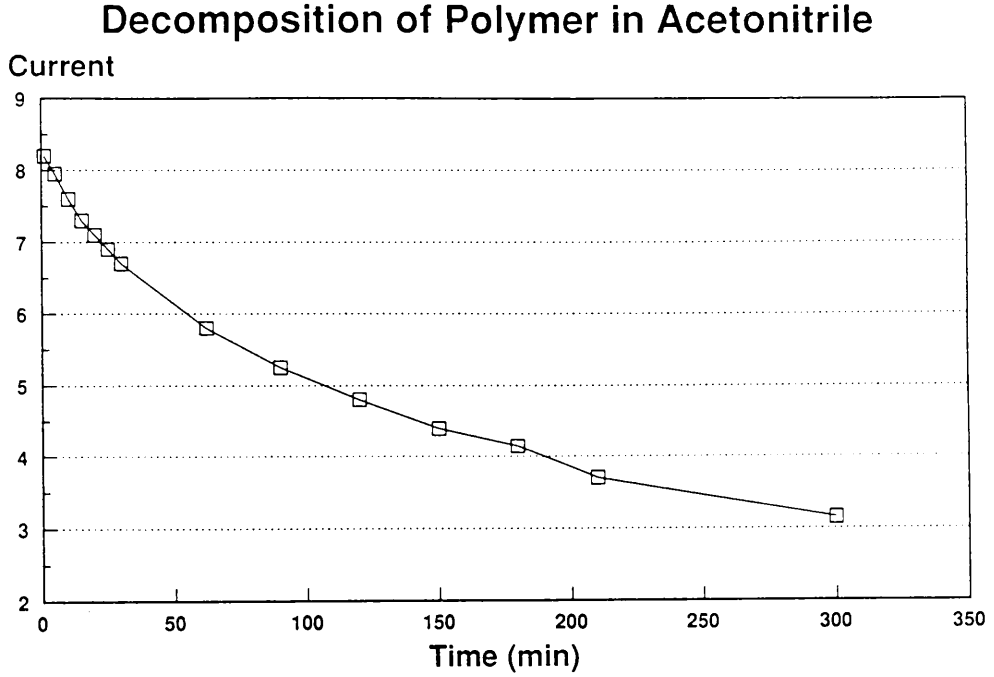


Fig. 35. Graph of decomposition of a Pt/poly-(-)-$[Ru(bipy)_2(vbpy)]^{2+}$ electrode while immersed in a 0.1 mol $l^{-1}$ solution of TBA $BF_4$ in acetonitrile.

This would make it virtually impossible to do any kind of peak height comparisons as they will be decreasing continuously. Also, since there are no voltage shifts due to the different interactions between the polymer and the various forms of the $[Ru(bipy)_3]^{2+}$, it is unlikely that, even if there are differences in the C.V.'s, that they will ever be detected under these conditions.

There are several different ways to continue this work. As was discovered later, the poly-$[Ru(bipy)_2(vbpy)]^{2+}$ polymer seems to have a much longer lifetime in aqueous solution. This is probably due to the fact that the

polymer was grown in acetonitrile with hexafluorophosphate as the counter ion. This means that in organic solvents, the polymer is more likely to re-dissolve back into solution, whereas in aqueous solution, it will be relatively insoluble. If the $[Ru(bipy)_3]^{2+}$ was converted to the chloride and the above work done in water, the rate of decay of the polymer might be reduced enough to show any detectable differences in the C.V.'s (if they are present).

Another possibility lies in the fact that $[Ru(vbpy)_3]^{2+}$, when polymerised, has a much longer lifetime with the literature reporting no reduction of the $Ru^{II/III}$ peak height in acetonitrile over several hours. Although these polymers do not have the ordered structure that the $[Ru(bipy)_2(vbpy)]^{2+}$ polymers have, they have the crosslinking which provides the stability required of a sensor.

The inherent problem with this system is the fact that the peak of the $[Ru(bipy)_3]^{2+}$ in solution lies at the exact potential of the peak for the $[Ru(bipy)_2(vbpy)]^{2+}$ polymer. This means that a background must be run and the peak subtracted from the original because small changes within a peak are harder to detect than small changes in a flat line.

As such the work in this field was discontinued.

Poly-$[Ru(bipy)_2(vbpy)]^{2+}$ in aqueous solution

It seems that poly-$[Ru(bipy)_2(vbpy)]^{2+}$ has a limited lifetime in organic solvents so its use as a chemical sensor lies in aqueous solvents.

A Pt/poly-$[Ru(bipy)_2(vbpy)]^{2+}$ electrode was immersed in different aqueous solutions primarily to find out what the working potential range of such electrolytic solutions would be.

From the C.V., the $Ru^{II/III}$ peak could be observed in 0.1mol $l^{-1}$ sulphuric acid (see fig. 36). There was no "drop off" in the base line until after +1.3V vs. SSCE and was fairly "flat" until approximately -0.5V.

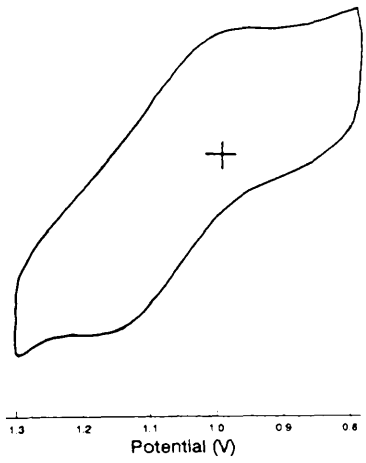


Fig. 36. Cyclic voltammogram of a Pt/poly-(-)-$[Ru(bipy)_2(vbpy)]^{2+}$ electrode immersed in 0.1 mol $l^{-1}$ solution of sulphuric acid in water.

For KCl, no peaks were observed because there was base-line cut-off at +1.1V due to oxidation of $Cl^-$. When the polymer was scanned down to +1.1V, the lifetime of the polymer was reduced. This was presumably due to the attack of the polymer by $Cl_2$. This would then break up the polymer making it soluble in the electrolyte solution. (This is confirmed by the solution turning yellow.)

With a solution of 0.1 mol $l^{-1}$ (+)-tartaric acid the C.V. can be scanned down to approximately +1.3V and up to approximately +0.1V. Although the "range" of (+)-tartaric went positive enough, no peaks could be detected for $Ru^{II/III}$ (see fig. 37).

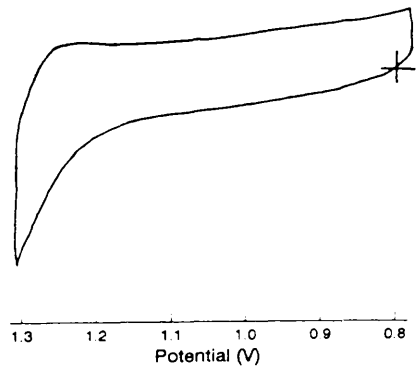


Fig. 37. Cyclic voltammogram of a Pt/poly-(-)-$[Ru(bipy)_2(vbpy)]^{2+}$ electrode immersed in a 0.1 mol $l^{-1}$ solution of (+)-tartaric acid in water.

While working with the above set up, the C.V. of the ruthenium polymer seemed to produce small, sharp peaks unlike standard diffusion controlled C.V. peaks (see fig.

38). These were not observed in either the aqueous KCl or the sulphuric acid even after prolonged soaking.

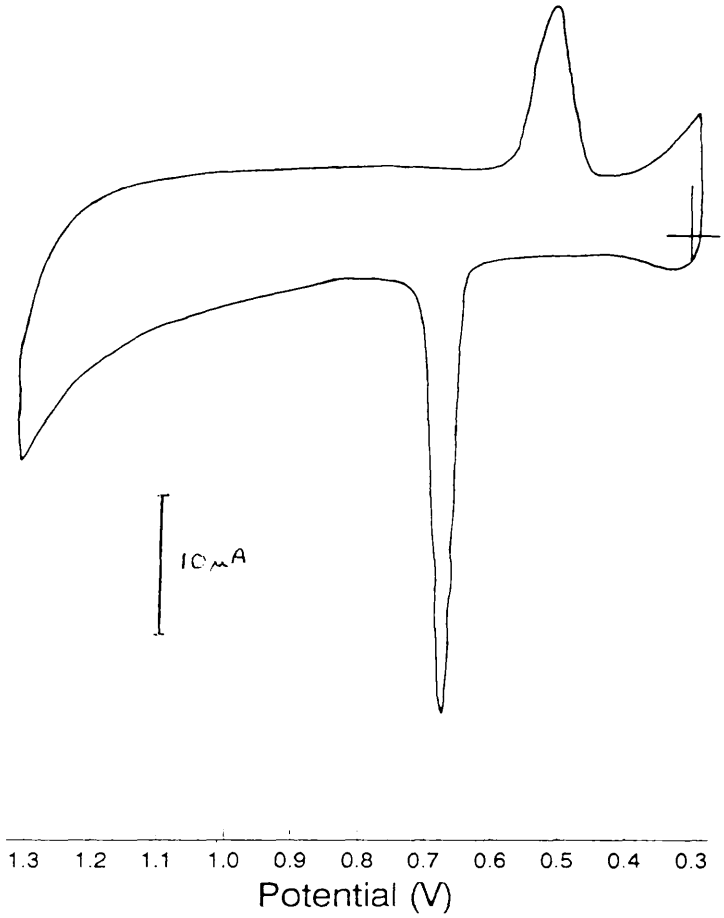


Fig. 38. Cyclic voltammogram of a Pt/poly-(-)-$[Ru(bipy)_2(vbpy)]^{2+}$ electrode immersed in a 0.1 mol $l^{-1}$ solution of (+)-tartaric acid in water after a period of time.

A C.V. of 0.1mol $l^{-1}$ (+)-tartaric acid was then run using a clean platinum electrode and no peaks were observed (see fig. 39). There seems to have been some kind of "reaction" between the tartaric acid and the polymer to produce certain peaks which are not otherwise present.

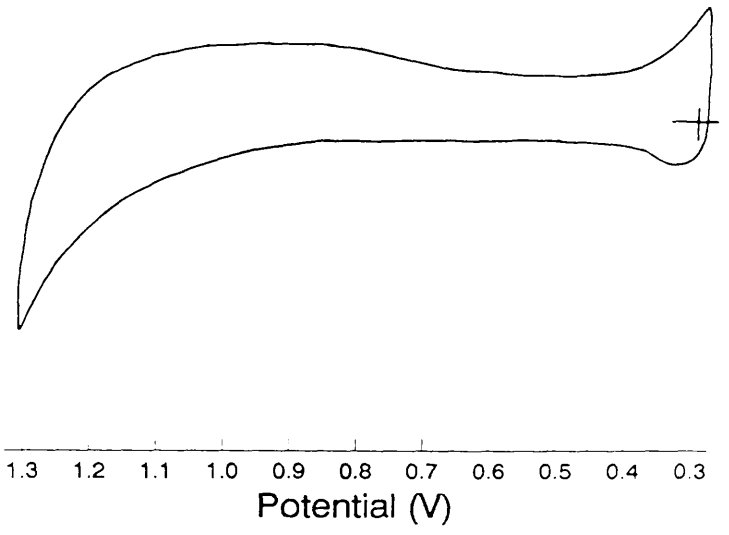


Fig. 39. Cyclic voltammogram of a Pt electrode immersed in a 0.1 mol $l^{-1}$ solution of (+)-tartaric acid in water.

The subsequent work done was on the interactions between poly-$Ru(bipy)_2(vbpy)^{2+}$, both racemic and the (-)-enantiomer, and tartaric acid, (+)-, (-)- and the racemate.

## poly-$[Ru(bipy)_2(vbpy)]^{2+}$ electrodes in tartaric acid

### Racemic poly-$[Ru(bipy)_2(vbpy)]^{2+}$ electrodes

#### Results

An electrode coated with racemic poly-$[Ru(bipy)_2(vbpy)]^{2+}$ $.2PF_6^-$ which is immersed in a 0.1 mol $l^{-1}$ solution of tartaric acid produces a C.V. like that in fig. 40. The C.V. produced was run at different scan speeds to compare the peak heights. The peak heights are of the order of 30μA when run at 200 mV/s (all spectra run at this speed). The peaks come at ~+0.65V (vs. SSCE) for the oxidation and ~+0.45V (vs. SSCE) for the reduction.

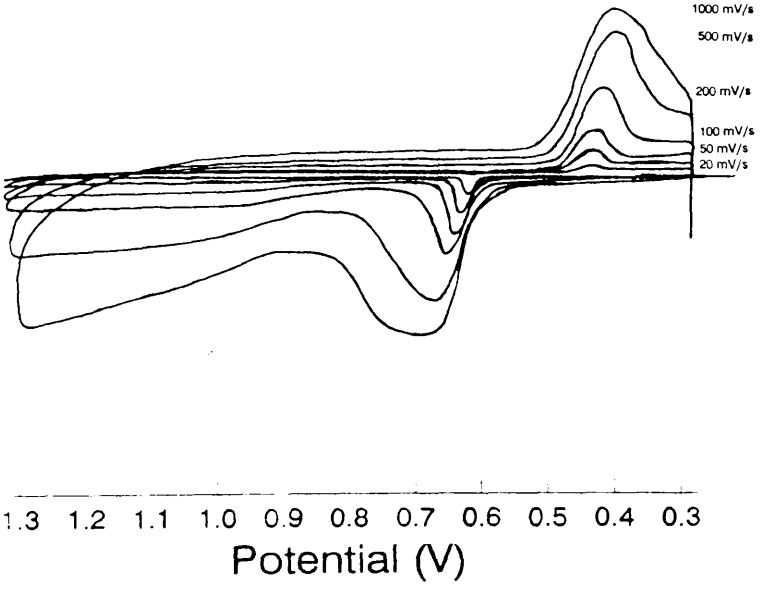


Fig. 40. Cyclic voltammogram of a Pt/poly-(±)-$[Ru(bipy)_2(vbpy)]^{2+}$ electrode immersed in a 0.1 mol $l^{-1}$ solution of (+)-tartaric acid in water scanned at different rates.

On repeatedly scanning, the peak heights reduce until an "equilibrium" height is achieved (see fig. 41) or the peak height drops to zero (see fig. 42). If the electrode is then left immersed in the solution, the peaks reappear with the peak heights being the same as the original peak heights. The time required for the immersion, however, differs from polymer to polymer. The time can be as short as one minute even when the reduction in peak height is quite considerable.

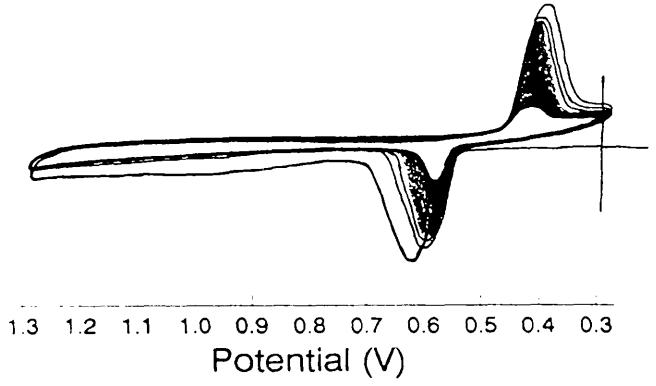


Fig. 41. Cyclic voltammogram of a Pt/poly-(±)-$[Ru(bipy)_2(vbpy)]^{2+}$ electrode immersed in a 0.1 mol $l^{-1}$ solution of (+)-tartaric acid in water.

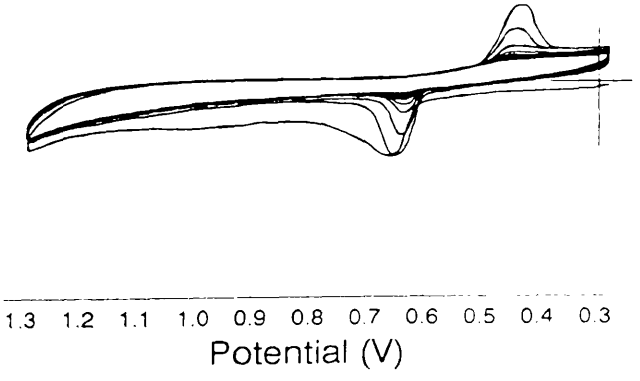


Fig. 42. Cyclic voltammogram of a Pt/poly-(±)-$[Ru(bipy)_2(vbpy)]^{2+}$ electrode immersed in a 0.1 mol $l^{-1}$ solution of (+)-tartaric acid in water.

It can be clearly seen that these peaks are not standard, diffusion controlled, solution C.V. peaks but are in fact relatively sharp peaks separated by approximately 0.2V.

The peaks were observed initially while scanning in the range +0.3V to +1.3V vs. SSCE. This range was chosen because a flat plot was obtained when scanning a platinum electrode in 0.1 mol $l^{-1}$ tartaric acid. If this scan range is reduced from +1.3V to +1.0V the peaks disappear even though the scan range should incorporate them. If the range is then increased back to +1.3V, the peaks reappear although not in the first half of the cycle. This absence of a peak in the first half of the cycle also occurs if the cell is switched off between scans.

This can be illustrated in the following set of experiments carried out one after another on an already conditioned electrode in (-)-tartaric acid (although (+)-tartaric acid would produce exactly the same results).

Fig. 43 shows the first C.V. after switching on the apparatus. Note the lack of peak at +0.65V in the first half of the scan.

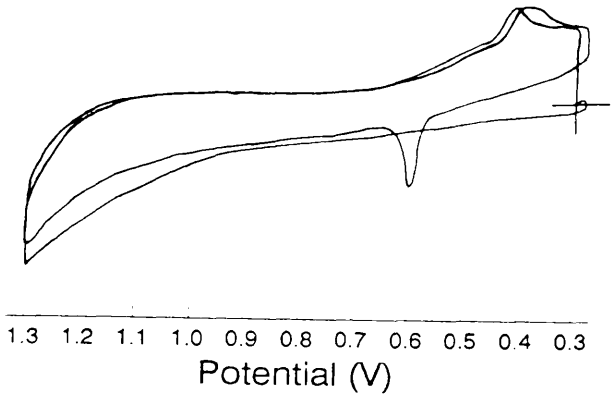


Fig. 43. Cyclic voltammogram of a Pt/poly-(±)-$[Ru(bipy)_2(vbpy)]^{2+}$ electrode immersed in a 0.1 mol $l^{-1}$ solution of (-)-tartaric acid in water after switching apparatus on.

Fig. 44 shows what happens if the scan range is reduced to +0.3V ↔ +1.0V. Note that the peak disappears. It should be noted that the apparatus was not switched off between fig. 43 and fig. 44.

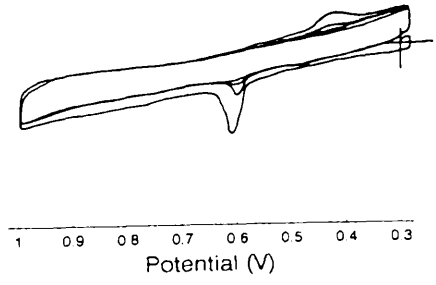


Fig. 44. Cyclic voltammogram of a Pt/poly-(±)-$[Ru(bipy)_2(vbpy)]^{2+}$ electrode immersed in a 0.1 mol $l^{-1}$ solution of (-)-tartaric acid in water (scan range reduced from +1.3V to +1.0V).

If the C.V is then run again still in the range +0.3V ↔ +1.0V, the C.V. produces no peaks (see fig. 45).

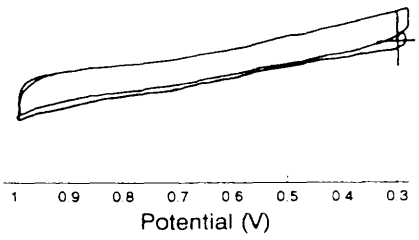


Fig. 45. Cyclic voltammogram of a Pt/poly-(±)-$[Ru(bipy)_2(vbpy)]^{2+}$ electrode immersed in a 0.1 mol $l^{-1}$ solution of (-)-tartaric acid in water.

On scanning again in the range +0.3V ↔ +1.3V, the C.V. in fig. 46 is produced. Note that there is again a lack of peak at +0.65V in the first scan.

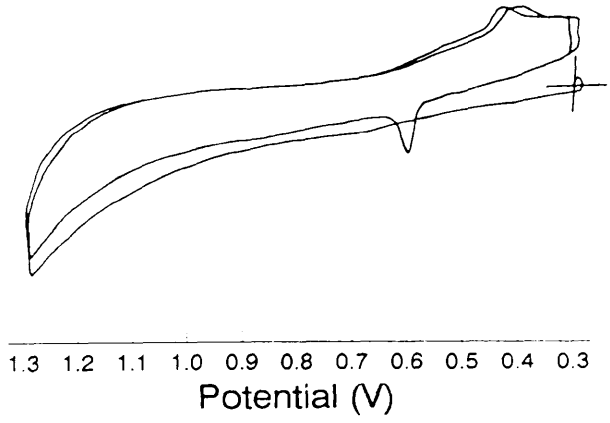


Fig. 46. Cyclic voltammogram of a Pt/poly-(±)-$[Ru(bipy)_2(vbpy)]^{2+}$ electrode immersed in a 0.1 mol $l^{-1}$ solution of (-)-tartaric acid in water (scan range increased from +1.0V to +1.3V).

If the apparatus is switched off for just a few seconds, a reduced peak at +0.65V is produced (see fig. 47(a) ) and if it is switched off for over 30 seconds then no peak appears at +0.65V (see fig. 47(b) ). Switching off

and on immediately produces no noticeable reduction in peak height (see fig. 47(c) ).

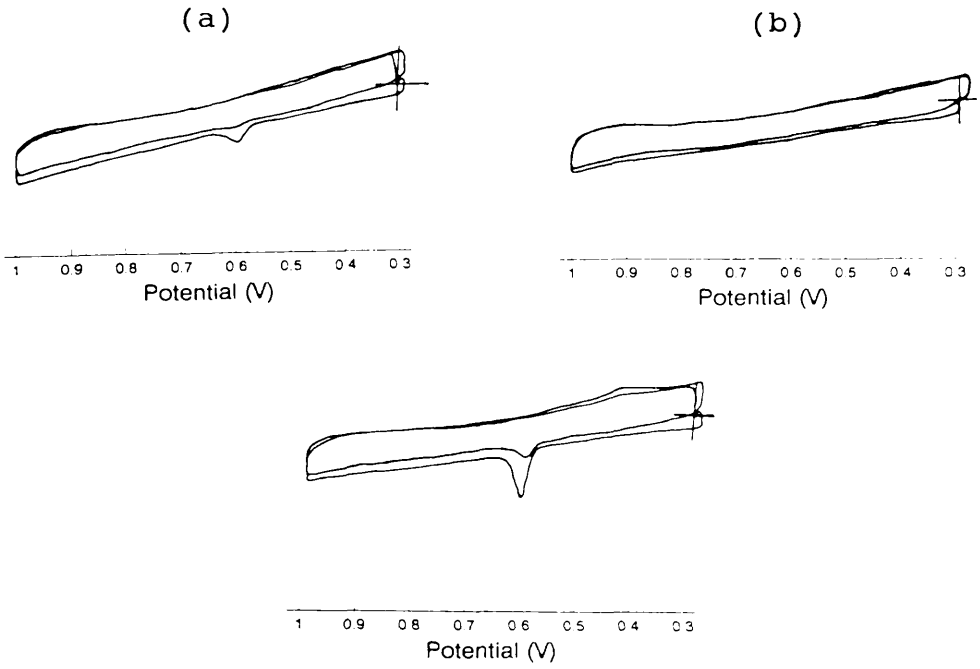


Fig. 47. Cyclic voltammogram of a Pt/poly-(±)-$[Ru(bipy)_2(vbpy)]^{2+}$ electrode immersed in a 0.1 mol $l^{-1}$ solution of (-)-tartaric acid in water after switching off apparatus for (a) a few seconds, (b) over 30 seconds and (c) less than a second.

If the polymer is then scanned from +0.3V to +1.3V, the standard peaks return. Without switching off, a scan from +0.55V ↔ +1.3V produces the C.V in fig. 48(a). This shows that the potential must be scanned below this (see fig. 48(b) ) in order that the peak at +0.65V is present on the second scan i.e. the reduction at +0.45V is necessary in order that the oxidation at +0.65V occurs.

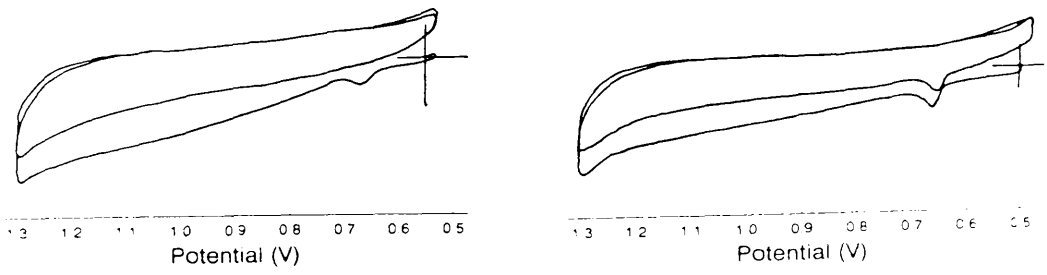


(a) (b)

Fig. 48. Cyclic voltammogram of a Pt/poly-(±)-$[Ru(bipy)_2(vbpy)]^{2+}$ electrode immersed in a 0.1 mol $l^{-1}$ solution of (-)-tartaric acid in water scanned to (a) +0.55V and (b) +0.50V.

If the polymer coated electrode is cleaned with 5μ diamond paste, then no peaks occur. This is the equivalent of a pure platinum electrode scanned in tartaric acid (care should be taken to make sure that the auxiliary electrode is cleaned or else peaks can occur without any polymer being present on the working electrode).

The previous discussion is made more complicated with the results obtained when scanning the polymers when initially dipped in tartaric acid (see fig. 49). To begin with the C.V.'s obtained are complex and require some time to become the standard "spikes" at +0.45V and +0.65V.

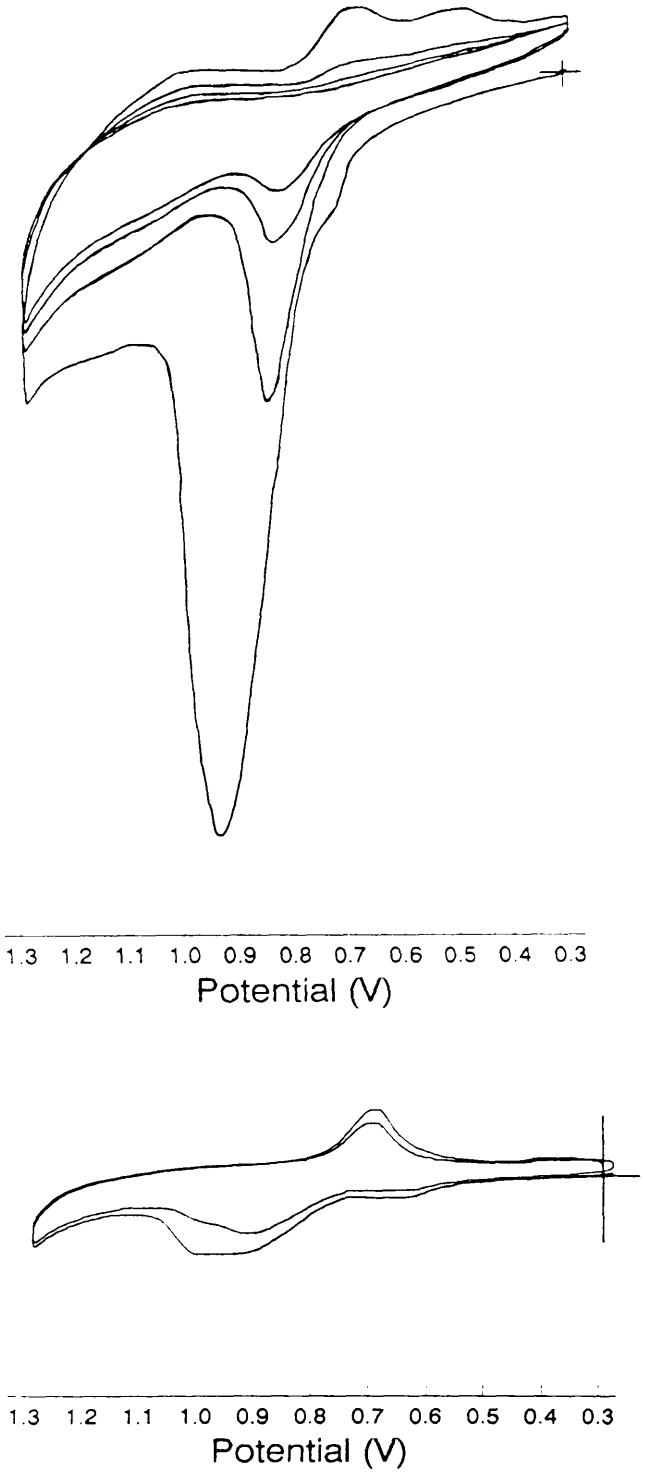


Fig. 49. Cyclic voltammogram of a Pt/poly-(±)-$[Ru(bipy)_2(vbpy)]^{2+}$ electrode initially immersed in a 0.1 mol $l^{-1}$ solution of tartaric acid in water.

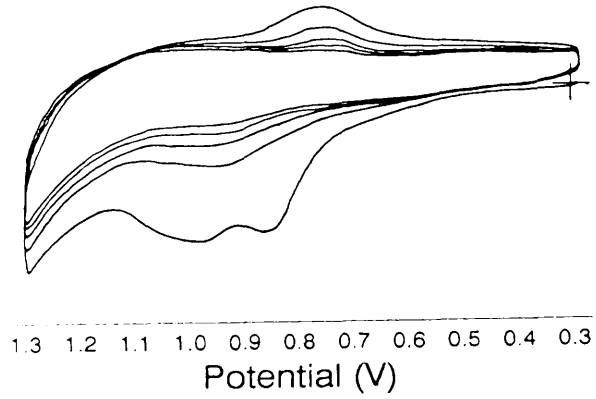


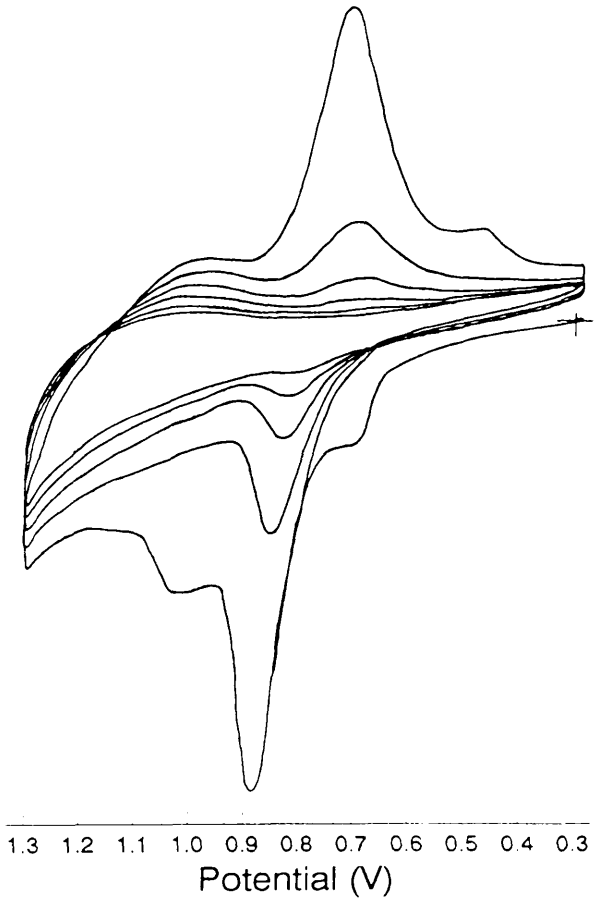


Fig. 49. Cyclic voltammogram of a Pt/poly-(±)-$[Ru(bipy)_2(vbpy)]^{2+}$ electrode initially immersed in a 0.1 mol $l^{-1}$ solution of tartaric acid in water.

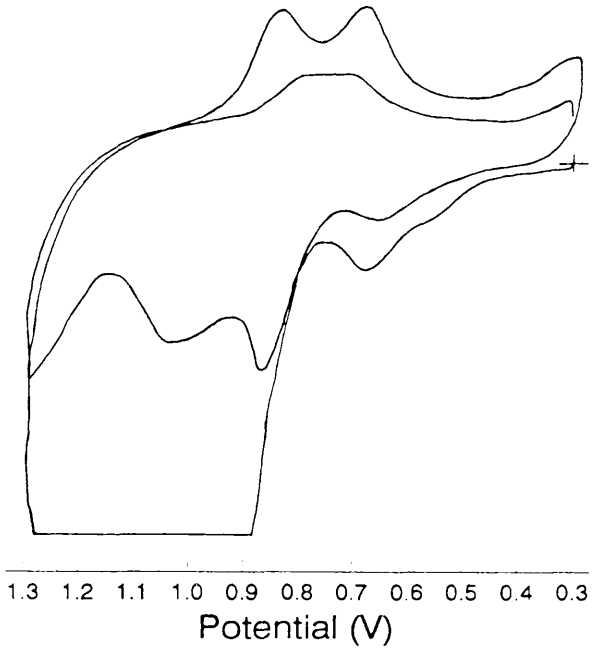


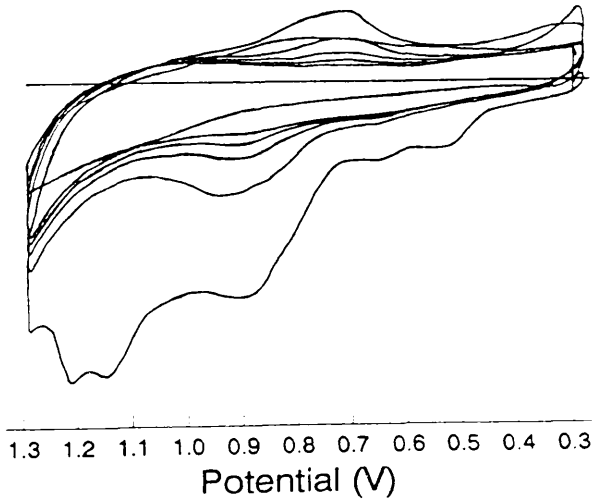


Fig. 49. Cyclic voltammogram of a Pt/poly-(±)-$[Ru(bipy)_2(vbpy)]^{2+}$ electrode initially immersed in a 0.1 mol $l^{-1}$ solution of tartaric acid in water.

Discussion

The sharp peaks obtained are characteristic of polymer films that have been poorly solvated due to being used in aqueous solvent or are of high molecular weight. Since both of these conditions occur in the above system (the polymer films are relatively thick), sharp peaks would be expected. This indicates that the interactions within the polymer are strong due to lack of solvation effects.

What is unusual compared with the literature is the potential difference between the oxidation and reduction peaks. Normally when the peaks are "spiked", the potential difference is very small. This is due to the scans being carried out at relatively low scan rates. If the scan rate is increased, the "spiking" disappears and the return to standard C.V. waves occurs.

Literature has reported "spiking" with a large potential gap between the oxidation and reduction peaks. This is observed in bilayer systems where the redox reaction of the outer layer is restricted by that of the inner layer. In the example on page 70, the peaks were separated by several volts. The possibility of a bilayer being produced in the above system is not immediately apparent but cannot be discounted at present.

What is more likely is that we have an ion exchange type polymer similar to Nafion. Work done on Nafion polymer electrodes with tetrathiofulvalenium ($TTF^+$) incorporated in them and immersed in a solution of 1.0 mol $l^{-1}$ KBr produces C.V.'s similar to those obtained for our system above. The spiking is explained as above in that we have a poorly solvated polymer (high molecular weight) which results in the "incorporated species" having strong interactions between them. The large gap between the peaks (in the Nafion case approximately 0.2V) is explained by a species being produced which is very similar to the original but slightly more stable which results in it having a longer lifetime when scanned in the opposite direction. In the Nafion case the more stable species is thought to be $TTFBr_{0.7}$, the Br picked up from the aqueous solution of 1.0 mol $l^{-1}$ KBr. This causes the corresponding C.V. peak to occur at the slightly different potential. In our system it is conceivable that the species responsible for the peaks is in some way modified by one of the solution species to cause the shifting of one of the C.V. peaks. In the Nafion example, this occurs as a square reaction scheme (see page 63) so therefore it would be assumed that our system would undergo a similar sort of reaction.

In the above system, no peaks occur for poly-$[Ru(bipy)_2(vbpy)]^{2+}$ at or close to +0.5V vs. SSCE. Neither are any peaks observed at this potential when

running the C.V. of tartaric acid using a plain platinum electrode. As such, the peaks can only be explained by some kind of reaction between the poly-$[Ru(bipy)_2(vbpy)]^{2+}$ and the tartaric acid.

These peaks are not present in their spiked form until a period of time (and a certain amount of potential scanning) has occurred. This also implies that some sort of reaction between the polymer and the electrolyte has taken place.

These peaks are made more complex with the observation that on scanning the polymer and then leaving it for a range of times (between a few seconds and a few minutes) and then scanning again, the reduction peak occurs at two different potentials. If the rest time is short (time = 5 seconds), the peak occurs at +0.37V (see fig. 50(a) ). If the rest time is long (time > 5 minutes ), the peak occurs at +0.45V (see fig. 50(g) ). If, however, a compromise is obtained (time = 40 seconds ), then both peaks can be observed simultaneously (see fig. 50(d) ). The transition between these states can be seen in figs. 50(b), 50(c), 50(e) and 50(f).

These times differ for different polymers but the intermediate state occurs within the range 0-2 minutes.

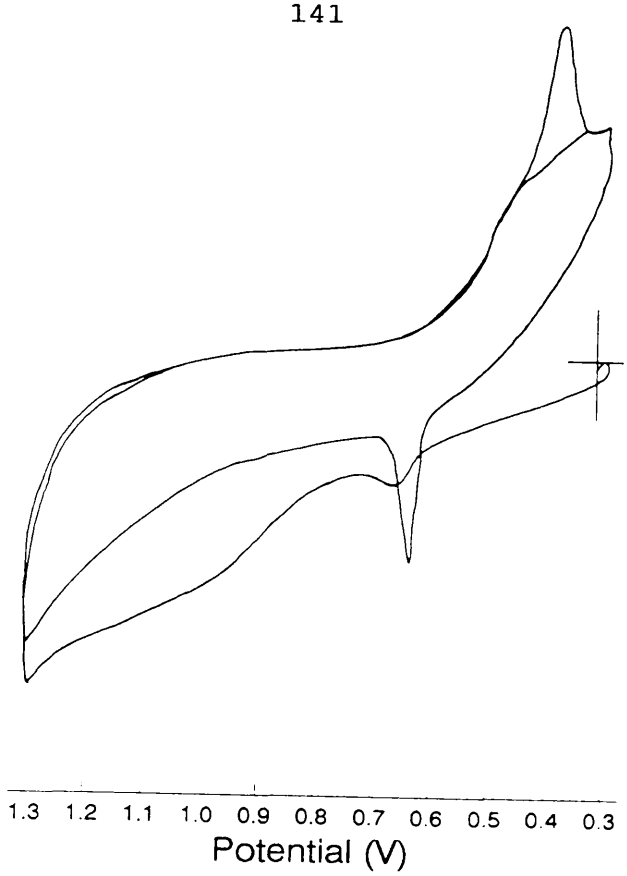


Fig. 50(a). Cyclic voltammogram of a Pt/poly-(±)-$[Ru(bipy)_2(vbpy)]^{2+}$ electrode immersed in a 0.1 mol $l^{-1}$ solution of (-)-tartaric acid in water after 5 seconds.

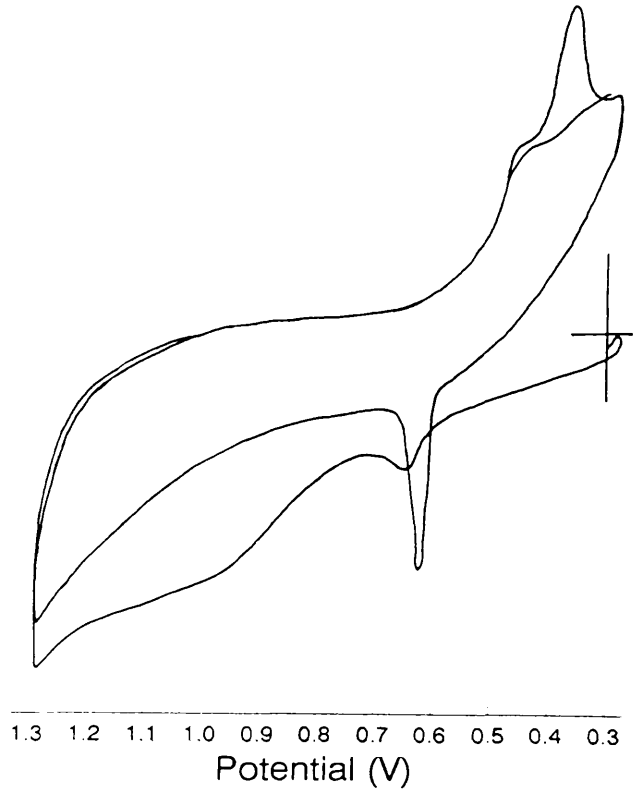


Fig. 50(b). Cyclic voltammogram of a Pt/poly-(±)-$[Ru(bipy)_2(vbpy)]^{2+}$ electrode immersed in a 0.1 mol $l^{-1}$ solution of (-)-tartaric acid in water after 15 seconds.

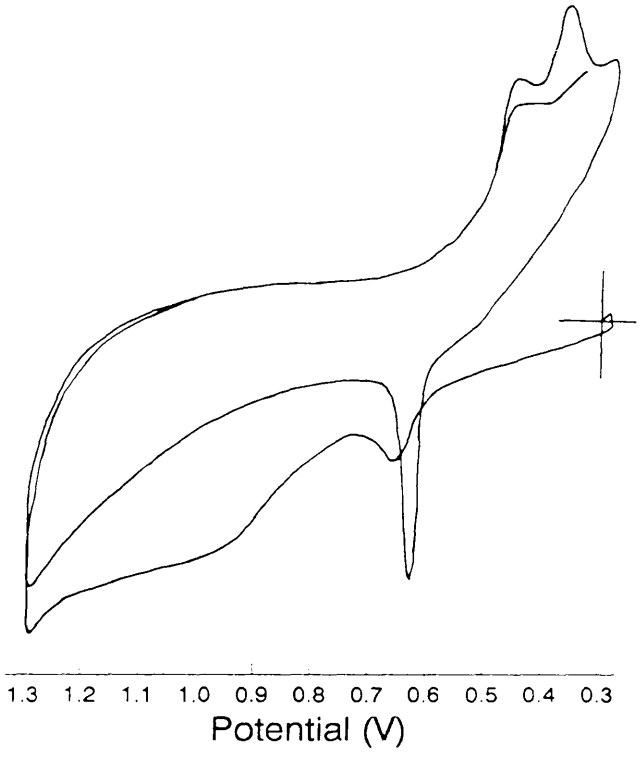


Fig. 50(c). Cyclic voltammogram of a Pt/poly-(±)-$[Ru(bipy)_2(vbpy)]^{2+}$ electrode immersed in a 0.1 mol $l^{-1}$ solution of (-)-tartaric acid in water after 25 seconds.

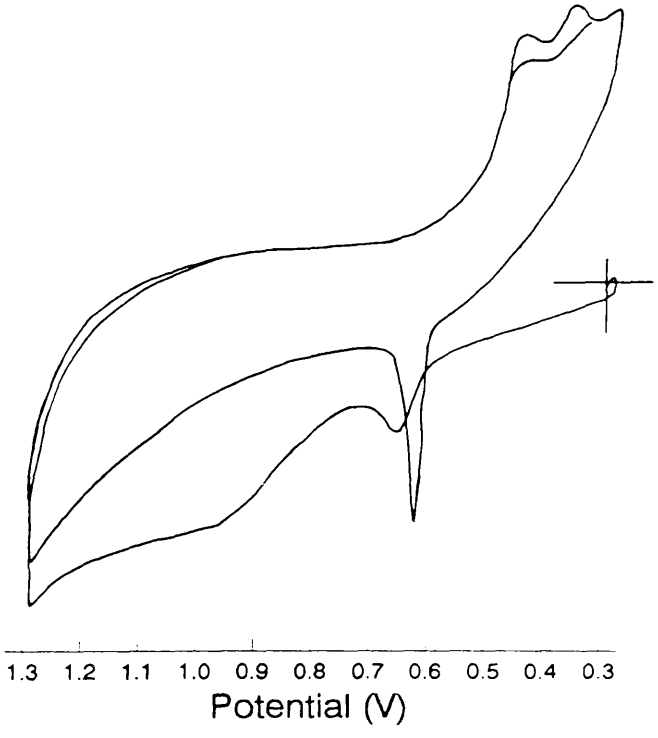


Fig. 50(d). Cyclic voltammogram of a Pt/poly-(±)-$[Ru(bipy)_2(vbpy)]^{2+}$ electrode immersed in a 0.1 mol $l^{-1}$ solution of (-)-tartaric acid in water after 40 seconds.

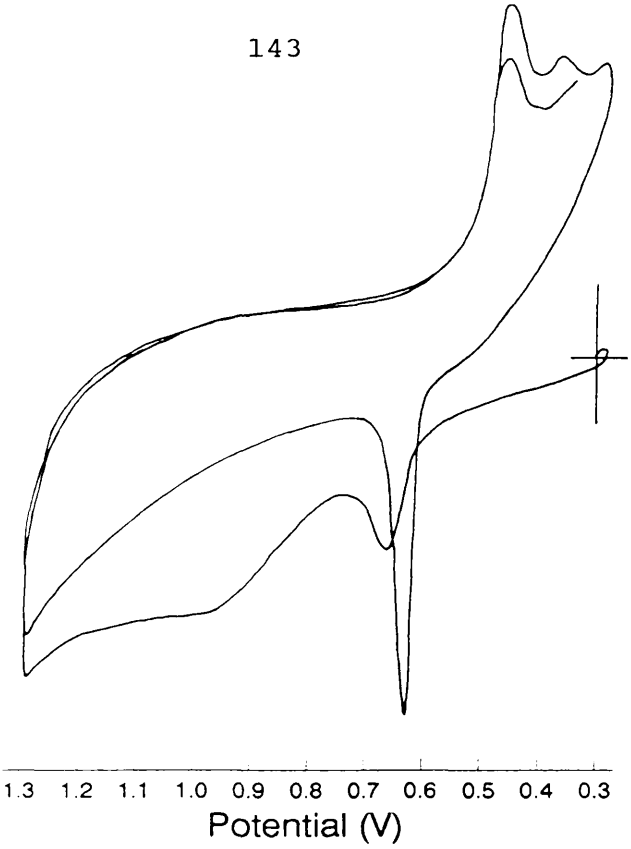


Fig. 50(e). Cyclic voltammogram of a Pt/poly-(±)-$[Ru(bipy)_2(vbpy)]^{2+}$ electrode immersed in a 0.1 mol $l^{-1}$ solution of (-)-tartaric acid in water after 1 minute.

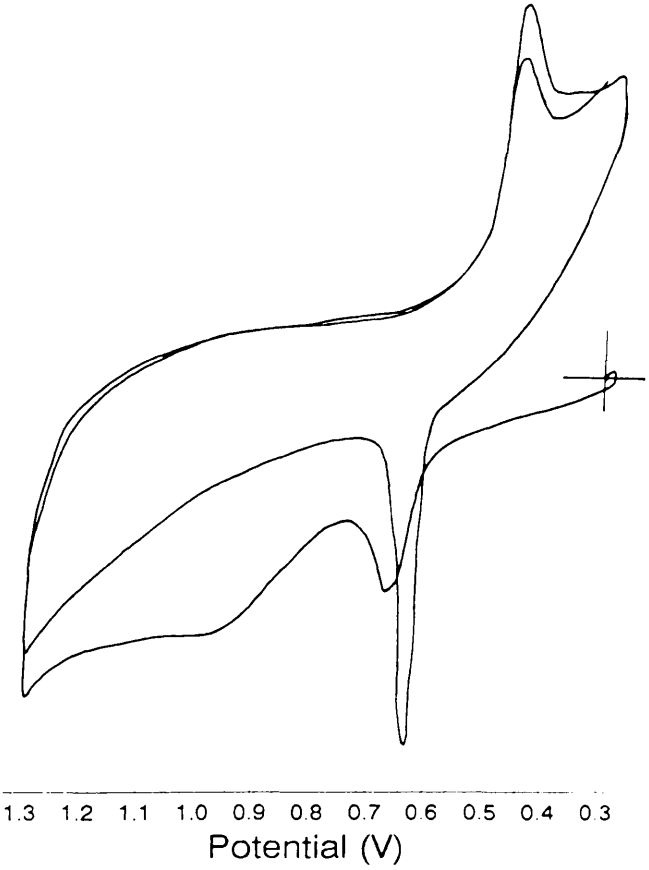


Fig. 50(f). Cyclic voltammogram of a Pt/poly-(±)-$[Ru(bipy)_2(vbpy)]^{2+}$ electrode immersed in a 0.1 mol $l^{-1}$ solution of (-)-tartaric acid in water after 2 minutes.

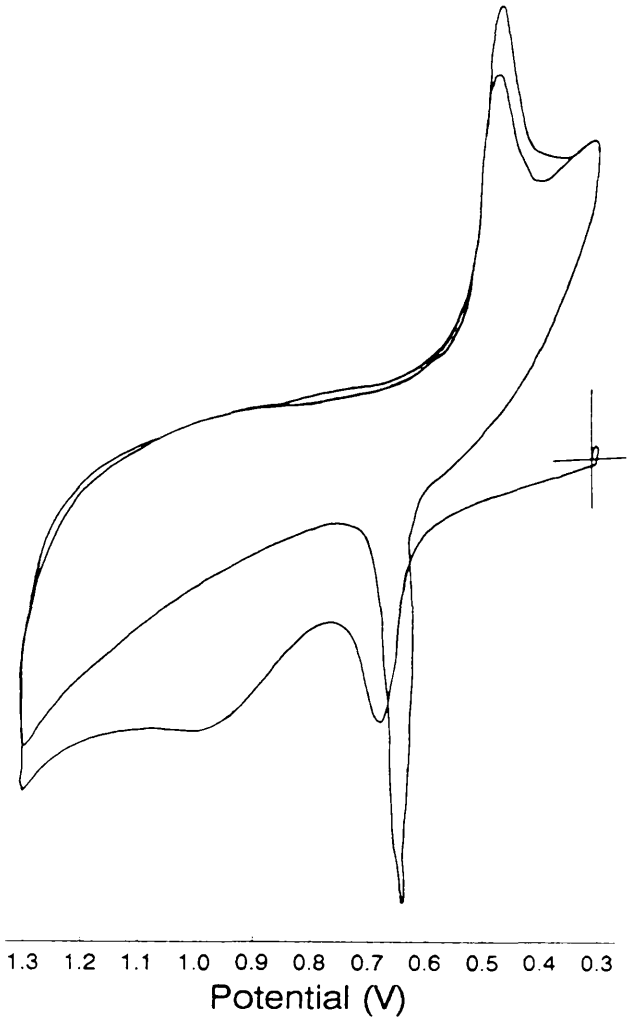


Fig. 50(g). Cyclic voltammogram of a Pt/poly-(±)-$[Ru(bipy)_2(vbpy)]^{2+}$ electrode immersed in a 0.1 mol $l^{-1}$ solution of (-)-tartaric acid in water after 5 minutes.

This result seems to agree with the idea that a reaction between the polymer and the electrolyte causes the observed peaks. It implies that the reaction takes several minutes to occur to completion (in an already conditioned electrode) and that it goes via an intermediate species which corresponds to the C.V. peak at +0.37V.

The fact that the peak at +0.65V has no voltage shift (even at short soaking times) implies that the reaction occurs after the voltage has passed +0.65V. This combined with the results of reducing the scan from +1.3V to +1.0V (peaks disappear) seems to indicate that the reaction between the polymer and the electrolyte occurs between +1.3V and +1.0V. This voltage range ties in with the oxidation of $Ru^{II}$ to $Ru^{III}$, the only electrochemical process within this system between the above potentials.

Although tartaric acid has no electrochemical processes occurring between +1.3V and +0.3V, the Ru of the polymer could be catalysing some sort of reaction between the tartaric acid and the polymer or alternatively catalysing a reaction of tartaric acid which produces a species which reacts with the polymer.

The possibility exists that the peaks could be due to dissolved species (perhaps from the polymer dissolving) in solution. This was discounted by setting up several (up to 3 at a time) working electrodes in the same electrochemical cell. The working electrode was then switched about and the C.V.'s recorded. Peaks could be present in the C.V. of one electrode but not in the other C.V.'s recorded seconds later. This confirms that the C.V. peaks correspond to a reaction at (or in) the electrode. This was confirmed by doubling the volume of tartaric acid in the cell by adding fresh solution. The

peak heights would half if the C.V. peaks were due to dissolved species. This did not happen.

As mentioned before, if the electrochemical cell is switched off between the scans, the oxidation peak at +0.65V disappears from the first half of the scan. This also agrees with the above theory in that no peak is observed until the potential is scanned to the +1.0V to +1.3V range. The "species" produced in this manner must only be stable if the cell is kept at +0.3V. If it is switched off, the species must return to its original state (polymer and electrolyte) thus the first oxidation peak is not present on a subsequent scan.

Experiments done with different starting points and held at different potentials all produced results consistent with this theory.

Starting at +1.0V, it can be seen that the peaks are present immediately (see fig. 51). If, however, the scan is started at +0.8V then no peaks are visible until one complete cycle (see fig. 52). At +0.9V (an intermediate state) small peaks are visible in the first cycle although they become bigger on the second cycle (see fig. 53). [The apparatus is switched off between each experiment.] This again indicates how important it is to scan beyond +1.0V. Without this no peak occurs at +0.45V and therefore no peak occurs at +0.65V.

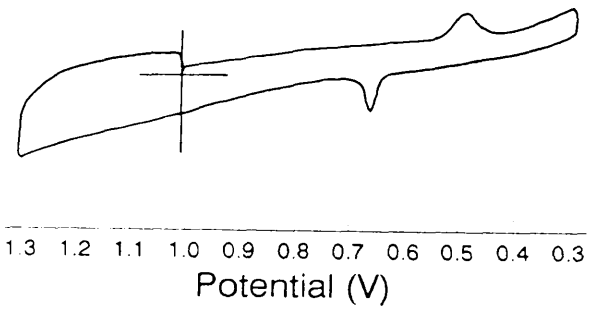


Fig. 51. Cyclic voltammogram of a Pt/poly-(±)-$[Ru(bipy)_2(vbpy)]^{2+}$ electrode immersed in a 0.1 mol $l^{-1}$ solution of (-)-tartaric acid in water scanned from +1.0V.

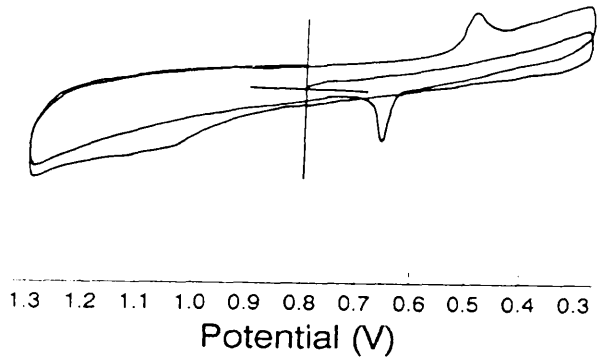


Fig. 52. Cyclic voltammogram of a Pt/poly-(±)-$[Ru(bipy)_2(vbpy)]^{2+}$ electrode immersed in a 0.1 mol $l^{-1}$ solution of (-)-tartaric acid in water scanned from +0.8V.

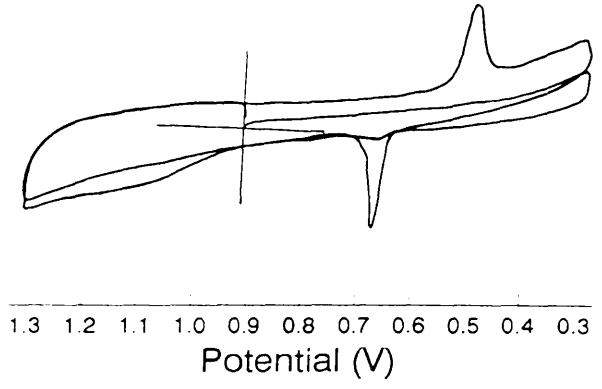


Fig. 53. Cyclic voltammogram of a Pt/poly-(±)-$[Ru(bipy)_2(vbpy)]^{2+}$ electrode immersed in a 0.1 mol $l^{-1}$ solution of (-)-tartaric acid in water scanned from +0.9V.

It seems apparent at this stage that we have a three way cycle. Firstly a reaction above +1.0V (no peak visible), secondly a peak at +0.45V (not present without scanning above +1.0V) and lastly a peak at +0.65V (not present without the peak at +0.45V having occurred before).

Work done on sodium tartrate produced what might have been peaks at the corresponding voltages (see fig. 54) but were of such small magnitude that it can be assumed that the above process is either acid sensitive or requires that a hydrogen ion counter species is used with the tartrate ion as opposed to a sodium counter ion (perhaps because of the size or the reactivity).

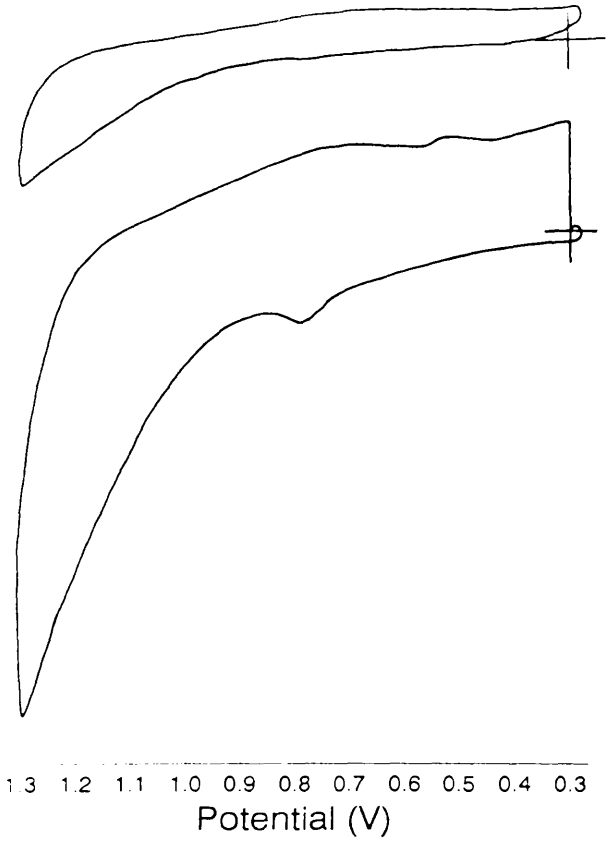


Fig. 54. Cyclic voltammogram of a Pt/poly-(±)-$[Ru(bipy)_2(vbpy)]^{2+}$ electrode immersed in a 0.1 mol $l^{-1}$ solution of Na(+)-tartrate in water.

The initiation procedure is, however, much more complex. The C.V.'s for this process seems to be different but on closer inspection, the peaks do have similarities. The first scan is the most complex and varies considerably from polymer to polymer (although this is probably due to sensitivity settings). From the second scan on, however, a standard diffusion controlled C.V. peak seems to be present centred at approximately +0.8V vs. SSCE. The oxidation peak is at ~+0.9V and the reduction peak is at ~+0.7V. These peaks diminish to zero at which point the peaks at +0.65V and +0.45V then become apparent. The peaks at +0.65V and +0.45V can appear almost immediately (actually before the peaks at +1.0V and +0.7V disappear) or they can also appear some time after the peaks at +1.0V and +0.7V have disappeared.

The peak heights are not consistent from one polymer to another. Peak heights can be large for one half of the scan but small for the opposite scan. In general the oxidation (+0.3V to +1.3V) produces peaks with greater magnitude than the reduction (+1.3V to +0.3V) although in some cases they can be of similar sizes. This is probably due to the initiation process being (to a certain extent) irreversible. The polymers that have a large difference between oxidation and reduction peaks have undergone a process which is perhaps more "irreversible" than those with equal peak heights. This would result in a longer lifetime when the polymer is left in solution for an

elongated period. The polymer growth might result in different morphologies which are more conducive to the initiation reaction than others.

In some polymer initiation, these complex peaks are not present. The C.V.'s scanned immediately on immersion produce the peaks at +0.65V and +0.45V so it can be assumed that the "complexities" occur so quickly that they are not recorded.

This lack of complex peaks during the initiation seems to occur when the polymer film is relatively thin. This implies that the "initiation reaction" is dependant on some kind of permeation within the polymer.

An electrode was produced by scanning a solution of monomer for 25 scans. The electrode did not visibly have a polymer coating but it did produce peaks at +0.45V and +0.65V. No initiation complexities were recorded which seems to imply that initiation occurred before the process could be recorded. This agrees with the idea that a thicker polymer will take longer to have the tartrate permeate it and as such will undergo any relevant initiation more slowly.

If the polymer is left immersed in solution for an extended time, an oxidation peak appears at +0.9V but no corresponding reduction peak occurs at +0.7V. This peak can be reduced in magnitude by the second cycle

(see fig. 55) or can be nonexistent by the second cycle (see fig. 56). Unlike the peak at +0.65V, the single peak at +0.9V occurs even when the cell is switched off between scans (see fig. 57).

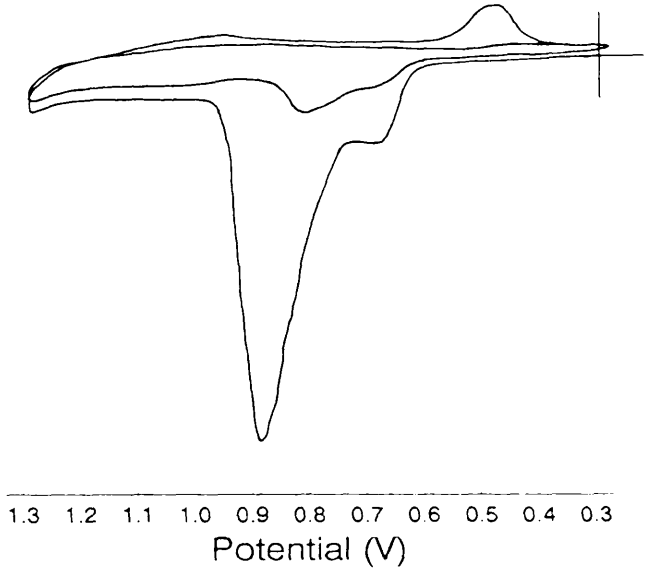


Fig. 55. Cyclic voltammogram of a Pt/poly-(±)-$[Ru(bipy)_2(vbpy)]^{2+}$ electrode immersed in a 0.1 mol $l^{-1}$ solution of (-)-tartaric acid in water after soaking for several hours.

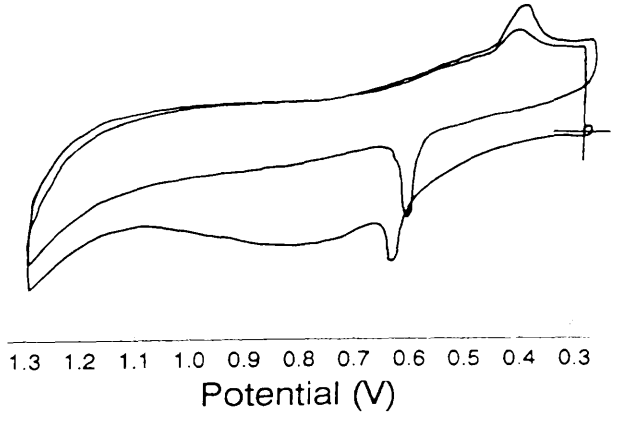


Fig. 56. Cyclic voltammogram of a Pt/poly-(±)-$[Ru(bipy)_2(vbpy)]^{2+}$ electrode immersed in a 0.1 mol $l^{-1}$ solution of (-)-tartaric acid in water after soaking for several minutes.

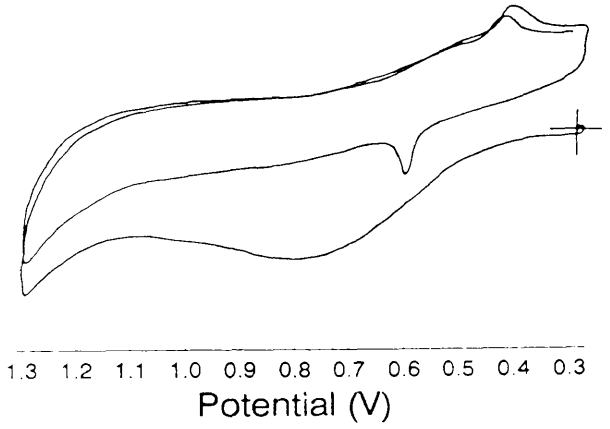


Fig. 57. Cyclic voltammogram of a Pt/poly-(±)-$[Ru(bipy)_2(vbpy)]^{2+}$ electrode immersed in a 0.1 mol $l^{-1}$ solution of (-)-tartaric acid in water after soaking for several minutes (switched off).

This implies that a permeation type reaction occurs when the electrode is immersed in solution (and not scanned positively) and is immediately reversed when the electrode is scanned to a positive potential. In fact it is likely that the reverse "initiation" reaction occurs when the electrode is left to soak and that the reverse initiation is itself reversed by the first scan of the electrode to positive potential.

The nature of the "initiation" is, however, unclear at this time.

## poly-(-)-$[Ru(bipy)_2(vbpy)]^{2+}$ electrodes

### Results and Discussion

A polymer coating of poly-(-)-$[Ru(bipy)_2(vbpy)]^{2+}$ produces many of the same results obtained with a poly-(±)-$[Ru(bipy)_2(vbpy)]^{2+}$ polymer coating. The same peaks at +0.45V and +0.65V are obtained with the same magnitude (see fig. 58). The peaks behave in the same manner with respect to the range of scanning and the time elapsed between scans. It also produces no peaks at all if the polymer is cleaned off with 5μ diamond paste.

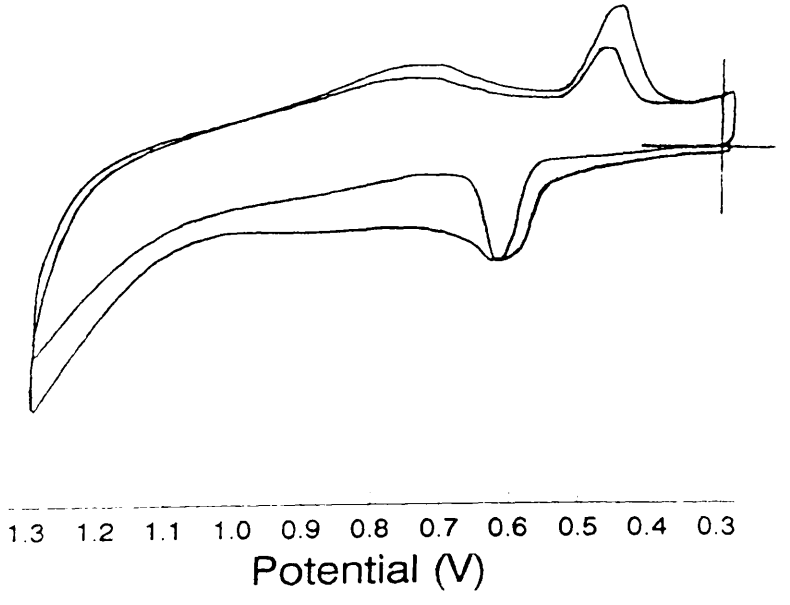


Fig. 58. Cyclic voltammogram of a Pt/poly-(-)-$[Ru(bipy)_2(vbpy)]^{2+}$ electrode immersed in a 0.1 mol $l^{-1}$ solution of (+)-tartaric acid in water.

Where there are differences is when the electrode is initially dipped into the tartaric acid solution and

scanned (see fig. 59), no complex peaks appear. The peaks at +0.45V and +0.65V appear either immediately or after some time.

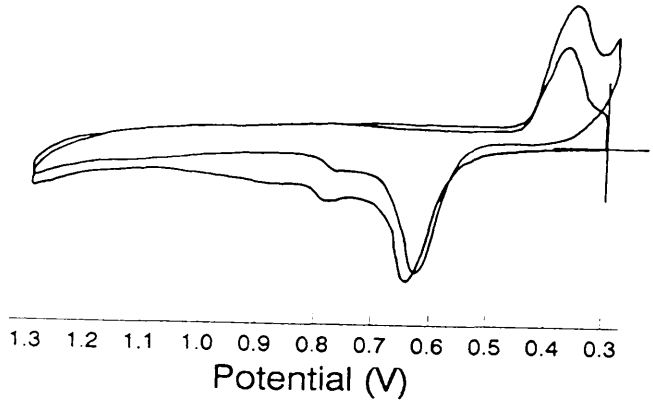


Fig. 58. Cyclic voltammogram of a Pt/poly-(-)-$[Ru(bipy)_2(vbpy)]^{2+}$ electrode initially immersed in a 0.1 mol $l^{-1}$ solution of (+)-tartaric acid in water.

This could be to do with several different possibilities:-

(i) The polymers may have always been thin and as such, the complex peaks have been missed due to their relatively short lifetime. This is probably not the case as polymerisation on some of the electrodes was carried out for a relatively long time.

(ii) Polymerisation of the chiral monomer is energetically less favourable than for the polymerisation of the racemic monomer due to steric interactions. As such, the chiral polymer layers on the electrodes would be relatively thin resulting in the phenomenon of (i).

This too is also unlikely as the polymer on the electrode could be visibly seen to be relatively thick.

(iii) Because the polymer is chiral (possible spiralling in one direction), it is thought that the tartrate (chiral also) interacts differently than with a racemic polymer. In effect, the tartaric acid reacts with the racemic polymer thus inducing some kind of "chiral nature". This, however, can not happen with the chiral polymer as the "chiral nature" is already present.

Point (iii) cannot be proven with the evidence so far but this theory is given strength with the results that follow.

poly-$[Ru(bipy)_2(vbpy)]^{2+}$ electrodes transferred from one aqueous solution to another

poly-(±)-$[Ru(bipy)_2(vbpy)]^{2+}$ electrodes

Results and discussion

When a poly-(±)-$[Ru(bipy)_2(vbpy)]^{2+}$ electrode is immersed in a solution of (+)-tartaric acid, the C.V. finally produced is that in fig. 59.

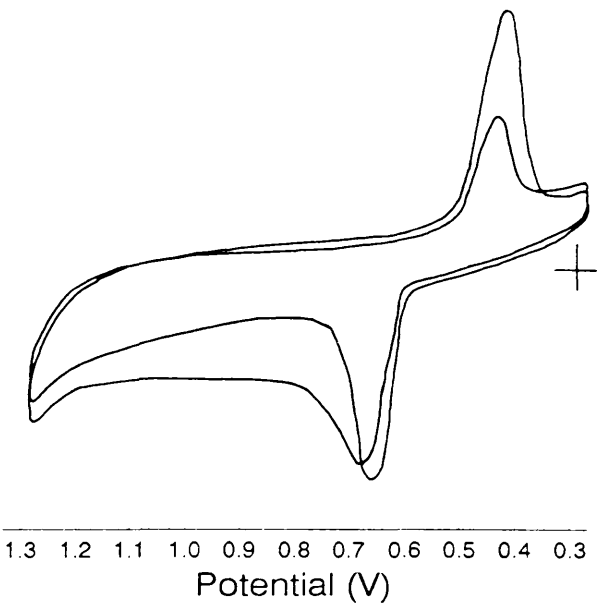


Fig. 59. Cyclic voltammogram of a Pt/poly-(±)-$[Ru(bipy)_2(vbpy)]^{2+}$ electrode immersed in a 0.1 mol $l^{-1}$ solution of (+)-tartaric acid in water.

If the electrode is then taken out, carefully washed and immersed in a solution of (-)-tartaric acid, the C.V. produced is that of fig. 60.

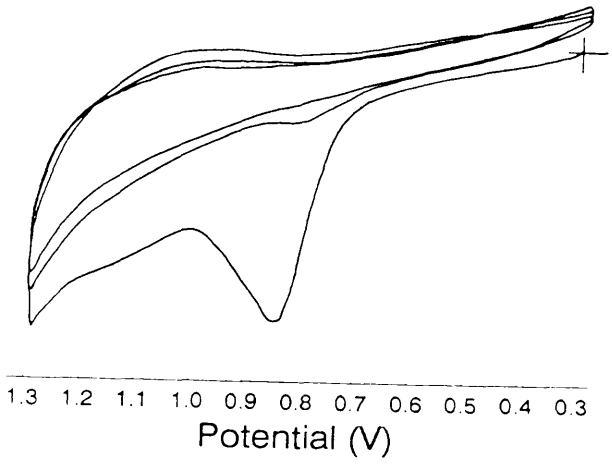


Fig. 60. Cyclic voltammogram of a Pt/poly-(±)-$[Ru(bipy)_2(vbpy)]^{2+}$ electrode immediately immersed in a 0.1 mol $l^{-1}$ solution of (-)-tartaric acid in water.

The peak at +0.85V is present on the first half of the cycle but no peaks are present there after. The standard peaks gradually reappear after a period of time (several minutes to several hours depending on the polymer) (see fig. 61). This time seems to be as a result of the (+)-tartaric acid in the polymer exchanging with the (-)-tartaric acid of the solution. No peaks occur until this process has occurred.

If this process is reversed i.e. the electrode is placed back into a solution of (+)-tartaric acid, the C.V. again becomes blank and a period of time is required before the peaks at +0.45V and +0.65 are visible again. The period of time is similar to that of (+)-tartaric acid changed to (-)-tartaric acid (using the same polymer electrode).

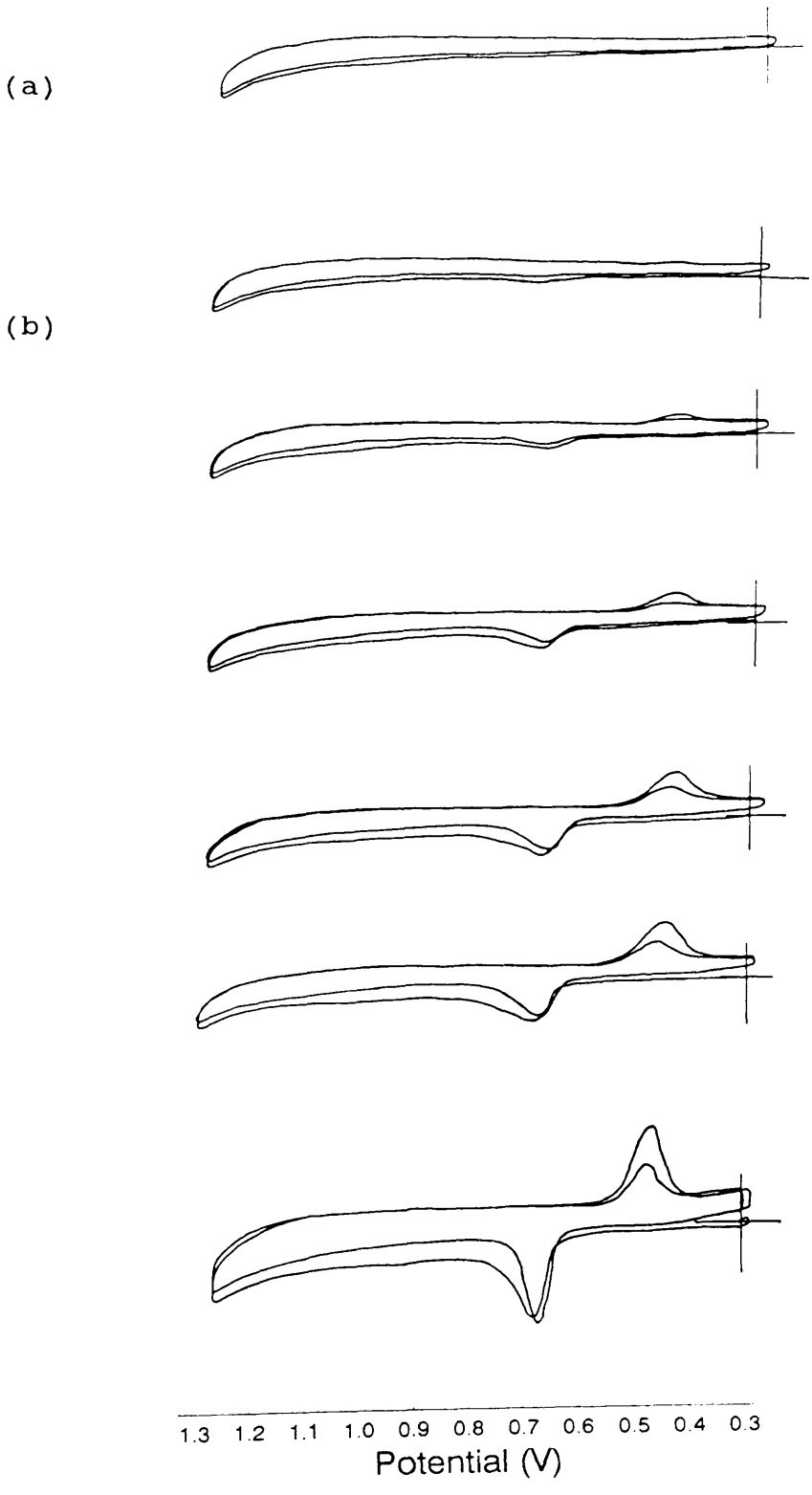


Fig. 61. Cyclic voltammogram of an already conditioned (in (+)-tartaric acid) Pt/poly-(±)-$[Ru(bipy)_2(vbpy)]^{2+}$ electrode immersed in a 0.1 mol $l^{-1}$ solution of (-)-tartaric acid in water (a) immediately and (b) over a period of about 1 hour after.

This process can be repeated again and again with only a small decrease in peak height from change to change. This is probably due to the slow degradation of the polymer (due to its slight solubility in water).

In the above experiments, using the same solution from two steps previous does not produce the peaks immediately i.e. going from (+)-tartaric acid to (-)-tartaric acid and then back to the same solution of (+)-tartaric acid does not produce results any different from those stated above. This again indicates that the peaks are not due to dissolved species in solution but due to adsorption of species on or into the electrode itself.

To test whether the above theories were correct, the electrode was then transferred from a solution of (+)-tartaric acid to a new solution of (+)-tartaric acid using the same method of transfer as used above. This resulted in peaks immediately at +0.45V and +0.65V. This proves that the tartaric acid is reacting with the polymer and that changing the "hand" of the tartaric acid results in the polymer re-reacting with the new enantiomer. If, however, as in this case, the same enantiomer is used, no reaction is necessary and therefore the peaks occur immediately.

These results prove to be very interesting and provide a basis for an electrode capable of chiral recognition.

The above experiment was repeated i.e. (+)-tartaric acid → (-)-tartaric acid → (+)-tartaric acid and then the electrode was transferred into a solution of racemic tartaric acid. This resulted in the peaks being present but at a much reduced peak height. Quantitative values for peak heights were difficult due to the changes due to many other factors i.e. time between scans, number of scans before, etc. . As such, being able to say that the peak height has halved would be impossible. What can be said with confidence, however, is that the peak heights reduce considerably and consistently (see fig. 62).

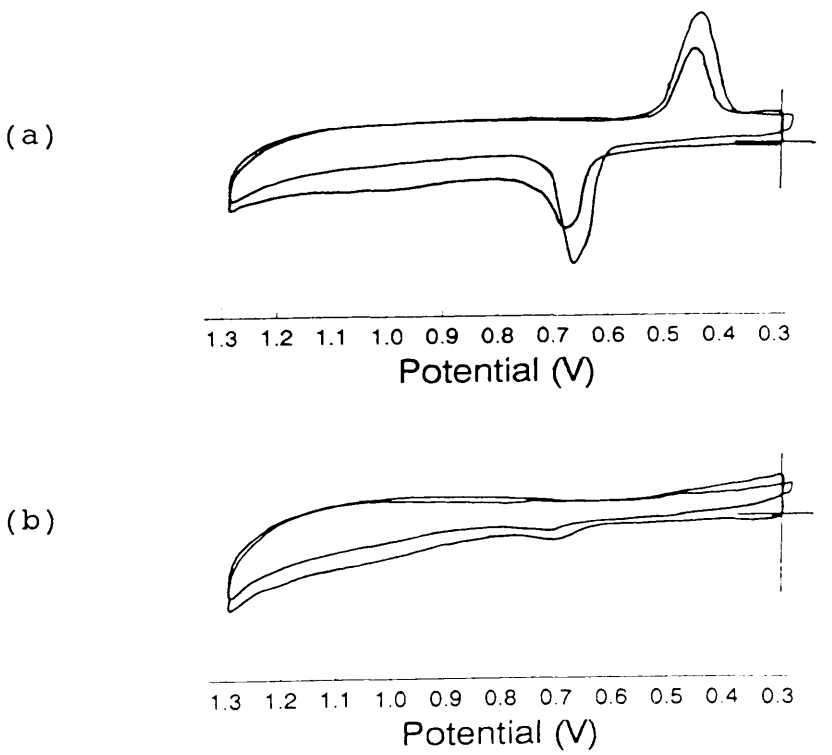


Fig. 62. Cyclic voltammogram of a Pt/poly-(±)-$[Ru(bipy)_2(vbpy)]^{2+}$ electrode immersed in a 0.1 mol $l^{-1}$ solution of (a) (+)-tartaric acid in water followed immediately by (b) (±)-tartaric acid in water.

If left, the peak heights again rise and on changing the solution to (+)- OR (-)- tartaric acid the peak heights reduce by a factor consistent with the change from (+)-tartaric acid (although (-)-tartaric acid would produce the same results) to (±)-tartaric acid (see fig. 63).

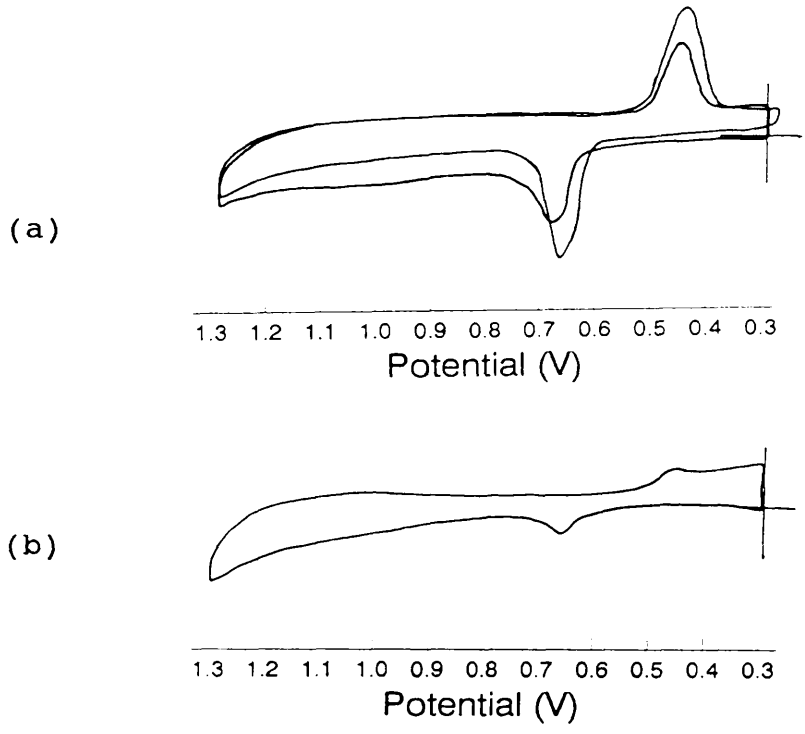


Fig. 63. Cyclic voltammogram of a Pt/poly-(±)-$[Ru(bipy)_2(vbpy)]^{2+}$ electrode immersed in a 0.1 mol $l^{-1}$ solution of (a) (±)-tartaric acid in water followed immediately by (b) (-)-tartaric acid in water.

This seems to strengthen the idea of a "chiral" reaction occurring between the polymer and the tartaric acid.

One final complexity is on the transferral of a conditioned electrode to a 0.1 mol $l^{-1}$ KCl solution, peaks are observed at +0.58V (large and sharp) and +0.38V

(small and broad) (see fig. 64). These peaks persist throughout continuous cycling. The peak heights stay the same although the solution becomes more coloured. Since it has been theorised that immersion in KCl causes the degradation of the polymer, then the peaks present are in fact due to the continuously produced surface of polymer which has been conditioned with tartaric acid rather than a solution species which would increase in quantity with time. The potential shift of approximately 0.07V could be due to the different pH of the solution (run in neutral solution rather than acidic).

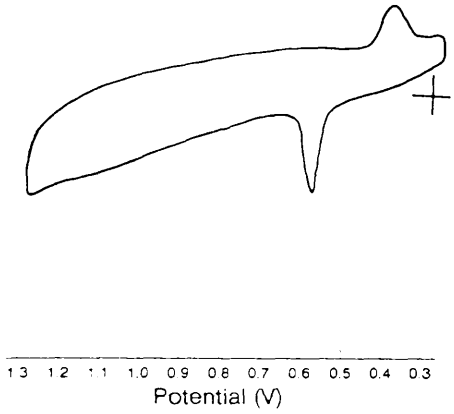


Fig. 64. Cyclic voltammogram of a Pt/poly-(±)-$[Ru(bipy)_2(vbpy)]^{2+}$ electrode immersed in a 0.1 mol $l^{-1}$ solution of KCl.

Alternatively, if an electrode is immersed in a 0.1 mol $l^{-1}$ solution of Na(+)tartrate and then $H^+$ is slowly added, peaks gradually appear proving the importance of the tartrate being present as the acid rather than the sodium salt.

## poly-(-)-$[Ru(bipy)_2(vbpy)]^{2+}$ electrodes

### Results and discussion

When a chiral polymer electrode ( poly-(-)-$[Ru(bipy)_2(vbpy)]^{2+}$ ) is immersed in a solution of (+)-tartaric acid, the C.V. produced is that in fig. 65.

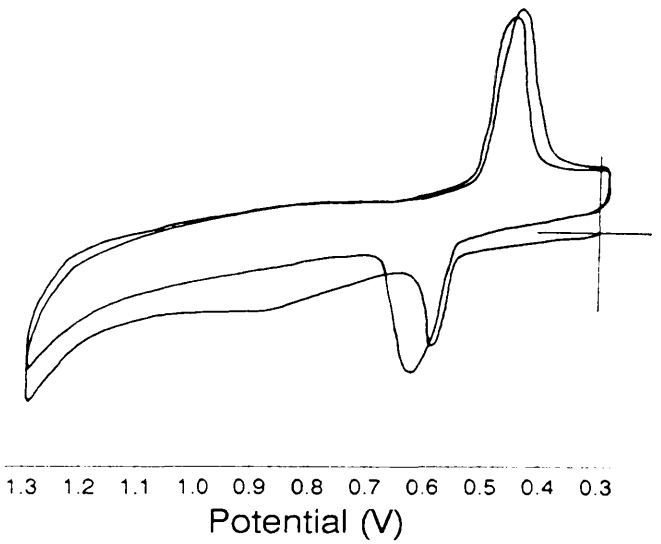


Fig. 65. Cyclic voltammogram of a Pt/poly-(-)-$[Ru(bipy)_2(vbpy)]^{2+}$ electrode immediately immersed in a 0.1 mol $l^{-1}$ solution of (+)-tartaric acid in water.

If the electrode is then washed and transferred to a solution of (-)-tartaric acid, the initial C.V. is that in fig. 66. After some time the C.V. becomes like that in fig. 67. As in the case of the (±)-poly-$[Ru(bipy)_2(vbpy)]^{2+}$ electrode, this process can be repeated with the loss in peak height being very small between stages.

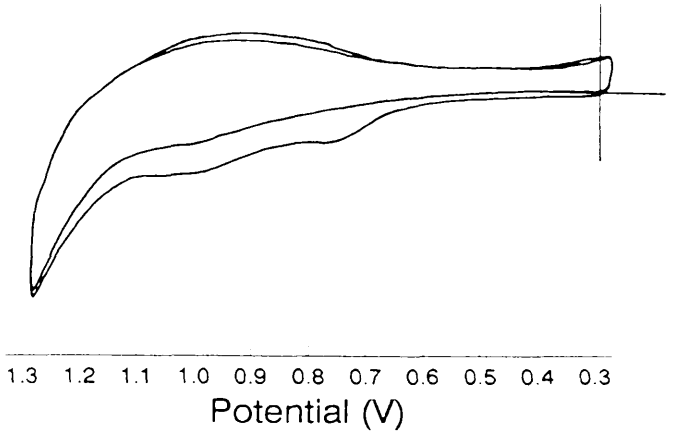


Fig. 66. Cyclic voltammogram of a Pt/poly-(-)-$[Ru(bipy)_2(vbpy)]^{2+}$ electrode immediately immersed in a 0.1 mol $l^{-1}$ solution of (-)-tartaric acid in water.

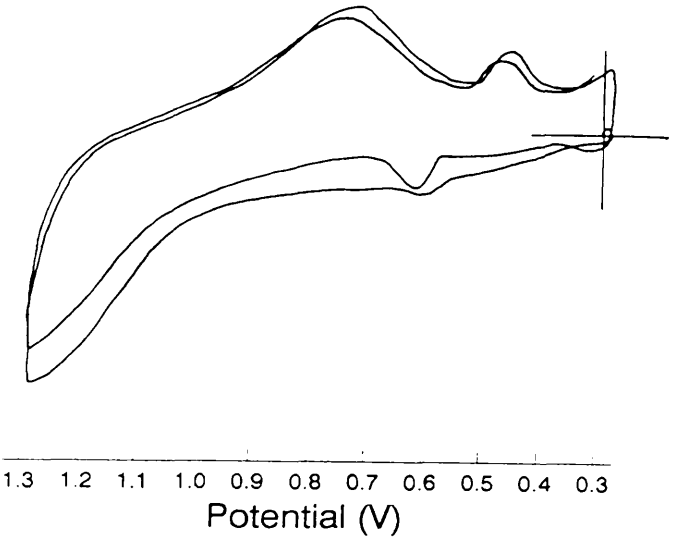


Fig. 67. Cyclic voltammogram of a Pt/poly-(-)-$[Ru(bipy)_2(vbpy)]^{2+}$ electrode immersed in a 0.1 mol $l^{-1}$ solution of (-)-tartaric acid in water after being left to soak.

If, however, the electrode is transferred from (+)-tartaric acid to (+)-tartaric acid, the C.V. peaks disappear. This is different from the racemic electrode case but seems to tie in with the above theories.

With the polymer being chiral, the conditioning process will not be exactly that undergone with the racemic polymer. This is due to the inability of the chiral polymer to be "chirally" conditioned obviously due to its already existent chiral structure. As such the interactions between the tartaric acid and the chiral polymer will be less although there is still some sort of reaction (due to the existence of the peaks at +0.45V and +0.65V).

On changing from (+)-tartaric acid to (+)-tartaric acid, the peaks disappear. This must be due to the weakness of the interactions. The transferral process must be too harsh to maintain the weakly bonded tartaric acid to the chiral polymer.

On changing from (for example) (+)-tartaric acid to (-)-tartaric acid, the peaks go as would be expected but this is probably due more to the transferral process rather than the chiral nature of the polymer. Since no chiral conditioning is possible of an already chiral polymer, this is the last piece of the puzzle to fit in. Although it seemed that the chiral polymer was behaving the same as the racemic polymer, it was in fact behaving differently and how it would be expected to behave.

For completeness a chiral electrode was transferred from (+)-tartaric acid to (±)-tartaric acid and then to (-)-

tartaric acid. At both transferral stages, the peaks disappeared confirming the theory that the interaction between a chiral polymer electrode and tartaric acid is less than for a racemic polymer electrode and tartaric acid. Therefore the chiral poly-$Ru(bipy)_2(vbpy)^{2+}$ electrode can not be used (at least using the above system) as a chiral sensor.

As an aside, if the C.V.'s of a poly-(-)-$[Ru(bipy)_2(vbpy)]^{2+}$ electrode immersed in (+)-tartaric acid (see fig. 68), (-)-tartaric acid (see fig. 69) and (±)-tartaric acid (see fig. 70) are compared, it can be seen that the peak at approximately +0.45V for the (±)-tartaric acid is broader. Originally it was thought that a chiral electrode might produce a voltage shift for the interactions between itself and different enantiomers. In the case of the (±)-tartaric acid, there seems to be two peaks very close to one another but still slightly resolvable. This initially seems to indicate that the electrode can differentiate between the (+)-tartaric acid and the (-)-tartaric acid. Unfortunately on comparing the voltammograms of the electrode immersed in separate solutions of (+)-tartaric acid and (-)-tartaric acid, no voltage difference is detected. Whether this is due to a lack of sensitivity within the cell/apparatus or just an unexplainable broadening of the peaks with the (±)-tartaric acid is not known. At present the apparatus being used is not capable of solving this dilemma and a new C.V. apparatus would be required to do so.

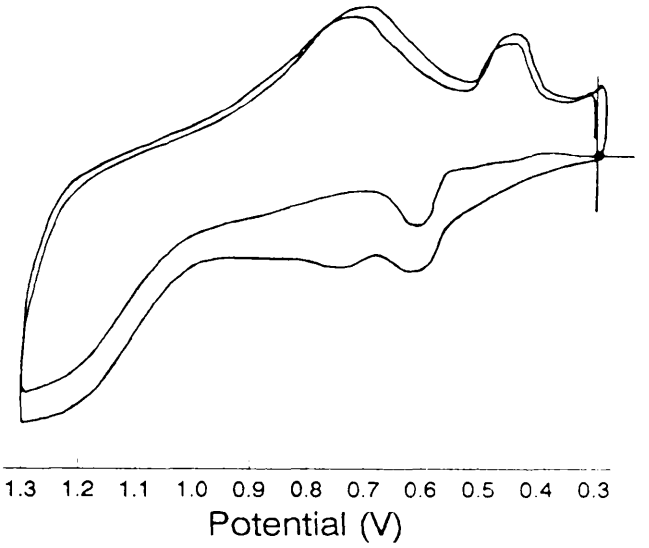


Fig. 68. Cyclic voltammogram of a Pt/poly-(-)-$[Ru(bipy)_2(vbpy)]^{2+}$ electrode immersed in a 0.1 mol $l^{-1}$ solution of (+)-tartaric acid in water.

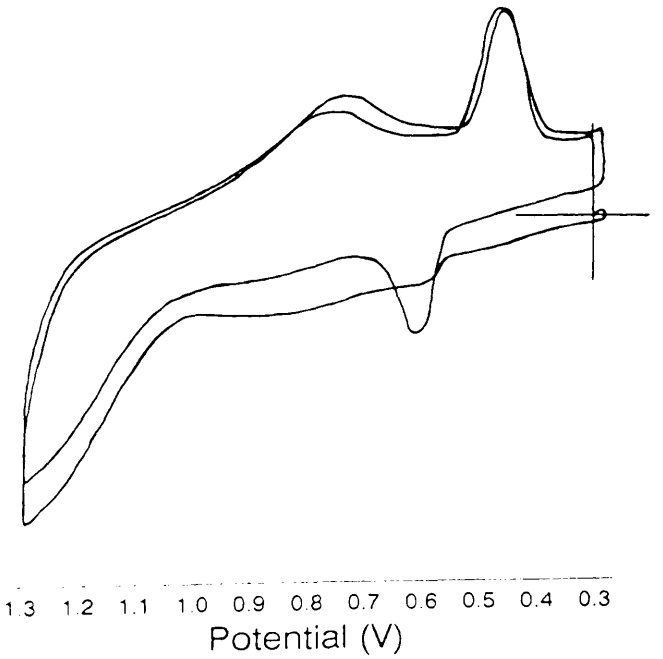


Fig. 69. Cyclic voltammogram of a Pt/poly-(-)-$[Ru(bipy)_2(vbpy)]^{2+}$ electrode immersed in a 0.1 mol $l^{-1}$ solution of (-)-tartaric acid in water.

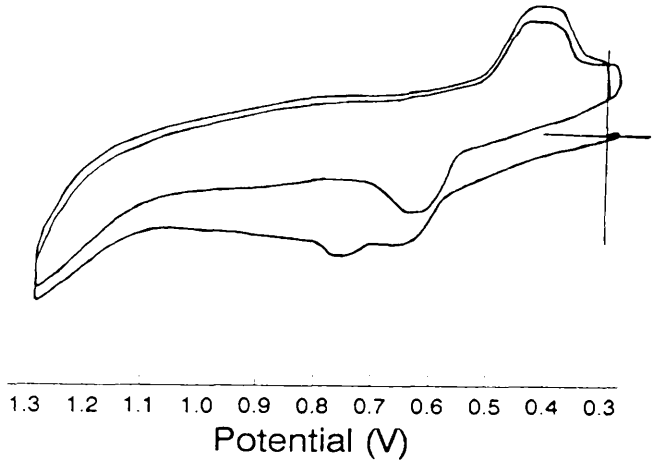


Fig. 70. Cyclic voltammogram of a Pt/poly-(-)-$[Ru(bipy)_2(vbpy)]^{2+}$ electrode immersed in a 0.1 mol $l^{-1}$ solution of (±)-tartaric acid in water.

# Chapter 4

# CONCLUSIONS

## Resolution Experiments

Resolution of ruthenium complexes with a vinyl substituent on one of the ligands seems to be more difficult than the resolution of the analogous complexes without the vinyl substituent. Successful resolution of these complexes was most successful when using silver antimonyl-(+)-tartrate.

This process produces silver salts as a precipitate and some of the ruthenium complex seems also to be precipitated at this stage (silver salts are coloured deep red). This is probably due to the adsorption of the vinyl substituent to the surface of the silver salt. This reduces the quantity of diastereoisomers produced thus ultimately making the resolution more difficult due to a decrease in the quantities used.

Once the silver salt has been filtered, however, resolution is still a slow process. Resolution gradually increases as a sample is recrystallised time after time. This must be due to the vinyl substituent causing complications.

## Electrode Experiments

Polymerisation, unlike literature reports, does occur with quite substantial build-up of polymer possible. The "exhaustion" of the monomer solution (polymer build-up no longer possible) must be due to polymerisation of the monomer to produce short chains which are not bonded to the electrode but which redissolve back into the acetonitrile solution. These short chain polymers now no longer have the vinyl group necessary for polymerisation. Once all the remaining monomer in solution has been polymerised onto the electrode or alternatively into these short chain polymer chains, the solution will no longer contain complexes capable of polymerisation.

The U.V. of this solution was identical to that of the original monomer solution. This agrees with the above theory since the electronic structure of the ruthenium in both the monomer and the polymer would be almost identical.

This is confirmed by building up a polymer (using electropolymerisation) onto a $SnO_2$ coated glass electrode. The U.V. of the polymer produced was identical (as far as the accuracy of the spectrometer could be extended) to that of the monomer solution.

On dipping an electrode into aqueous solutions the polymer seems to have a much longer lifetime than in acetonitrile solutions. This is due simply to the fact that the small polymer chains produced in the electropolymerisation above (which were very soluble in acetonitrile) are not soluble in water.

The insolubility of the polymer chains are due to the following factors:
Water is not a good solvent for permeating polymers whereas acetonitrile is good. The longer it takes the solvent to permeate the polymer, the longer it takes the polymer to dissolve.
Once the polymer has been permeated with solvent, the outer polymer chains can dissolve if they are soluble in the solvent being used. Whether the small polymer chains are soluble or not depends on the counterion of the monomer unit. When the counter ion is $[PF_6]^-$ or $[BF_4]^-$, the polymer will be soluble in acetonitrile and not in water and when the counterion is $Cl^-$, $Br^-$, [(+)-tartrate]$^{2-}$, $[SO_4]^{2-}$, etc. then the polymer will be soluble in water and not in acetonitrile. This is not necessarily the case for all polymers since the solubility induced by the counterion might be outweighed by the insolubility of the polymer chain length.

In the case of singly vinylated complexes the small polymer lengths are due to the steric interactions

between the monomer units during polymerisation. A singly vinylated polymer is a spiralling chain with no cross-linking. Since a ruthenium monomer is relatively bulky, this spiralling will cause high steric crowding and as such reduce the expected length. Di- or tri- vinylated polymers will not experience this steric crowding (see p. 58).

Ultimately, I suspect, the polymer system devised owes all of its properties to its ion exchange type nature. When the polymer is grown, the counterion of the monomer is $PF_6^-$ and the electrolyte solution that it is grown in has a $BF_4^-$ counterion. Both of these have very similar properties in that both are bulky and soluble in organic solvent solutions and not aqueous solutions. When grown, the polymer will have a mixture of both as the counterion but since both have the same properties they can be considered as one.

When the polymer is dipped into a 0.1 mol $l^{-1}$ solution of tartaric acid ( (+) or (-) ) and scanned in the range +1.3V ↔ +0.3V, the tartrate must exchange with the $PF_6^-$/ $BF_4^-$. Two $PF_6^-$ ions are required to neutralise each ruthenium monomer so two $PF_6^-$ ions would exchange with one tartrate. Tartrate has the structure:

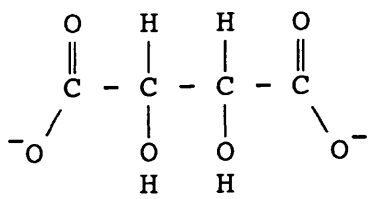

If one tartrate neutralises one "unit" of the polymer then we have a straightforward polymer chain of the type:

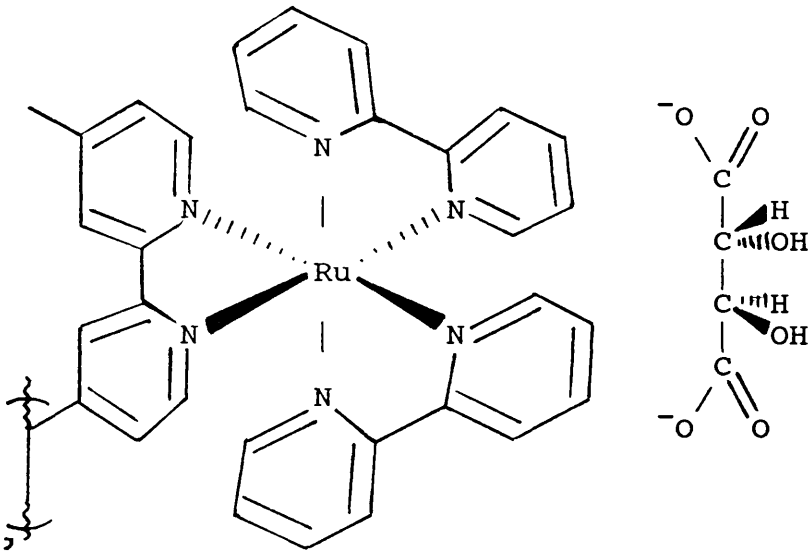

The possibility, however, of the tartrate bridging two units of the polymer exists so that the following structure exists:

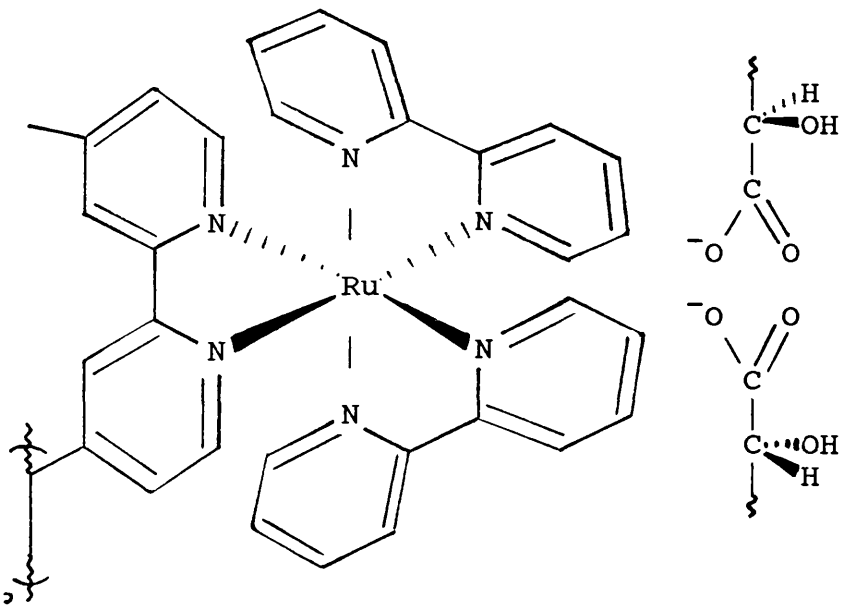

In reality a mixture of the above two would occur with the added complexity of having "crosslinking" of the tartrate from one sight on the polymer chain to a site on another adjacent polymer chain or to a sight on the same polymer chain where the chain has doubled back on itself.

This incorporation of the tartrate into the polymer induces a chiral structuring which can be used to detect chirality in other systems (as long as the chiral nature of the original conditioning solution is known).

As theorised earlier, these polymer chains grow with a spiralling akin to the secondary structure of proteins. In the pure poly-(-)-$[Ru(bipy)_2(vbpy)]^{2+}$ polymers the chiral structuring was not induced as it already was chiral. In the poly-(±)-$[Ru(bipy)_2(vbpy)]^{2+}$, however, the polymer does not have chiral structuring. The incorporation of tartrate into the polymer can therefore induce a psuedo-chiral structuring into the polymer structure. If this "chiral" polymer (conditioned electrode) is then transferred to the opposite handed tartaric acid, the polymer will then restructure into the other pseudo-chiral form.

During the period of conditioning and "re-conditioning" (transferral to new solution), the peaks at +0.45V and +0.65V are not observed. During this process, the polymer

must restructure to its new "chiral" state and the new tartrate must diffuse into the polymer. No peaks are observed because of the changing state of the system. With the polymer changing from one chiral structuring to another, the new tartrate will be unable to bind until the new structuring is complete. As such, no peaks are observed initially but gradually appear as more of the polymer changes state.

Tentatively suggested in the results and discussion chapter was the reason for the peaks themselves. The peaks are only present when the polymer and tartrate (in the form of tartaric acid) are present together. (They do not appear when run in systems separately.). Thus the peaks must be due to the interaction between the polymer and the tartrate. The peaks themselves do not occur if the polymer is not scanned beyond +1.0V. This means that the reaction occurring is catalysed by the $Ru^{III}$ produced at this potential.

Tartaric acid is not oxidised at this potential but in the presence of $Ru^{III}$, the tartrate could be oxidised. Tartrate can be oxidised to several different products The possibilities are:

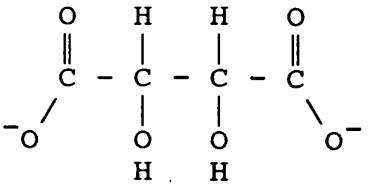

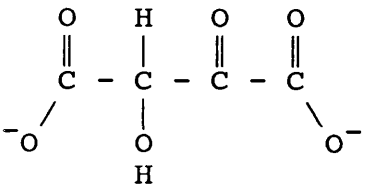

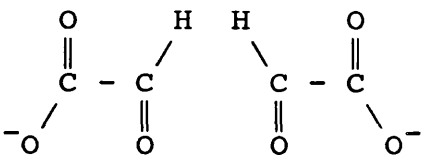

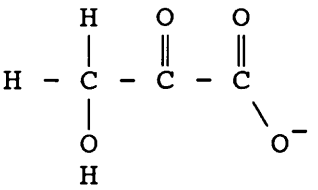

AND

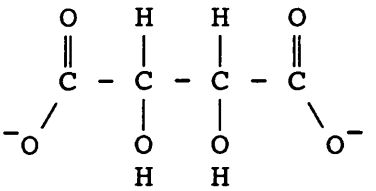

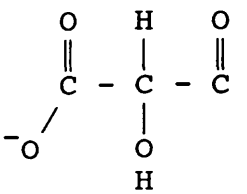

One of these products is probably responsible for the peaks at +0.45V and +0.65V. Whether this substance is responsible for the restructuring of the polymer or only for the peaks (and as such merely an indication of the completion of the chiral structuring) is not known. The polymer could obtain its chiral structuring from the tartrate and then this tartrate could be oxidised within the polymer or it could be the oxidised tartrate product which reacts with the polymer to induce the chiral structuring.

To date which of these mechanisms is responsible for the reported phenomenon is not totally clear but further conclusions can not be made at present. Further work will be required to elucidate the remaining outstanding points and this is discussed in the following chapter.

# Chapter 5

# FUTURE WORK

Future work includes work on the following systems:

(i) Attempting to grow the polymer with tartrate as the counter ion. Dipping the "unconditioned" polymer into a solution of the same handed tartaric acid would produce peaks immediately if the incorporation of tartrate is responsible for the peaks at +0.45V and +0.65V. Problems arising with this would be the ability to scan to -2.05V in aqueous solution. No aqueous systems used within this work are capable of being scanned negative enough for polymerisation of the ruthenium monomers.

(ii) On a similar vein, attempted polymerisation of the polymer with any water soluble counterion should be attempted since these polymers will have longer life-times in acetonitrile. As such the polymer, when used in acetonitrile, will have a greater working potential since the base-line "cut off" will not occur until +1.5V and +2.5V. As with (i), however, finding an aqueous system capable of scanning to -2.05V will be difficult.

(iii) Other work to discover the nature of the interaction between the polymer and the tartrate could be carried out using ethylene glycol ($HO-CH_2-CH_2-OH$), succinic acid ($HOOC-CH_2-CH_2-COOH$) and Glycolic Acid ($HO-CH_2-COOH$). These compounds contain all of the functional groups of tartaric acid in all of the possible combinations. Depending on which (if any) of these

substances produce the peaks at (or close to) +0.45V and +0.65V it will be possible to determine how the tartaric acid is reacting with the polymer.

(iv) As mentioned before, sketchy results were obtained when using the chiral polymer in the different hands of tartaric acid. With the use of more accurate C.V. apparatus, further work could be carried out to see if the broadening of the peaks in (±)-tartaric acid was due to different interactions between the (+)-tartaric acid and the polymer and the (-)-tartaric acid and the polymer.

Chapter 6

# APPENDICES

## Appendix 1 - Electrode Systems

All electrochemical work was done using the two reference electrodes described in the experimental section.
Aqueous work used a 0.1 mol $l^{-1}$ SSCE electrode while work carried out in acetonitrile used a 0.1 mol $l^{-1}$ $Ag/AgNO_3$ reference electrode.
These electrodes are compared with other reference electrodes in the table below:-

| Electrode System | Relative Potential (V) | |
|---|---|---|
| $Hg/Hg_2SO_4$, sat'd $K_2SO_4$ | +0.06 | +0.44 |
| $Ag/AgNO_3$ (0.1 mol $l^{-1}$) | **0.00** | +0.38 |
| 0.1 mol $l^{-1}$ KCl calomel | -0.24 | +0.14 |
| 1.0 mol $l^{-1}$ KCl calomel | -0.30 | +0.08 |
| S.C.E. (saturated calomel) | -0.34 | +0.04 |
| Ag/AgCl (Sat'd) - S.S.C.E | -0.38 | **0.00** |
| Hg/HgO, 1.0 mol $l^{-1}$ NaOH | -0.48 | -0.10 |
| N.H.E. (Normal Hydrogen Electrode) | -0.58 | -0.20 |
| Tl/TlCl 40 wt % in Hg (Thalamid) | -1.16 | -0.78 |

## Appendix 2 - Abbreviations

| | |
|---|---|
| bipy | 2,2'-bipyridine |
| Bu | Butyl |
| C.V. | Cyclic Voltammogram |
| DMF | Dimethylformamide |
| EDTA | Ethane diamine tetra-acetic acid |
| HOPG | Highly Orientated Pyrolytic Graphite |
| nic | Nicotinic acid |
| phen | 1,10-phenanthroline |
| PVP | Poly(vinylpyridine) |
| py | Pyridine |
| SUBS | Substrate |
| SSCE | Saturated Sodium Chloride Electrode |
| TBA $BF_4$ | Tetrabutylammonium Borofluoride |
| THF | Tetrahydrofuran |
| TPP | Tetra(aminophenyl)porphyrin |
| $TTF^+$ | Tetrathiofulvalenium |
| vbpy | 4-vinyl-4'-methyl-2,2'-bipyridine |
| vpy | 4-vinylpyridine |
| XPS | X-ray Photoelectron Spectroscopy |

Chapter 7

# REFERENCES

1. J. R. Lenhard, Ph.D. thesis, University of North Carolina, 1979.

2. R. F. Lane and A.T. Hubbard, *J. Phys. Chem.*, 1973, **77**, 1401.

3. R. F. Lane and A.T. Hubbard, *J. Phys. Chem.*, 1973, **77**, 1411.

4. H. D. Abruña, P. Denisevich, M. Umana, T.J. Meyer, and R.W. Murray, *J. Am. Chem. Soc.*, 1981, **103**, 1.

5. P. Denisevich, K.W. Willman, and R.W. Murray, *J. Am. Chem. Soc.*, 1981, **103**, 4727.

6. B. F. Watkins, J. R. Behling, E. Kariv, and L. L. Miller, *J. Am. Chem. Soc.*, 1975, **97**, 3549.

7. E. Laviron, *J. Electroanal. Chem.*, 1979, **100**, 263.

8. H. Angerstein-Kozlowska, J. Klinger, and B. E. Conway, *J. Electroanal. Chem.*, 1977, **75**, 45.

9. J. C. Lennox and R. W. Murray, *J. Am. Chem. Soc.*, 1978, **100**, 3710.

10. D. F. Smith, K. Willman, K. Kuo, and R. W. Murray, *J. Electroanal. Chem.*, 1979, **95**, 217.

11. A. P. Brown and F. C. Anson, *Anal. Chem.*, 1977, **49**, 1589.

12. W. J. Albery, N. G. Boutelle, P. Colby, and A. R. Hillman, *J. Electroanal. Chem.*, 1982, **133**, 135.

13. H. Abruña, T. J. Meyer, and R. W. Murray, *Inorg. Chem.*, 1979, **18**, 3233.

14. F. B. Kaufman, A. H. Schroeder, E. M. Engler, S. R. Kramer, and J. Q. Chambers, *J. Am. Chem. Soc.*, 1980, **102**, 483.

15. P. Daum, J. R. Lenhard, D. R. Rolison, and R. W. Murray, *J. Am. Chem. Soc.*, 1980, **102**, 4649.

16. P. J. Peerce, A. J. Bard, *J. Electroanal. Chem.*, 1980, **112**, 11.

17. P. Daum and R. W. Murray, *J. Phys. Chem.*, 1981, **85**, 389.

18. K. W. Willman, R. D. Rocklin, R. Nowak, K. Kuo, F. A. Schultz, and R. W. Murray, *J. Am. Chem. Soc.*, 1980, **102**, 7629.

19. J. B. Kerr, L. L. Miller, and M. R. Van De Mark, *J. Am. Chem. Soc.*, 1980, **102**, 3383.

20. P. R. Moses, L. Wier, and R. W. Murray, *Anal. Chem.*, 1975, **47**, 1882.

21. M. Fujihira, T. Matsue, and T. Osa, *Chem. Lett.*, 1976, 875.

22. P. Kirkov, *Electrochim. Acta.*, 1972, **17**, 519.

23. P. R. Moses and R. W. Murray, *J. Electroanal. Chem.*, 1977, **77**, 393.

24. J. R. Lenhard and R. W. Murray, *J. Electroanal. Chem.*, 1977, **78**, 195.

25. M. S. Wrighton, M. C. Paiazzotto, A. B. Bocarsly, J. M. Bolts, A. B. Fischer, and L. Nadjo, *J. Am. Chem. Soc.*, 1978, **100**, 7264.

26. P. R. Moses and R. W. Murray, *J. Am. Chem. Soc.*, 1976, **98**, 7435.

27. J. M. Bolts and M. S. Wrighton, *J. Am. Chem. Soc.*, 1978, **100**, 5257.

28. J. M. Bolts and M. S. Wrighton, *J. Am. Chem. Soc.*, 1978, **101**, 6179.

29. M. S. Wrighton, R. G. Austin, A. B. Bocarsly, J. M. Bolts, O. Haas, K. D. Legg, L. Nadjo, and M. C. Palazzotto, *J. Am. Chem. Soc.*, 1978, **100**, 1602.

30. W. O'Grady, C. Iwakura, J. Huang, and E. Yeager, *Electrocatalysis*, (M. W. Breiter, Ed.), Electrochemical Society Softbound Symposium Series, Princeton, N. J., 1974, p. 286.

31. H. O. Finklea and R. W. Murray, *J. Phys. Chem.*, 1979, **83**, 353.

32. A. Louis Allred, C. Bradley, and T. H. Newman, *J. Am. Chem. Soc.*, 1978, **100**, 5081.

33. J. R. Lenhard and R. W. Murray, *J. Am. Chem. Soc.*, 1978, **100**, 7870.

34. K. Itaya and A. J. Bard, *Anal. Chem.*, 1978, **100**, 1487.

35. R. J. Burt, G. J. Leigh, and C J. Pickett, *J. Chem. Soc., Chem. Commun.*, 1976, 940.

36. L. M. Wier, Ph.D. thesis, University of North Carolina, 1977.

37. A. F. Diaz and K. K. Kanazawa, *IBM J. Res. Dev.*, 1979, **23**, 316.

38. S. Anderson, E. C. Constable, M. P. Dare-Edwards, J. B. Goodenough, A. Hamnett, K. R. Seddon, and R. D. Wright, *Nature*, 1979, **280**, 571.

39. M. A. Fox, F. J. Nabs, and T. A. Voynick, *J. Am. Chem. Soc.*, 1980, **102**, 4029.

40. R. E. Malpas, *J. Electroanal. Chem.*, 1981, **117**, 347.

41. G. R. Henning, *J. Chim. Phys.*, 1961, **58**, 12.

42. E. Yeager, *Electrocatalysis Workshop on on-Metallic Surfaces*, NBS Spec. Publ. No. 455, Dec. 1975, issued Nov. 1976.

43. J. F. Evans and T. Kuwana, *Anal. Chem.*, 1977, **49**, 1632.

44. C. M. Elliott and C. A. Marrese, *J. Electroanal. Chem.*, 1981, **119**, 395.

45. R. D. Rocklin and R. W. Murray, *J. Electroanal. Chem.*, 1979, **100**, 271.

46. C. P. Jester, R. D. Rocklin, and R. W. Murray, *J. Electrochem. Soc.*, 1980, **127**, 1979.

47. C. A. Koval and F. C. Anson, *Anal. Chem.*, 1978, **50**, 223.

48. N. Oyama and F. C. Anson, *J. Am. Chem. Soc.*, 1979, **101**, 1634.

49. T. Matsubara and C. Creutz, *J. Am. Chem. Soc.*, 1978, **100**, 6255.

50. F. J. Evans, T. Kuwana, M. T. Henne, and G. P. Royer, *J. Electroanal. Chem.*, 1977, **80**, 409.

51. T. Matsue, M. Fujihira, and T. Osa, *J. Electrochem. Soc.*, 1979, **126**, 500.

52. T. Matsue, M. Fujihira, and T. Osa, *J. Electrochem. Soc.*, 1981, **128**, 1473.

53. T. Matsue, M. Fujihira, and T. Osa, *J. Electrochem. Soc.*, 1981, **128**, 2565.

54. A. M. Yacynych and T. Kuana, *Anal. Chem.*, 1978, **50**, 640.

55. A. W. C. Lin, P. Yeh, A. M. Yacynych, and T. Kuana, *J. Electroanal. Chem.*, 1977, **84**, 411.

56. P. R. Moses, L. M. Wier, J. C. Lennox, H. O. Finklea, J. R. Lenhard, and R. W. Murray, *Anal. Chem.*, 1978, **50**, 576.

57. S. Mazur, T. Matusinovic, and K. Camman, *J. Am. Chem. Soc.*, 1977, **99**, 3888.

58. N. Oyama, A. P. Brown, and F. C. Anson, *J. Electroanal. Chem.*, 1978, **87**, 435.

59. N. Oyama, A. P. Brown, and F. C. Anson, *J. Electroanal. Chem.*, 1978, **88**, 289.

60. R. Nowak, F. A. Schultz, M. Umana, H. Abruña, and R. W. Murray, *J. Electroanal. Chem.*, 1978, **94**, 219.

61. R. Ravichandran and R. P. Baldwin, *J. Electroanal. Chem.*, 1981, **126**, 293.

62. R. C. Bowers and A. M. Wilson, *J. Am. Chem. Soc.*, 1959, **81**, 1840.

63. G. H. Fricke, *Anal. Chem.*, 1980, **52**, 259R.

64. N. Oyama, K. Shigihara, and F. C. Anson, *Inorg. Chem.*, 1981, **20**, 518.

65. Y. S. Lipatov and L. M. Sergeeva, *Adsorption on Polymers*, Wiley, New York, 1974.

66. J. B. Kerr, L. L. Miller, and M. R. Van De Mark, *J. Am. Chem. Soc.*, 1980, **102**, 3383.

67. L. L. Miller and M. R. Van De Mark, *J. Am. Chem. Soc.*, 1978, **100**, 639.

68. M. F. Dautartas, J. F. Evans, and T. Kuwana, *Anal. Chem.*, 1979, **51**, 104.

69. S. Nakahama and R. W. Murray, *J. Electroanal. Chem.*, 1983, **158**, 303

70. K. N. Kuo and R. W. Murray, *J. Electroanal. Chem.*, 1982, **131**, 37.

71. G. J. Samuels and T. J. Meyer, *J. Am. Chem. Soc.*, 1981, **103**, 307.

72. A. Merz and A. J. Bard, *J. Am. Chem. Soc.*, 1978, **100**, 3222.

73. K. K. Kanazawa, A. F. Diaz, R. H. Geiss, W. D. Gill, J. F. Kwak, J. A. Logan, J. F. Rabolt, and J. B. Street, *J. Chem. Soc., Chem. Commun.*, 1979, 854.

74. P. Denisevich, H. D. Abruña, C. R. Leidner, T. J. Meyer, and R. W. Murray, *Inorg. Chem.*, 1982, **21**, 2153.

75. Tokuji Ikeda, C. R. Leidner, and R. W. Murray, *J. Am. Chem. Soc.*, 1981, **103**, 7422.

76. J. R. Hollanhan and A. T. Bell, Eds., *Techniques and Applications of Plasma Chemistry*, Wiley, New York, 1974.

77. F. C. Anson, *J. Phys. Chem.*, 1980, **84**, 3336.

78. L. L. Miller and M. R. Van De mark, *J. Am. Chem. Soc.*, 1978, **100**, 3223.

79. N. Oyama and F. C. Anson, *Anal. Chem.*, 1980, **52**, 1192.

80. A. Diaz, J. M. Vasquez Vallejo, and A. M. Duran, *IBM J. Res. Dev.*, 1981, **25**, 42.

81. K. Doblhofer, D. Nolte, and J. Ulstrup, *Ber. Bunsenges. Phys. Chem.*, 1978, **82**, 403.

82. J. Facci and R. W. Murray, *J. Phys. Chem.*, 1981, **85**, 2870.

83. C. D. Jaeger and A. J. Bard, *J. Am. Chem. Soc.*, 1979, **101**, 1690.

84. H. Angerstein-Kozlowska and B. E. Conway, *J. Electroanal. Chem.*, 1979, **95**, 1.

85. V. Plichon and E. Lavison, *J. Electroanal. Chem.*, 1976, **71**, 143.

86. H. D. Abruña, J. L. Walsh, T. J. Meyer, and R. W. Murray, *Inorg. Chem.*, 1981, **20**, 1481.

87. J. M. Calvert and T. J. Meyer, *Inorg. Chem.*, 1981, **20**, 27.

88. N. Oyama and F. C. Anson, *J. Am. Chem. Soc.*, 1979, **101**, 3450.

89. J. M. Calvert, R. H. Schmehl, B. P. Sullivan, J. S. Facci, T. J. Meyer, and R. W. Murray, *Inorg. Chem.*, 1983, **22**, 2151.

90. N. Oyama and F. C. Anson, *J. Am. Chem. Soc.*, 1979, **101**, 739.

91. N. S. Scott, N. Oyama, and F. C. Anson, *J. Electroanal. Chem.*, 1980, **110**, 303.

92. E. Tsuchida and N. Nischide, *Adv. Polym. Sci.*, 1977, **24**, 1.

93. J. M. Calvert, B. P. Sullivan, and T. J. Meyer, *Adv. Chem. Ser.*, 1982, **192**, 159.

94. N. Oyama and F. C. Anson, *J. Electrochem. Soc.*, 1980, **127**, 640.

95. T. F. Guarr and F. C. Anson, *J. Phys. Chem.*, 1987, **91**, 4037.

96. T. Ikeda, C. R. Leidner, and R. W. Murray, *J. Am. Chem. Soc.*, 1981, **103**, 7422.

97. D. R. Rolison, M. Umana, P. Burgmayer, and R. W. Murray, *Inorg. Chem.*, 1981, **20**, 2996.

98. A. H. Schroeder, F. V. Kaufman, V. Patel, and E. M. Engler, *J. Electroanal. Chem.*, 1980, **113**, 193.

99. N. Oyama and F. C. Anson, *J. Electrochem. Soc.*, 1980, **127**, 247.

100. N. Oyama, K. Sato, and H. Matsuda, *J. Electroanal. Chem.*, 1980, **115**, 149.

101. I. Rubinstein and A. J. Bard, *J. Am. Chem. Soc.*, 1980, **102**, 6641.

102. L. Horner, Organic Electrochemistry, M Baizer, Ed., Marcel Dekker, New York, NY, 1973.

103. B. E. Firth, L. L. Miller, M. Mitani, T. Rogers, J. Lennox, and R. W. Murray, *J. Am. Chem. Soc.*, 1976, **98**, 8271.

104. L. Horner and W. Brich, *Liebigs, Ann. Chem.*, 1977, **8**, 1354.

105. M. Fujihira, A. Yokozawa, H. Kinoshita, and T. Osa, *Chem. Lett.*, 1982, **7**, 1089.

106. S. Abe and T. Nonaka, *Chem. Lett.*, 1983, **10**, 1541.

107. T. Komori and T. Nonaka, *J. Am. Chem. Soc.*, 1984, **106**, 2656.

108. T. Komori and T. Nonaka, *Chem. Lett.*, 1984, **4**, 509.

109. M. Salmon and G. Bidan, *J. Electrochem. Soc.*, 1985, **132**, 1897.

110. M. Salmon, M. Saloma, G. Bidan, and E. M. Genies, *Electrochim. Acta*, 1989, **34**, 117.

111. A. Fitch, A. Lavy-Feder, S. A. Lee, and M. T. Kirsh, *J. Phys. Chem.*, 1988, **92**, 6665.

112. A. Yamagishi, *Chem. Aust.*, 1987, **54**, 278.

113. G. Villemure and A. J. Bard, *J. Electroanal. Chem.*, 1990, **283**, 403.

114. R. D. Mariani and H. D. Abruña, *J. Electrochem. Soc.*, 1989, **136**, 113.

115. M. Lemaire, D. Delabouglise, R. Garreau, A. Guy, and J. Roncali, *J. Chem. Soc., Chem. Commun.*, 1988, **10**, 658.

116. F. Garnier, *Adv. Materials*, 1989, **4**, 117.

117. T. Kato, M. Gondaira, T. Amemiya, and A. Fujishima, *Chem. Lett.*, 1991, 713.

118. J. F. Price and R. P. Baldwin, *Anal. Chem.*, 1980, **52**, 1940.

119. N. S. Lewis and M. S. Wrighton, *Science*, 1981, **211**, 944.

120. R. M. Ianniello and A. M. Yacynych, *Anal. Chem.*, 1981, **53**, 2090.

121. P. K. Ghosh and T. G. Spiro, *J. Am. Chem. Soc.*, 1980, **102**, 5543.

122. B. P. Sullivan, D. J. Salmon, and T. J. Meyer, *Inog. Chem.*, 1978, **17**, 3334.

123. B. Bosnich and F. P. Dwyer, *Aust. J. Chem.*, 1966, **19**, 2229.

124. G. Schlessinger, *Inorg. Synth.*, **12**, 267.

125. J. N. Braddock and T. J. Meyer, *J. Am. Chem. Soc.*, 1973, **95**, 3158.

126. F. P. Dwyer and E. C. Gyarfas, *J. Proc. R. Soc. N. S. W.*, 1949, **83**, 174.